THE JOURNAL
OF
CHEMICAL PHYSICS

VOLUME 8 MAY, 1940 NUMBER 5

The Negative Bands of the Heavy Nitrogen Molecules

R. W. WOOD AND G. H. DIEKE
Johns Hopkins University, Baltimore, Maryland

(Received February 24, 1940)

The so-called negative bands emitted by the N_2^+ molecule have been photographed in the second order of a 21-ft. concave grating with a dispersion of about 0.6A per mm. The principal bands of $N^{15}-N^{15}$ and $N^{14}-N^{15}$ are analyzed. A comparison of the constants of the three isotopic molecules shows that the changes except for the spin-doubling and perturbations are well represented by the elementary theory of band spectra. The intensity alternations in the $N^{15}-N^{15}$ bands give $\frac{1}{2}h$ as the value for the nuclear spin of N^{15}.

§1

IN a previous communication[1] we reported the principal bands of the so-called negative group of $N^{14}-N^{15}$. In the meantime we obtained from Professor H. C. Urey a small quantity of ammonium nitrate in which 70 percent of the nitrogen was the heavy isotope N^{15}. With this concentration the bands of the three isotopic molecules[2] $N^{14}-N^{14}$, $N^{14}-N^{15}$ and $N^{15}-N^{15}$ appear approximately with the relative intensities 9 : 42 : 49. The conditions are therefore very favorable for the study of the $N^{15}-N^{15}$ bands. The ordinary $N^{14}-N^{14}$ bands are so weak that they do not interfere seriously with the stronger $N^{15}-N^{15}$ or $N^{14}-N^{15}$ bands. Although there is still considerable overlapping of the $N^{14}-N^{15}$ bands, this is not serious if we restrict ourselves to the stronger bands which are given in this paper. For the weaker bands originating from the higher vibrational states, the situation is less favorable, and it seemed best to leave their study until heavy nitrogen of even higher concentration becomes available.

For this reason we restrict ourselves in this paper to the bands originating from the two lowest initial vibrational levels. They are given in Table I for $N^{15}-N^{15}$ and in Table II for $N^{14}-N^{15}$. We were now able to photograph the $N^{14}-N^{15}$ bands at the optimum conditions (concentration of 50 percent N^{15}) and therefore could obtain them much more completely than was possible in our previous paper.

Table III gives the analysis of the $1\rightarrow0$ band of ordinary nitrogen which seems never to have been published before.

Essentially the same method was followed for the production of the nitrogen as in our previous paper. Also the remarks made there concerning the wave-length measurements and their accuracy apply to the present case.

Figures 1–3 give reproductions of the regions near the heads of the principal bands. In the $0\rightarrow0$ band near 3914A (Fig. 1) the heads of the $N^{14}-N^{14}$, $N^{14}-N^{15}$ and $N^{15}-N^{15}$ bands fall so closely together that they do not appear separate

[1] R. W. Wood and G. H. Dieke, J. Chem. Phys. **6**, 734 (1938).

[2] Throughout this paper, whenever the nitrogen molecule is mentioned, the N_2^+ ion is meant. To indicate this explicitly in symbols like $N^{14}-N^{15}$ would give rise to a rather awkward notation.

TABLE I.* *The negative bands of* $N^{15}-N^{15}$.

K	P BRANCH ν	P BRANCH I		R BRANCH ν	R BRANCH I	
	The 0→0 band					
0	—	—				
1	25,559.13	2		25,570.74	2	
2	555.82	1		575.18	2	
3	552.80	3*d*		579.90	8	
4	550.04	1*d*		584.86	2*D*	
5	547.63	5		590.23	7	
6	545.46	2		595.78	2*d*	
7	543.57	4	*	601.60	10	*A*
8	541.96	2	*	607.75	7	*A*
9	540.52		*	614.22	10	*A*
10	539.68		*	620.91	3	
11	538.82		*	627.86	8	
12	538.27		*	635.16	3*b*	
13	538.27		*	642.71	8*D*	
14	538.27		*	650.54	4*D*	
15	538.82		*	658.64	8*D*	
16	539.68		*	667.02	4*D*	
17	540.52		*	675.67	8*D*	
18	541.53		*	684.59	3*D*	
19	542.53		*	693.61	5	
	543.04		*	693.89	5	
20	544.34		*	701.73	1	
	544.60		*	703.30	3	
21	546.86	2	*	713.36	5	
	547.06	2		712.90	5	
22	547.63	(5)	*C*	723.26	2	
	549.33	1		722.32	3	
23	552.30	2	*A*	733.45	3	
	551.84	2	*A*	737.25	3*r*	
24	555.46	0	*A*	743.16	1	
	554.14	3	*B*	745.40	3	
25	558.21	3*r*	*A*	755.61	4	
	561.98	2		755.78	4	
26	560.92	(2)		766.68	2*b*	*C*
	563.02	1				
27	566.28	3*D*		778.92	4	
				777.09	4	
28	—	—		789.75	1	
	570.13	1	*AC*	790.94	1	
29	574.40	2		801.75	3	
	573.44	2		802.54	3	

K	P BRANCH ν	P BRANCH I		R BRANCH ν	R BRANCH I	
	The 0→0 band					
30	579.01	0		814.01	1	
	—	—	Too close to the very strong line R_3	814.72	1	
31	583.99	1		826.60	3	
	584.86	2*D*	*C*	827.24	3	
32	589.19	0		839.47	0	
	—	—	Too close to R_5	840.06	0	
33	594.71	1		852.57	2	
	95.35	0		853.19	2	
34	600.50	0		866.00	0	
	601.03	0		866.56	0	
35	606.71	1*D*	*A*	879.66	1	
	607.18	1		880.24	1	
36	613.00	00		893.63	00	
	613.62	0		894.29	00	
37	619.62	1		907.88	0	
	620.21	1		908.45	1	
38	626.66	00				
	—	—				
39	634.36	0	?			
	The 0→1 band					
0	—	—		23,464.21	00	
1	23,456.79	2		468.42	3	
2	453.54	1		472.92	1	
3	450.62	4		477.76	6	
4	448.04	5*r*	*A*	482.90	4	
5	445.75	10		488.37	8	
6	443.79	5		494.15	3	
7	442.13	8	*B*	500.28	10	
8	440.86		*	506.67	4	
9	439.83		*	513.37	6	
10	439.03		*	520.32	10*D*	*B*
11	438.76		*	527.81	7*b*	
12	438.47		*	535.45	2*b*	
13	438.76		*	543.46	8*D*	
14	439.48		*	551.74	3*D*	

K	P BRANCH ν	P BRANCH I		R BRANCH ν	R BRANCH I	
	The 0→1 band					
15	440.44		*	560.36	8*D*	
16	441.62		*	569.19	2	
				569.40	2	
17	443.21	7*b*		578.44	7	
				578.67	7	*B*
18	445.05	4*b*		587.95	3	
				588.17	3	
19	447.27	10*b*	*B*	597.75	6	
				598.02	6	
20	449.33	0		606.48	3	
	449.72	2*D*		608.11	3	
21	452.33	4		618.88	6	
	452.64	3		618.43	6	
22	454.18	2*b*		629.58	(4)	Lines in head of 14–15 1–2 band
	455.69	10*b*	*A*	628.82	1*c*	
23	459.40	4		640.51	5	
	458.95	5	*B*	644.48	3*D*	*A*
24				651.04	1	
	462.09	1*d*		653.48	1*c*	
25	466.84	10	*B*	664.37	5	*C*
	470.73	2		664.57	5	
26	470.42	2		676.32	4*b*	*A*
	472.65	1				
27	476.86	4*D*		688.56	4*c*	
				687.65	3*c*	
28	481.50	2		701.28	2	*b*
				702.36	4	*B*
29	486.92	3		714.26	2	
	485.98	3		715.06	3	
30	492.57	2				*B*
	493.85	0		728.27	0	
31	398.51	5*c*	*A*	741.23	2	
	499.36	2		741.85	2	
32	504.86	00		754.376	00	
	505.56	0		755.17	00	
33	511.54	5	*B*	739.47	1	
	512.15	2*b*		770.03	1	
34	518.56	0		783.97	00	
	519.13	0		784.59	00	
35	525.82	1		798.87	1	
	526.41	1		799.37	2*b*	
36	533.44	00		814.07	00	
	534.03	00		814.61	1*v*	
37	541.34	1		829.56	0	
	541.94	1		830.16	1*c*	

* Overlapping with other classified lines is indicated by a letter *A*, *B*, *C* in the column to the right of the intensity column.
A means that the overlapping line is a $N^{14}-N^{14}$ line,
B that it is a $N^{14}-N^{15}$ line,
C that it is a $N^{15}-N^{15}$ line.

When the overlapping line is much stronger than the line in question, the intensities are put between parentheses. In such a case very little reliance can be put on the value of the frequency. The congested region of the head is indicated in a band by an asterisk. Intensity estimates are uncertain in this region and also the frequencies are less reliable.

TABLE I.—*Continued.*

K	P BRANCH ν	I		R BRANCH ν	I	
	The 0→2 band					
0	—	—		21,392.59	1*D*	*A*
1	21,385.12	3*D*	*	396.60	4	*C*
2	381.92	4*bb*	*	401.20	1	
3	379.09	3*br*	*	406.23	4*D*	*C*
4	376.63	4*b*	*	411.42	2	
5	374.64	4*D*	**B*	417.01	4*bb*	*B*
6	372.74	4*b*	*	423.03	2	
7	371.26	4*b*	*	429.32	3*b*	*C*
8		3*b*	*	436.09	3*b*	*B*
9	369.55	4*b*	*	443.11	3*b*	
10	369.14	4*b*	*	450.50	2	
11	369.14	4*b*	*	458.21	5	
12	369.55	4*b*	*	466.35	2*b*	
13		3*b*	*	474.77	8	
14	371.26	4*b*	*	483.53	2*b*	
15	372.74	4*b*	*	492.81	5*D*	
16	374.64	4*D*	**B*	502.17	2*b*	
17	376.63	4*b*	*	511.98	6*D*	
18	379.09	3*br*	*	522.04	2	
				522.25	2	
19	381.92	4*bb*	*	532.46	4	
				532.77	4	
20	385.12	3*D*	*	541.95	0	
				543.53	1	
21	388.48	4		555.01	2	
	388.73	4		554.55	3	
22	390.97	0		566.45	1	
	392.59	1*D*		565.52	2	
23	397.08	3		378.20	4	
	396.60	4	*C*	582.06	3*b*	
24	401.53	1				Con-
	400.58	1		591.84	1	*B*
25	406.23	4*D*	*C*	603.85	3*D*	
	410.10	2				
26	410.67	1*bd*		616.60	1*bd*	
	412.92	1				
27	418.06	3*D*		629.79	2	
				628.84	2	
28	423.83	1		443.49	0*b*	
				444.63	0	
29	430.09	2		457.50	4*br*	
	429.32	3*b*	*C*	458.25	3	
30	436.80	0		471.82	0	
	437.94	0				*B*
31	443.89	1		686.49	2	
	444.66	1		687.14	2*c*	
32	451.30	0		701.39	2	*B*
	451.99	0		701.93	1*d*	*B*

K	P BRANCH ν	I		R BRANCH ν	I	
	The 0→2 band					
33	459.10	1		716.96	2	
	459.72	1		717.58	1	
34	467.22	00				
	467.74	(2)	*B*			
35	475.71	1				
	476.32	1				
36	484.59	00				
	485.16	00				
37	493.83	1*d*	*A*			
	491.31	1*d*	*A*			
38	503.38	00				
	503.92	00				
39	513.29	0				
	513.85	0				
40						
41	534.16	0				
	534.73	0				
	The 1→0 band					
0	—	—				
1	27,852.26	0		27,863.84	1	
2	848.92	00		868.34	3	*B*
3	845.88	2		872.78	2	*B*
4	843.00	1		877.25	0	*B*
5	840.38	4		882.71	3	*B*
6	838.02	1*b*		888.04	1*b*	*B*
7	835.87	4		893.37	4*D*	*B*
8	834.02	1*D*		899.16	1*D*	*B*
9	832.38	3*D*		905.28	3*r*	
10	830.89	0		911.57	1	*A*
	831.14	0				
11	829.64	3*b*	*	917.78	2	
	829.95	2	*	918.05	2	
12	828.77	1	*	(924.11)	0*b*	*A*
	829.21	1	*			
13	828.15		*	931.46	3	*A*
	828.41		*	931.78	3	
14	827.84		*	938.64	0	
	828.15		*	939.02	1	*A*
15	827.52		*	946.11	4	*A*
	827.84		*	946.49	4	*A*
16	827.84		*			
	828.15		*			
17	828.15		*			
	828.41		*			
18			*			
			*			
19	829.21		*			
	829.64		*			

K	P BRANCH ν	I		R BRANCH ν	I	
	The 1→0 band					
20			*			
			*			
21	831.49	0				
	831.92	1				
22	832.99	00				
	833.61	00				
23	834.78	1				
	835.22	1				
24						
25	839.02	1				
	839.52	1				
26	841.49	00				
	841.97	00				
27	844.24	1				
	844.73	1				
28						
29	850.41	0				
	850.93	0				
30						
31	857.53	0				
	858.09	0				
	The 1→2 band					
0	—	—		23,685.64	(4)	*B*
1	23,678.15	(2)		689.59	(4)	*B*
2	774.69	(5)	*B*	693.99	0*d*	
3	671.94	2		698.78	2*d*	
4	669.67	(5)	*A*	703.84	0	
5	667.09	4	*A*	709.16	2*D*	
6	665.13	00		715.06	(4)	*C*
7	663.47	3*b*		720.84	3*c*	
				721.07	3*c*	
8	662.20		*	727.17	0	
	662.54		*	727.48	(5)	*Б*
9	661.18		*	733.79	2	
	661.40		*	734.07	2	
10	660.30		*	740.68	1	
	660.54		*	741.02	2	*C*
11	659.74		*	748.00	3	
	660.02		*	748.30	3	
12	659.74		*	755.92	3*Db*	
	660.02		*			
13	660.02		*	763.41	3	
	660.30		*	763.71	3	
14	660.54		*	771.44	(5)	*B*
	660.97		*	771.96	(5)	*B*
15	661.40		**C*	780.05	3	
	661.67		**B*	780.40	3	
16	662.54		*	788.80	2	
	662.84		**A*	789.19	1	

TABLE I.—*Continued.*

K	P BRANCH ν	I		R BRANCH ν	I		K	P BRANCH ν	I		R BRANCH ν	I		K	P BRANCH ν	I		R BRANCH ν	I	
	The 1→2 band—Continued							*The 1→2 band*							*The 1→2 band*					
17	664.09		*B	797.93	1		23	679.41	6	B	858.90	3	B	30				944.00	0	
	664.37		*C	798.33	2			679.73	6	B	859.42	2						944.53	0	
18	665.92	2vc	B	807.32	3v		24	682.81	1		870.21	0		31	717.29	(4)	A	957.43	1	
				807.77	0			683.06	0		870.64	2	B		717.80	00		957.85	1	
19	667.91	3		817.05	3		25	687.04	1		881.74	2		32						
	668.33	3		817.48	3			687.44	1c		882.24	2		33	729.93	0		985.03	1	
20	670.33	0		827.04	0		26				893.45	0						985.51	1	
	670.75	0c		827.47	0						893.98	1v		34						
21	673.05	2		837.37	1		27	695.92	3		905.73	1		35				24,013.85	0	
	673.43	2		837.84	1			696.35	1b		906.20	1						14.32	0	
							28	700.80	0		918.18	00								
22			Con fused	846.90	(4bb)	B	29	706.02	1		930.98	2								
				48.20	(3bd)			706.48	1		931.42	2								

in the figure. The corresponding rotational lines are, however, well separated. The band of the heaviest isotope lies always nearer to the electronic transition of the band system which is not far from the 0→0 band than the corresponding bands of the lighter isotopes. Accordingly in the 1→0 band (Fig. 2) the $N^{14}-N^{15}$ and $N^{15}-N^{15}$ bands lie to longer wave-lengths of the $N^{14}-N^{14}$ band. This means that the heads of the heavier isotopes appear in a region which is free from lines in the ordinary nitrogen spectrum. On the other hand, in the 0→1 band near 4270A (Fig. 3) the heads of the heavier isotopes appear inside the head of the ordinary nitrogen band. For this reason they cannot be observed so easily for small concentrations of N^{15}. This explains why most of the preliminary investigations which were done when only nitrogen of small N^{15} concentration was available were carried out with the 1→0 band.

The analysis of the bands could be carried out with the same degree of completeness and certainty as that of the corresponding bands of ordinary nitrogen. The chances for overlapping

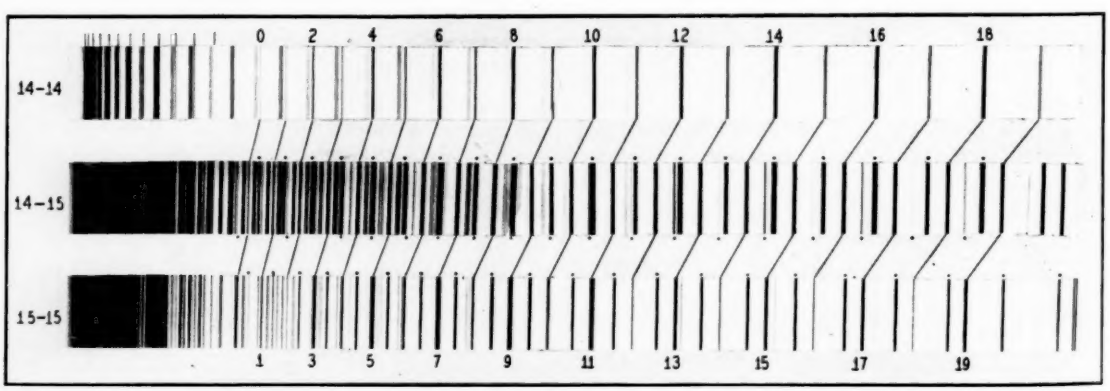

FIG. 1. The 0→0 band at 3914A of the negative nitrogen bands (N_2^+). The upper spectrum is that of ordinary nitrogen $N^{14}-N^{14}$. The lines of the *R* branch are marked and the alternating intensities are seen. The strong lines are numbered (even *K*). The beginning of the *P* branch is also indicated. The middle spectrum is taken with a concentration of about 30 percent of the heavy isotope N^{15}. The lines of the *R* branch of $N^{14}-N^{15}$ are marked. Those of $N^{14}-N^{14}$ are indicated by a dot above, those of $N^{15}-N^{15}$ by a dot below the line. It is seen that there are no intensity alternations for $N^{14}-N^{15}$. (Perhaps better seen on the lower spectrum where the lines are not overexposed.) The lower spectrum is taken with about 70 percent of N^{15}. The $N^{14}-N^{15}$ and the $N^{15}-N^{15}$ lines have about the same intensity, but the $N^{14}-N^{14}$ are only faintly visible. The intensity alternations of the $N^{15}-N^{15}$ lines are now of such a nature that the odd numbered lines are the strong ones.

TABLE II. *The negative bands of* $N^{14}-N^{15}$.*†

K	P BRANCH ν	P BRANCH I		R BRANCH ν	R BRANCH I	
The 0→0 band						
0	—			25,568.41	1	
1	25,560.72	1		572.73	2	
2	557.28	2		577.32	2	
3	554.14	3	*C*	582.20	3	
4	551.31	3		587.39	4	*B*
5	548.78	4		592.86	4	
6	546.55	4		598.66	4	
7	544.60	4*c*	*C*	604.70	5	
8	543.04		*	611.07	5	
9	541.53		*	617.74	5*D*	
10	540.52		*	624.60	4	
				624.76	4	
11	539.68		*	631.82	4	
				632.01	4	
12	539.23		*	639.34	4	
				639.55	4	
13	539.23		*	647.18	4	
				647.37	4	
14	539.23		*	655.29	5	
				655.51	5	
15	539.68		*	663.66	5	
				663.91	5	
16	540.52		*	672.38	5	
				672	5	
17	41.53		*	681.35	5	
				681.62	5	
18	42.53		*	690.59	5	
				690.88	5	
19	544.10	1		709.19	5	
	4.34	1		700.46	5	
20	546.00	1		710.04	4	
	6.26	1		710.31	4	
21	548.15	1		720.17	4	
	8.44	1		720.47	4	
22	550.65	1		730.61	4	
	0.89	1		730.90	4	
23	553.41	2		741.29	4	
	553.68	2		741.60	4	
24	556.48	2		752.32	4	
	556.74	2		752.61	4	
25	559.82	2		763.62	3	
	560.10	2		763.88	3	
26	563.47	2		775.13	3	
	563.73	2		775.43	3	
27	567.41	2		786.96	2	
	567.70	2		787.27	2	
The 0→0 band						
28	571.64	1		798.94	2	
	571.92	1		799.34	2	
29	576.12	1		812.85	2	
	576.40	1		811.63	2	
30	580.78	1		824.46	2	
	581.18	1		824.05	3	
31	587.39	(8)	*B*	837.22	3	
	586.14	1		835.78	2	
32	591.70	0		849.53	2	
	591.22	0*r*		854.15	1	
33	597.14	0		865.33	2	
	595.78	2*dr*	*C*	865.79	2	
34	602.01	1*c*		878.80	2	
			AC	879.19	2	
35	610.44	00		892.81	1*c*	
			B	892.49	1*c*	
36	616.85	0		907.18	1	
	617.21	0		08.45	1	*C*
37	623.35	0		921.90	0*c*	
	623.64	0		22.72	1	
38				936.89	0	
				37.66	0	
39				52.13	0	
				52.82	0	
				67.59	00	
				68.28	1	
The 0→1 band						
0	—	—		23,429.50	1	
1	23,421.79	1		433.83	3*rd*	*A*
2	418.46	2		438.58	3*c*	*C*
3	415.41	3	*A*	443.50	2*c*	
4	412.68	3		448.83	3	
5	410.32	3		454.54	4	
6	408.35	3		460.54	5*b*	
7	406.67	3		466.84	8*b*	
8	405.07		*	473.46	3*b*	
9	404.24		*	480.46	6*D*	*A*
10	403.64		*	487.74	4*D*	
11	403.17		*	495.32	3*c*	
	3.35		*	495.45	3*c*	
12	403.17		*	503.25	4*c*	
	3.35		*	503.47	4*c*	
The 0→1 band						
13	403.35		*	511.54	3	
	3.64		*	511.77	3	
14	404.04		*	520.14	4	*C*
	4.24		*	520.41	4	*C*
15				529.07	3	
				529.31	3	
16	406.15		*	538.38	3	
	6.36		*	538.62	3	
17	407.77	3		547.94	3	
	8.01	3		548.20	3	
18	409.70	3		557.84	3	
	9.93	3	*A*	558.09	3	
19	412.20	2		568.11	3	
	2.40	2		568.36	3	
20	414.61	2		578.67	6	*C*
	4.84	2		578.93	3	
21	417.55	2		589.58	3	
	7.79	2		589.83	3	
22	420.84	2*d*		600.76	3	
	1.08	2*d*	*A*	601.08	3	
23	424.42	2		612.33	3	
	4.69	2		612.61	3	
24	428.34	2		624.13	2	
	8.64	2		624.47	2	
25	432.62	2		636.34	2	*A*
	432.88	2		636.64	2	*B*
26	437.20	2		648.84	2	
	437.48	2		649.13	3	*B*
27	442.13	4	*C*	661.67	3	*B*
	442.38	1		661.95	2	
28	447.27	4	*C*	674.69	2	
	447.65	1		675.05	2	
29	452.90	1	*C*	689.59	2	
	453.18	1		688.33	1	
30	458.65	3		702.36	1	
	458.95	5	*C*	701.90	2*d*	
31	466.34	1		718.21	1	
	465.12	3		714.79	2	
32	471.83	10*b*	*A*	729.66	0	
	471.41	1		734.30	0	
33	478.46	2		746.82	0*b*	
	476.86	4*D*	*C*	747.13	0	
34	484.72	3		761.36	0	
	489.47	3*c*	*A*	761.76	0	
35	494.70	1		776.57	3*D*	
	495.02	2				
36	502.00	2		792.27	2	
	502.36	2				

* Overlapping with other classified lines is indicated by a letter *A*, *B*, *C* in the column to the right of the intensity column.
A means that the overlapping line is a $N^{14}-N^{14}$ line,
B that it is a $N^{14}-N^{15}$ line,
C that it is a $N^{15}-N^{15}$ line.
When the overlapping line is much stronger than the line in question, the intensities are put between parentheses. In such a case very little reliance can be put on the value of the frequency. The congested region of the head is indicated in a band by an asterisk. Intensity estimates are uncertain in this region and also the frequencies are less reliable.

† For the 1→0 band see our previous paper (reference 1).

TABLE II.—*Continued.*

K	P BRANCH ν	I		R BRANCH ν	I	
The 0→1 band—Continued						
37	510.09	1		808.33	1r	
				809.21	2	
38	518.56	0	C	824.70	1	
				825.43	1	
39	527.53	(2b)	C	841.36	0	
	528.30	(6)	A	841.92	3b	
40	536.64	0		858.34	2	B
	537.40	0		858.90	3	B, C
41	546.20	0		875.81	1b	
	546.87	0d		876.42	0	
42	556.15	00				
	556.77	00				
The 0→2 band						
0	—	—		21,322.19	0	
1	21,314.51	0		326.55	2	
2	311.23	1		331.30	2	
3	308.31	2		336.40	3	
4	305.77	3		341.87	4	A
5	303.57	3		347.72	3	
6	301.86	3D		353.92	4	
7	300.37	3b	*	360.51	4b	
8	299.38	3bb	*	367.44	3	
9	298.66	3b	*	374.64	4D	C
10	298.25	3b	*	382.42	3b	
11	298.25	3b	*	390.47	3D	
12	298.66	3b	*	398.75	4c	
				398.93	4c	
13	299.38	3bb	*	407.64	4D	
14	300.64	2	*	416.66	3c	
				417.01	4bc	C
15	301.86	3D	*B	426.15	3	
	302.17	3	*	426.41	3	
16	303.80	3		436.09	3b	C
	304.03	3				
17	305.04	3c		446.23	2	
	306.28	3c		446.50	2	
18	308.66	3c		456.79	2	
	308.90	3c		457.06	2	
19	311.61	3		467.74	2	
	311.86	3		468.00	2	
20	314.94	3		479.02	3	
	315.21	3		479.30	3	
21	318.64	3		490.66	2d	A
	318.91	3		490.96	2d	A
22	322.72	2		502.70	2	A
	322.97	2		503.00	2	
23	327.14	2		515.07	2	
	327.42	2		515.38	2	

K	P BRANCH ν	I		R BRANCH ν	I	
The 0→2 band						
24	331.94	2		527.79	2	
	332.21	2		528.09	2	
25	337.12	2		540.89	1	
	337.40	2		541.21	1	
26	342.64	2				head 1-3
	342 92	2		554.55	3r	C
27	348.53	2		568.12	2	B
	348.83	2		568.41	2	
28	354.79	1		582.06	3b	C
	355.08	1		582.52	2	
29	361.39	1		598.14	0	
	361 67	1		596.92	1	
30	368.25	1		611.93	2	A
	368.64	1		611.50	1	
31	—	—		626.91	1	
	375.85	1		625.50	0	
32	383.74	1		641.57	0	
	383.28	1		646.33	(2b)	B
33	—	—		659.96	0	
	391.60	1		660.28	0	
34				676.08	0	
				676.51	0	
The 1→2 band						
0	—	—		23,354.83	1	
1	23,647.23	0		659.11	2	
2	643.88	1		663.91	3	
3	640.91	2b	C	668.77	4	
4	638.18	3b		673.85	3	
				674.10	3	
5	635.82	3		679.41	6	C
				679.73	6	C
6	633.98	2b		685.33	4	
				685.64	4	
7	632.03	2		691.54	6*	A
	32.29	2		691.88	4	
8	630.53	3	*	698.09	4	
	30.94	2	*	698.44	4	
9	629.58	4	*C	704.94	4	
	.96	3	*	705.33	4	
10	628.82	8c	*	712.15	4	
	629.22	6c	*	712.54	4	A
11	628.58	6c	*	719.60	8	A
	628.82	6c	*	720.08	4	
12	628.36		*	727.48	5	
	628.82		*	727.96	5	
13	628.58		*	735.66	7D	A
	628.82		*	736.10	7	
14	629.22		*	744.14	4	
	629.58		*C	744.61	5	
15	629.96		*	752.88	7	
	630.53		*	53.41	7	

K	P BRANCH ν	I		R BRANCH ν	I	
The 1→2 band						
16	631.25	2	*	762.03	4	
	631.72	4		76.51	5	
17	632.79	2		771.44	5	C
	633.26	2		771.96	5	C
18	634.64	3		781.18	5	
	635.15	3		781.71	5	
19	636.64	6v	B	791.23	5	
	637.34	4		791.79	5	
20	639.32	4		801.62	4	
	639.85	4		802.19	4	
21	642.18	3		812.32	3	
	642.70	6		812.92	3	
22	645.33	4		823.37	2	
	645.86	4		823.94	5	
23	648.84	6	B	834.80	2b	
	649.43	4		835.28	2	
24	652.62	2		846.35	3	
	653.19	4		846.90	4b	C
25	656.72	3		858.34	2	
	657.29	3		858.90	3	C
26	661.18	3	C	870.64	2	C
	661.67	5	BC	871 21	1	
27	665.92	2v	A	883.20	2	
	666.57	2r		883.83	3	
28	671.10	1		896.10	2	
	671.65	2		896.71	1	
29	676.32	4b	AC	909.35	2	
	677.05	1		910.28	3bb	
30	682.20	1		922.90	3	
	682.81	1		3.53	1	
31	688.33	4c	B	24,036.75	1	
	688.89	1		037.35	1	
32	694.67	1		050.92	1	
	5.26	1		051.53	1	
33	701.28	2	C	065.39	1	
	.90	4	B			
34	708.44	2				
	709.16	2D	C			
The 1→3 band						
0	—	—				
1	21,571.35	1b	B	21,583.32	2bc	B
2	568.12	2	B	588.60	1b	B
3	565.30	2		593.05	1b	
4	562.71	2D	*	598.49	0b	B
				598.88	0D	B
5	560.61	2c	*	604.21	1b	B
				604.66	1b	B
6	559.24	2b	*	610.40	1d	
				610.79	1d	
7	557.38	2	*	616.88	1	
	557.78	2b	*	617.28	3	

TABLE II.—*Continued.*

K	P BRANCH ν	I		R BRANCH ν	I		K	P BRANCH ν	I		R BRANCH ν	I		K	P BRANCH ν	I		R BRANCH ν	I	
	The 1→3 band—Continued							*The 1→3 band*							*The 1→3 band*					
8	556.32	2	*	623.70	1		14	557.38	2	*	672.29	2		20	571.35	1*b*	*B*	33.69	1*d*	
	556.70	2	*	624.16	3*D*			557.78	2*b*	*	672.80	2			571.93	1		34.27	2*r*	
9	555.60	4	*	630.88	4		15	558.85	2	*	681.62	2		21	575.02	1				
	555.95	2	*	631.35	1			559.24	2*b*	*	682.15	2			575.53	1				
10	555.01	2	*	638.46	2		16	560.61	2*c*	*	691.36	2		22	578.98	1				
	555.60	4	*	638.92	2			561.06	1*bc*	*	691.85	2			579.52	1				
11	555.01	2	*C	646.33	2*b*		17	562.71	2*c*	*	701.39	2	*C*	23	583.32	2*b*	*B*			
	555.60	4	*	646.86	2			563.29	2*c*	*	701.93	1*d*	*C*		583.86	2*b*				
12	555.60	4	*	654.67	3		18	565.30	2		711.81	2		24	587.95	1*c*				
	555.95	2	*	655.16	3			565.81	1		712.34	2			588.60	1*c*				
13	556.32	2	*	663.32	2		19	568.62	2	*B*	722.57	1								
	556.70	2	*	663.80	2			568.69	2		723.12	1								

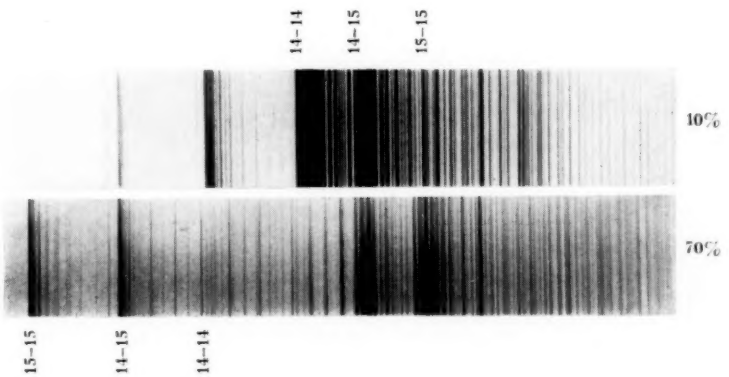

FIG. 2. The 1→0 bands with heads at 3582.4, 3587.3 and 3592.5A. (Marked below.) Above the figure are marked the heads of the 0→1 bands of the second positive group of N_2 with the 14–14 head at 3577A.

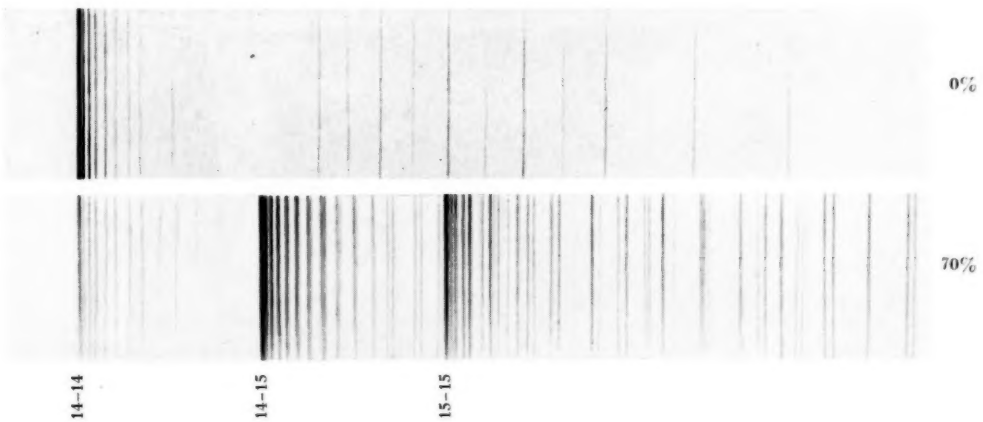

FIG. 3. The 0→1 bands with heads at 4278.2, 4271.7 and 4265.2A.

of different lines is naturally somewhat larger as now there are always three bands where there was only one for ordinary nitrogen. On the plates taken with the 70 percent concentration of N^{15}, however, the lines of the ordinary nitrogen molecule are so weak that they give very little trouble.

§2 Comparison of the Three Molecules

The bands of the three isotopic molecules are exactly analogous in almost all respects. The intensity alternations are different, however, as must be expected of molecules of this kind. Only molecules with two identical atoms should show intensity alternations, but not the mixed molecule $N^{14}-N^{15}$. This is in agreement with the observations, as is clearly shown in Fig. 1 or Fig. 4. The N^{14} nucleus having an even number of heavy particles follows the Bose-Einstein statistics, whereas the N^{15} nucleus with an odd number of heavy particles obeys the Fermi-Dirac statistics. Accordingly the lines which are strong in $N^{14}-N^{14}$ are weak in $N^{15}-N^{15}$ and vice versa, which also comes out in the Figs. 1 and 4.

There is one feature, however, which cannot be predicted for the other isotopes, when known for one molecule, without a more complete knowledge of the detailed structure of the molecule than is available at present. This is the occurrence of perturbations, which is quite different for the three molecules and therefore is of particular interest. We shall leave their discussion, however, for a separate paper.

Table III. *The 1→0 band of* $N^{14}-N^{14}$.*

K	P branch ν	P branch I		R branch ν	R branch I		K	P branch (cont'd.) ν	P branch (cont'd.) I	
0	—	—		27,941.80	4		19	27,908.76	2	*
				946.11	2			910.19	2	*B
1	27,933.75	2		946.49	2		20	909.61	5	*
2	930.32	10*b*	*B*	The rest of the *R*-branch coincides				911.11	5	*
3	926.95	2		with the strong			21	911.49	0	*
	927.16	2		0→1 band of the				912.49	5	*
				2nd positive group.						
4	923.91	3					22	913.09	2	
	924.11	3						914.11	2	
5	921.16	2					23	914.94	1	
	921.29	2						915.79	1	
6	918.62	10*b*					24	917.04	2	
								917.91	2	
7	916.32	4					25	919.48	1	
8	914.29	4						920.26	1	
9	912.41	5*b*					26	922.06	3	
10	910.85	5						922.86	3	
11	909.61	5	*				27	924.96	1	
	909.36	1	*					925.74	1	
12	908.20	2	*				28	928.09	2	
	907.50	10*bb*	*					928.90	2	
13	907.98	3					29	931.51	2	*C*
	906.41	3						932.29	2	
14	907.50	10*bb*	*				30	935.19	2	
	903.42	5						935.91	2	*B*
15	907.50	10*bb*	*				31	938.64	1	
	911.11	5	*					939.12	1	*C*
16	907.50	10*bb*	*				32	942.17	2	
	909.61	5	*					944.02	3	
17	907.50	10*bb*	*							
	909.36	1	*							
18	908.20	2	*							
	909.01	5	*							

* Overlapping with other classified lines is indicated by a letter *A*, *B*, *C* in the column to the right of the intensity column.
A means that the overlapping line is a $N^{14}-N^{14}$ line,
B that it is a $N^{14}-N^{15}$ line,
C that it is a $N^{15}-N^{15}$ line.
When the overlapping line is much stronger than the line in question, the intensities are put between parentheses. In such a case very little reliance can be put on the value of the frequency. The congested region of the head is indicated in a band by an asterisk. Intensity estimates are uncertain in this region and also the frequencies are less reliable.

Table IV. *Comparison of the rotational differences of* $N^{14}-N^{14}$ *and* $N^{15}-N^{15}$.

Final State

K	V″=0 Calc.	V″=0 Obs.	V″=1 Calc.	V″=1 Obs.	V″=2 Calc.	V″=2 Obs.	$N^{14}-N^{14}$ V″=1 Calc.	$N^{14}-N^{14}$ V″=1 Obs.
1	10.75		10.65	10.67	10.54	10.67*	11.40	11.42
2	17.92	17.94	17.74	17.77	17.56	17.65	19.00	19.07
3	25.09	25.13	24.84	24.87	24.58	24.57*	26.60	26.59
4	32.26	32.27	31.94	31.98	31.61	31.69	34.20	34.29
5	39.43	39.40	39.03	39.10	38.63	38.71	41.79	41.88
6	46.60	46.64	46.13	46.22*	45.65	45.69	49.39	49.69
7		53.82	53.22	53.25	52.67	52.67	56.99	57.16
					59.69	59.66		
20	146.80	146.78	145.33	145.33	143.82	144.01	155.57	155.66
21	153.94	153.97	152.39	152.36	150.82	150.96	163.14	163.22
22	161.08	161.06	159.43	159.48	157.81	157.94	170.71	170.76
23	168.22	167.80	166.53	166.73	164.80	164.93	178.27	178.32
24	175.36	175.25	173.59	173.75	171.79	171.96	185.83	185.83

Initial State

K	V′=0		V′=1	
1	11.61	11.62	11.48	11.51*
2	19.35	19.37	19.13	19.36*
3	27.09	27.12	26.79	26.87*
4	34.83	34.83	34.44	
5	42.57	42.61	42.09	42.07*
6	50.31	50.33	49.74	49.93
7	58.05	58.03	57.39	57.48*
17	135.31	135.34	133.78	133.90*
18	143.02	143.01	141.40	
19	150.73	150.61	149.02	149.14
20	158.44	158.39	156.64	156.71
21	166.14		164.25	164.37

* These differences are obtained from blends or other lines of questionable accuracy.

TABLE V. *Constants of the ionized* $N^{15}-N^{15}$ *molecule. (Derived from the analogous* $N^{14}-N^{14}$ *constants.)*

		FINAL STATE	INITIAL STATE
Y_{01}	B_e	1.8014	1.9462
$-Y_{11}$	α	0.0180	0.0219
$(-Y_{02})$	D	$2.5\cdot10^{-6}$	$3.7\cdot10^{-6}$
Y_{10}	ω_e	2132.57	2338.03
$-Y_{20}$	x	15.063	21.648
$-Y_{30}$	$-y$	0.03608	0.4878
$-Y_{40}$	$-z$		0.0431

In all other respects the bands behave exactly as predicted from the elementary theory of isotopic changes in band spectra. We shall not try to demonstrate this in very great detail, as it has been done for other molecules and no new points of interest appear.

Table IV gives a comparison of the rotational levels of $N^{15}-N^{15}$ and $N^{14}-N^{14}$. ($N^{14}-N^{15}$ behaves exactly in an analogous way.)

We compare the observed rotational differences of $N^{15}-N^{15}$ with those calculated from the constants of $N^{14}-N^{14}$. In order to do this, the constants for the negative bands of ordinary nitrogen obtained by Coster and Brons[3] are multiplied by the appropriate isotopic factors. The $N^{15}-N^{15}$ constants obtained in this way are listed in Table V. With the help of the formulae.

$$F(K)=B_VK(K+1)-DK^2(K+1)^2$$
$$B_V=B_e-\alpha(V+\tfrac{1}{2})+\beta(V+\tfrac{1}{2})^2 \quad \text{or}$$
$$B_V=Y_{01}+Y_{11}(V+\tfrac{1}{2})+Y_{21}(V+\tfrac{1}{2})^2,$$

the rotational differences of $N^{15}-N^{15}$ are then calculated. These are listed in the columns "calc." of Table IV, whereas the columns "obs." present the observed differences:

$R(K)-P(K)$ for the initial state
$R(K-1)-P(K+1)$ for the final state.

The differences from approximately $K=7$ to $K=18$ are omitted from the tables as they involve the P lines forming the head, the accuracy of which is so low that for them the comparison would be of no significance. The agreement between the observed and the calculated values is as good as may be expected for rotational differences of this kind. For comparison the analogous differences for the $V''=1$ level of ordinary nitrogen are given. The agreement is in general of the same order of magnitude as that for $N^{15}-N^{15}$. That the higher rotational levels of $N^{15}-N^{15}$ begin to show systematic deviations from the calculated values is not surprising, as any formula of the kind used here is only an approximation formula, supposed to be valid only for small values of K and V. In addition, if the variation of the constant D with the vibrational quantum number (which has been neglected here) were taken into account, the agreement could be considerably improved.

A comparison of the vibrational energies for the three molecules is given in Tables VI and VII. From the origins of the bands presented in Table VI, the vibrational differences for initial and final electronic states are found. They are compared with the values calculated from the expression

$$Y_{10}(V+\tfrac{1}{2})+Y_{20}(V+\tfrac{1}{2})^2+Y_{30}(V+\tfrac{1}{2})^3,$$

employing the values of Table V for the constants. The agreement is quite satisfactory considering the fact that the absolute wave numbers cannot be trusted to better than 0.1 cm^{-1}.[4]

TABLE VI. *Origins of the negative bands.*

ISOTOPE	0→0	0→1	0→2	0→3
14–14	25,566.0	23,391.2	21,249.0	
14–15	25,564.40	23,425.47	21,318.14	
15–15	25,562.70	23,460.32	21,388.50	
	1→0	1→1	1→2	1→3
14–14	27,937.68		23,620.5	21,511.3
14–15	27,897.27		23,650.86	21,575.01
15–15	27,855.88		23,681.56	

TABLE VII. *Vibrational differences.*

	14–14		14–15		15–15	
	OBS.	CALC.	OBS.	CALC.	OBS.	CALC.
1″–0″	2174.8	2174.78	2138.93	2138.88	2102.38	2102.32
2″–1″	2142.2	2142.15	2107.33	2107.33	2071.82	2071.89
3″–2″	2109.2	2109.28	2075.83	2075.56		
1′–0′	2371.6	2371.49	2332.80	2332.56	2293.12	2292.54

[3] D. Coster and H. H. Brons, Zeits. f. Physik **73**, 747 (1932).

[4] The different groups of bands were usually measured from plates of different exposures and therefore the possible shift between the nitrogen and the iron spectrum mentioned in our previous article would enter completely into the vibrational differences.

Finally the values for the electronic transition of the band system are

25 461.48	for $N^{14}-N^{14}$
25 461.59	for $N^{14}-N^{15}$
25 461.64	for $N^{15}-N^{15}$.

The agreement is within the limits of possible errors of measurement, so that there is no appreciable electronic shift.

§3 The Intensity Alternations and the Spin of N^{15} [5]

As is well known, successive rotational levels of diatomic molecules consisting of identical atoms have statistical weights in the ratio $I+1 : I$ if I is the value of the nuclear spin. In the spectrum of such molecules this manifests itself by the relative intensities of successive rotational lines alternating in this ratio. The measurement of these intensity alternations gives therefore an opportunity for determining the nuclear spin.

In the ordinary nitrogen spectrum this was done by Ornstein and van Wijk[6] who found that the intensities alternate in the ratio 2 : 1 and that therefore, the spin of N^{14} is one. For the determination of the spin of N^{15} this ratio may be measured in any of the $N^{15}-N^{15}$ bands. However, no very detailed and accurate intensity measurements are necessary, as the intensity ratio can have only the discrete values 3 : 1, 2 : 1, 5 : 3, 3 : 2 $\cdots$ corresponding to the nuclear spins $I=\frac{1}{2}$, 1, $1\frac{1}{2}$, 2 $\cdots$. The intensity measurements need only be sufficiently accurate to distinguish between these possible values. The situation is most favorable for small spins, as the ratios vary most strongly then, so that even qualitative methods may give the desired result quite unambiguously. We used two independent methods which gave identical results.

The only negative band of $N^{15}-N^{15}$ which is free from overlapping bands of $N^{14}-N^{15}$ and $N^{14}-N^{14}$ is the $1\rightarrow 0$ band with its head at 3591.5A (Fig. 2). This band seems therefore the most suitable one for the identification of the nuclear spin. Only the P branch is not confused with other bands and only the first few lines are sufficiently resolved, as the higher lines are crowded together near the head of the band.

If there are no intensity alternations, successive rotational lines vary gradually in intensity. Their intensities all lie on one smooth curve, the shape of which can be determined, if necessary, but which is immaterial for our purposes. It depends on the temperature of the gas and the conditions of the discharge. With intensity alternations present, the strong lines lie on one curve and the weak lines on another curve. For each value of K the ordinates of both curves are in the ratio $I+1 : I$. If we weaken all the strong lines by a factor $(I+1)/I$, the reduced intensities will lie on the curve for the weak lines.

Therefore if we weaken the strong lines of $N^{15}-N^{15}$ by a factor 3 and find that they fall on the original curve for the weak lines, we know that the spin of N^{15} must be $\frac{1}{2}$. Should weakening of the strong lines by a factor 3 not give the desired result, we can try successively the other factors until the reduced strong lines fall on the curve for the weak lines. The outcome for N^{15} is that the spin is actually $\frac{1}{2}$.

The intensity reduction for this purpose can most conveniently be accomplished by a sector rotating with sufficiently high frequencies as to be free from the intermittency effect. The sector is adjusted in such a way as to reduce the upper half of the line and leave the lower half unweakened, so that the unreduced curve for the weak lines and the reduced curve of the strong lines can be obtained from the same exposure. In this way irregularities in the discharge will not affect the result. It has been stated already that a reduction by a factor 3 brought the strong curve in coincidence with the unreduced weak curve. To make sure that the method had the required sensitivity, we repeated the experiment with reduction factors 2 and 5/3 which proved clearly too small, so that it is proved that the spin of N^{15} is $\frac{1}{2}$.

However, although these experiments were quite conclusive, we thought it advisable to

[5] A preliminary account of these results was given: J. Chem. Phys. **6**, 308 (1938). Unfortunately we were not aware at that time, due to absence of the *Naturwissenschaften* from our library, that H. Krüger (Naturwiss. **26**, 445 (1938)) had reported on experiments to determine the spin of N^{15} and had given $\frac{1}{2}$ as the most probable value. A more complete account of these measurements appeared in the meantime: H. Krüger, Zeits. f. Physik **71**, 467, 19 (1939).

[6] L. S. Ornstein and W. R. van Wijk, Zeits. f. Physik **49**, 315 (1928); see also van Wijk, Zeits. f. Physik **59**, 313 (1930).

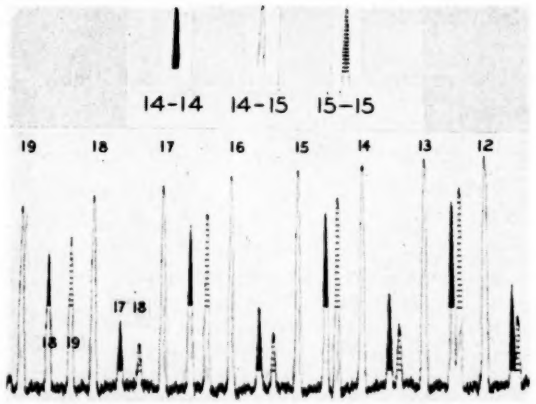

FIG. 4. Microphotometer curve of part of the 0→0 bands taken with a concentration of about 50 percent N^{15}. The lines can be recognized in Fig. 1. Note that the direction towards higher wave numbers is to the left here, whereas it is toward the right in Fig. 1.

determine the intensity ratio also by some other method, preferably in another band. The 1→0 band is rather weak and lies besides in the vicinity of the strong 3577 band of the second positive group. A certain amount of general background blackening could not be avoided. Furthermore, the measurements had to be made with the first few lines of the *P* branch where the intensities of the lines change rapidly as functions of *K*. In order not to lose any resolution it was necessary to employ a rather narrow slit, which is not as advantageous for intensity measurements as a wide one.

Fortunately after the analysis of the bands, the situation proved very favorable in the 0→0 band at 3914. The three isotopic 0→0 bands are practically superposed, but fortunately there is very little actual coincidence of the individual lines except very near the head. In the region of the maximum intensity of the *R* branch the lines are rather evenly spaced and the situation is ideal for a comparison of the intensities. Moreover, the $N^{14}-N^{14}$ lines can be used to calibrate the plates, so that we can dispense with the rotating sector or any other device for the reduction of intensities.

The plates were taken with a mixture of somewhat less than 50 percent N^{15}, so that the strong lines of $N^{14}-N^{14}$ and $N^{15}-N^{15}$ came out with approximately the same intensities. The weak $N^{15}-N^{15}$ lines are then considerably weaker than the corresponding weak $N^{14}-N^{14}$ lines, which shows that the intensity ratio for $N^{15}-N^{15}$ must be larger than 2 : 1. The only possibility is 3 : 1 which corresponds to the spin $\frac{1}{2}$. No measurements of any kind are therefore required for the determination of the spin in this case.

Figure 4 is a microphotometer curve of one of the plates. The strongest lines are the $N^{14}-N^{15}$ lines, which show, of course, no intensity alternations. The tops of the $N^{14}-N^{14}$ lines are filled in solid black whereas the $N^{15}-N^{15}$ are striped. To avoid the possibility of any question about the sensitivity of the method, the N^{15} concentration was chosen in such a way that the strong $N^{15}-N^{15}$ lines are slightly stronger than the neighboring strong $N^{14}-N^{14}$ lines. Nevertheless the weak $N^{15}-N^{15}$ lines are decidedly weaker than the weak $N^{14}-N^{14}$ lines. The illustrated part shows the most favorable section of the band. To the left the perturbations in the $N^{15}-N^{15}$ band may produce intensity irregularities which would make the comparison of the intensities of problematical value. To the right, toward the head, the lines come much closer together and interfere with each other.

We want to express again our sincere appreciation to Professor H. C. Urey for his generosity in supplying us with the needed amount of the heavy ammonium nitrate. Our thanks are also due to Dr. N. Ginsburg for the help he gave us with the photography of the spectrum and the microphotometer curves.

Infra-Red Absorption Studies

X. The Infra-Red Absorption of Hydrogen Fluoride in the Vapor State and in Solution in an Inert Solvent*

A. M. Buswell, R. L. Maycock and W. H. Rodebush
University of Illinois, Urbana, Illinois

(Received February 23, 1940)

The infra-red absorption of hydrogen fluoride has been observed both with the prism and the grating spectrometer. The absorption in the vapor for the single molecules is as previously reported by Imes. At slightly longer wave-lengths a very strong absorption band due to the hydrogen bonding in the associated molecules is observed. In solution in carbon tetrachloride the single molecule spectrum undergoes considerable modification and no association is observed. This fact is rather surprising. The infra-red absorption of a thin crystal of potassium hydrogen fluoride was studied in order to fix the frequency of the hydrogen in the FHF^- ion.

THE infra-red absorption spectrum of hydrogen fluoride was studied by Imes.[1] He obtained the P and R branches for the single molecule with a grating spectrometer with excellent resolution since the hydrogen fluoride molecule has a small moment of inertia. Because of the presence of water vapor he was not able to measure the absorption at wave-lengths greater than 2.6μ. Since nothing was known at that time about the association of hydrogen fluoride vapor, Imes made no attempt to investigate the absorption spectrum at longer wave-lengths.

Since the work of Imes the very strong tendency of hydrogen fluoride to associate through hydrogen bonding has been demonstrated by Simons[2] who found a vapor density which suggests the existence of a cyclical polymer $(HF)_6$. More recently Simons[3] and his collaborators have concluded that the polymers are not of definite size or configuration but form chains of variable length. From previous work[4] it was to be anticipated that the hydrogen bonded polymer would show strong absorption both in the vapor state and in solution at somewhat longer wave-lengths than that found by Imes for the single molecule. A further source of interest is the problem of free rotation in solution and since hydrogen fluoride has the smallest moment of inertia of any of the diatomic molecules that show infra-red absorption it is interesting to see what happens to the rotational structure when hydrogen fluoride is dissolved in a nonpolar solvent such as carbon tetrachloride.

The hydrogen fluoride used in this work was distilled from potassium acid fluoride which had previously been electrolyzed to remove water. In some cases the gas was passed through 90 percent sulfuric acid but in every case the water content was negligible. The carbon tetrachloride solvent was as free from water as any that we have been able to prepare. The absorption cells were provided with fluorite windows. Fluorite is attacked by hydrogen fluoride so that it is necessary to repolish the windows frequently. In some cases a platinum-lined cell was used, in other cases a brass cell coated with ceresin. The infra-red equipment used has been described previously.[1] The grating used was ruled for us by Professor Barker of the University of Michigan.

The potassium hydrogen fluoride used was recrystallized from water solution, the crystals having the form of thin plates. The crystals were dried in a vacuum desiccator and showed on analysis the theoretical amount of hydrogen fluoride. The water content should not be sufficient to affect the absorption appreciably. The absorption was measured directly upon the thin crystals.

* A preliminary note was published, J. Chem. Phys. **7**, 857 (1939).

[1] E. S. Imes, Astrophys. J. **50**, 25 (1919).

[2] J. H. Simons and J. H. Hildebrand, J. Am. Chem. Soc. **46**, 2183 (1924).

[3] S. H. Bauer, J. Y. Beach and J. H. Simons, J. Am. Chem. Soc. **61**, 19 (1939).

[4] A. M. Buswell, W. H. Rodebush *et. al.*, J. Chem. Phys. **3**, 84, 501 (1937); J. Am. Chem. Soc. **60**, 2239, 2444, 2528 (1938); **61**, 2809, 3252 (1939).

Results

As a preliminary experiment the work of Imes was repeated with the grating. Since Imes' results are in a journal not usually found in chemical libraries we have reproduced the absorption curves with a tabulation of the approximate wave-lengths measured by us which are good agreements with the very exact measurements of Imes. In Fig. 2 are shown measurements over a wider range with less resolution made with the prism spectrometer. The left-hand figure presents the absorption log I_0/I for the vapor measured against a cell containing dry air. The absorption due to the single molecule appears as small peaks with maxima at 2.59μ and 2.47μ while the stronger absorption with maxima at 2.85μ and 2.97μ is undoubtedly due to the hydrogen bonded polymers. At the higher concentrations the absorption due to the associated molecules increases very rapidly with increasing concentration while absorption due to the single molecules shows only a small increase as might be expected. The displacement of the bonded absorption is about the same as has been observed for the water molecule (2.67μ to 3.00μ). The doublet in the absorption peak has about the same separation as the maxima of the P and R branches of the single molecule but this is presumably only a coincidence. Since the associated molecules are of unknown size and configuration any analysis of the association bands is impossible.

The right-hand set of curves in Fig. 2 shows the absorption of hydrogen fluoride at different concentrations in carbon tetrachloride at three concentrations. The striking thing here is the small amount of absorption due to associated molecules. The absorption at 2.61μ is precisely similar to that obtained for hydrogen chloride in carbon tetrachloride, Fig. 3. Since the hydrogen chloride is known to be entirely unassociated this absorption is, therefore, characteristic of single molecules. The absolute concentrations of hydrogen fluoride molecules per cubic centimeter is greater than that in the vapor for some cases as shown yet little association is observed. We must conclude that the equilibrium between single molecules and associated molecules is displaced in solution very far toward complete dissociation. This behavior is difficult to explain particularly since no such phenomenon is observed in the case of the alcohols where the amount of association is large except in very dilute solution. Errera[5] has reported greater association in the vapor than in solution at some temperatures for alcohols, but no such abnormality as we find in the case of hydrogen fluoride. Water does not show association in carbon tetrachloride but the solubility of the single molecules is very slight, whereas the solubility of the single molecules of hydrogen fluoride is considerable.

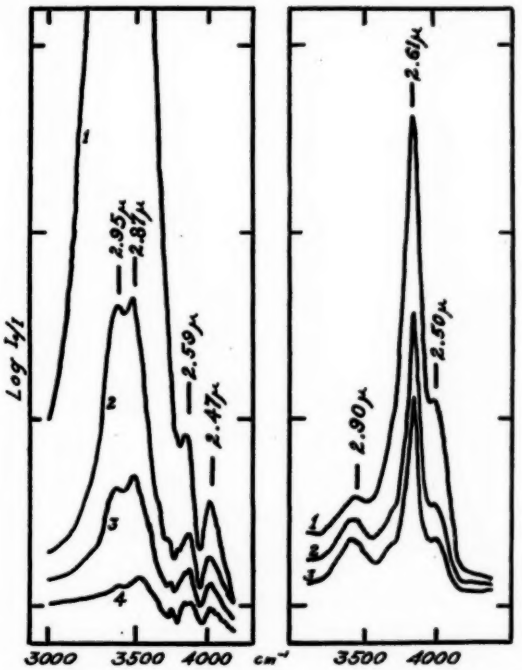

Fig. 2. Left. Hydrogen fluoride vapor (1) 0.1 mole HF per liter, (2) 0.05 mole HF per liter, (3) 0.02 mole HF per liter, (4) 0.01 mole HF per liter. Right. Hydrogen fluoride in carbon tetrachloride (1) 0.016 mole per liter, (2) 0.0092 mole per liter, (3) 0.0045 mole per liter.

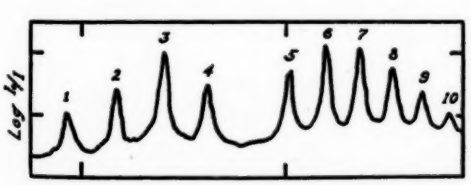

Fig. 1. Hydrogen fluoride vapor under high resolution (1) 2.640μ, (2) 2.608, (3) 2.578, (4) 2.550, (5) 2.498, (6) 2.475, (7) 2.453, (8) 2.433, (9) 2.413, (10) 2.396.

[5] J. Errera, P. Gaspart and H. Sack, J. Chem. Phys. **8**, 63 (1940).

Molecules such as hydrogen fluoride with a coordination number two form chain polymers. Apparently these polymers can vaporize whereas the four-dimensional polymers formed by water must of necessity constitute the liquid phase. Since hydrogen fluoride has the strongest tendency toward hydrogen bonding of any molecule, it is not surprising that it should be so much more strongly associated in the vapor state than any other substances but it is not easy to explain

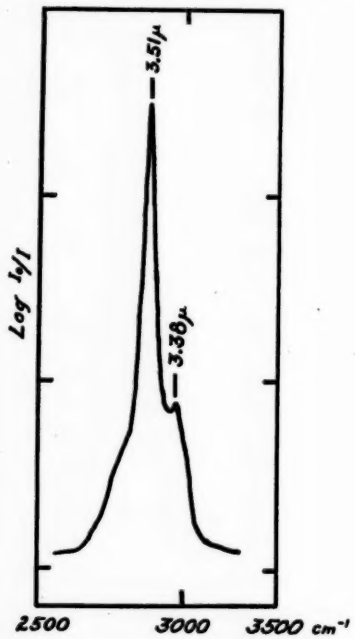

FIG. 3. Hydrogen chloride in carbon tetrachloride 0.13 molar.

why the single molecules should show so much greater solubility in carbon tetrachloride than the polymers. Errera supposed in the case of the alcohols that the increased dissociation in solution was due to the fact that the dielectric constant of the solvent was greater than unity. This explanation may be satisfactory in the case of the alcohols where the moment of a single molecule is perhaps greater than that of a dimer but there is no reason to suppose that this is the case for hydrogen fluoride.

Figure 4 shows the absorption curve for hydrogen fluoride in carbon tetrachloride solution as obtained with the grating spectrometer. Borst, Buswell and Rodebush[6] found that water in solution showed a fine structure resembling a rotational structure which was reproducible and distinct from that of water vapor. It was hoped that because of the small moment of hydrogen fluoride that a well-resolved fine structure could be observed. The results, however, were inconclusive because of the fact that the characteristic absorption of water in carbon tetrachloride overlays this region. Since it is impossible to remove all traces of water from carbon tetrachloride the absorption through the solvent as a blank was balanced against the solution. A difficulty now arose, however, in that the water in the solution is associated with the hydrogen fluoride and its absorption is diminished with the result that the absorption of water vapor cannot be entirely eliminated. Certainly one must grant that any absorption by hydrogen fluoride of a rotational character is very weak since it was impossible to differentiate it from that due to traces of water.

Figure 5 shows the absorption of a thin crystal of potassium hydrogen fluoride. The important unit structure in this crystal is the FHF^- ion. The spectrum obtained was rather more complicated than was anticipated. Some of the absorption might, of course, be due to excess free hydrogen fluoride or water but this seems unlikely since only very small amounts of these substances could be present. The strong narrow absorption at 2.67μ one would naturally attribute to the unsymmetrical linear vibration of the hydrogen in the FHF^- ion. This frequency is very near the frequency of the hydrogen in the hydrogen fluoride molecule and considerably higher than the frequency of the bonded hydro-

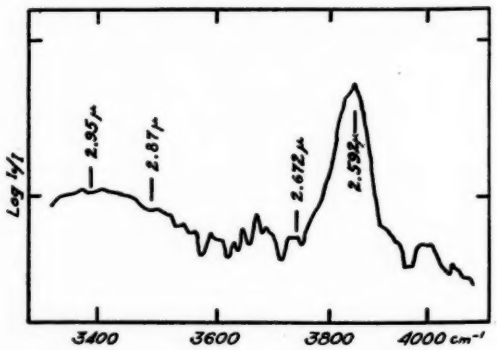

FIG. 4. Hydrogen fluoride in carbon tetrachloride, grating spectrometer.

[6] L. B. Borst, A. M. Buswell and W. H. Rodebush, J. Chem. Phys. **6**, 61 (1937).

gen in the polymerized molecules. The first fact is probably a coincidence but the second is to be anticipated. The other absorption peaks are probably overtones.

The internal structure of the hydrofluoride ion is probably predominantly ionic in character and if this is the case then there is very little room for the proton between the two fluorine ions since x-ray data shows the distance between fluorine atoms to be 2.26A which means a very close approach of the fluorine ions. One would, therefore, assume that the proton was located midway between the fluorine ions forming a symmetrical structure. One the other hand, the H–F distance in hydrogen fluoride is only 0.92A so that if the bond partakes of the covalent

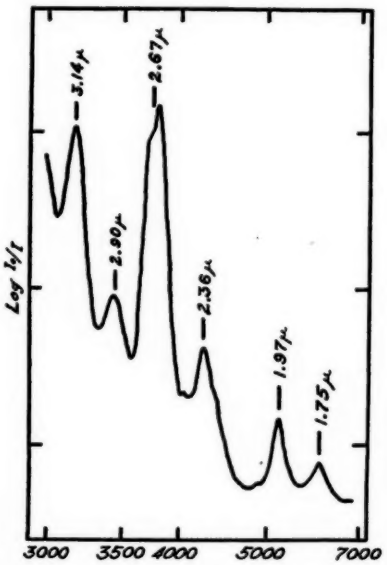

FIG. 5. Potassium hydrogen fluoride; thin crystal.

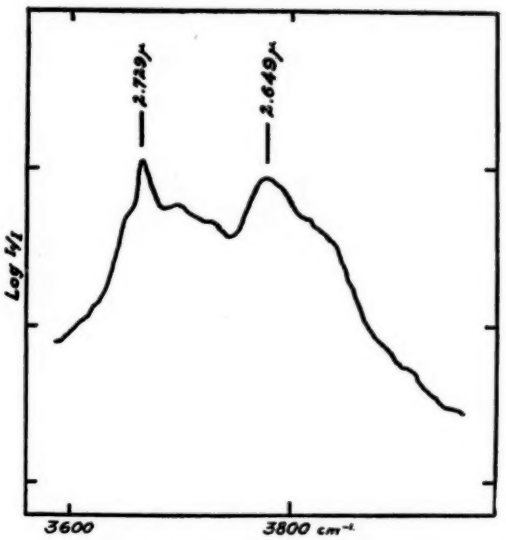

FIG. 6. Potassium hydrogen fluoride; 2.67μ peak on grating spectrometer.

character to a considerable degree two equilibrium positions might exist for the proton with a small potential hill between. In Fig. 6 is shown the absorption of the potassium hydrogen fluoride at 2.67μ as observed with the grating spectrometer. This curve was made primarily to show that the absorption could not be due to isolated water molecules but it is interesting to note that it shows a doublet characteristic which might be due to the existence of a double minimum with a low potential hill between as suggested above. A similar doublet of slightly greater separation is observed for hydrogen fluoride vapor. Here one might be quite sure that a double minimum exists although the proton could only shift from one atom to the other readily in a cyclic molecule.

The Raman Spectra of Phosphorus Methyl and Arsenic Methyl and the Force Constants of the Methyl Compounds of the Fifth Group Elements

E. J. Rosenbaum, Dorothy J. Rubin and C. Roger Sandberg
Department of Chemistry, The University of Chicago, Chicago, Illinois

(Received February 23, 1940)

The Raman spectra of $P(CH_3)_3$ and $As(CH_3)_3$ have been photographed and studied in relation to the spectra of the methyl compounds of nitrogen, antimony and bismuth. The low lying frequencies of all of these molecules can be interpreted in terms of a pyramidal structure with the methyl groups acting as units. The existence of only two low lying lines in the spectra of $Sb(CH_3)_3$ and $Bi(CH_3)_3$ is attributed to an accidental degeneracy resulting from the relatively large mass of the central atom and a particular value of the apex angle. The frequencies computed from a two-constant valence force potential function are in good agreement with those observed. The force constants obtained are tabulated.

FROM the point of view of molecular structure studies, the element methyls offer particular advantages. In many cases the approximation in which the methyl groups are treated as single particles turns out to be a fairly good one. As a consequence, by focusing attention on the Raman lines with frequencies below 1100 cm^{-1} it is possible to reach conclusions about the structure of molecules which contain a relatively large number of atoms. In addition, the behavior of the frequencies above 1100 cm^{-1}, which are ascribed to the inner vibrations of methyl groups, has some interesting aspects. That subject, however, will not be touched on in this paper but will be reserved until more data for other compounds are available.

Experimental

Particular efforts were made to assure the purity of the compounds studied. The methods of preparation and the physical properties of the samples used in this work will be described in a forthcoming publication in the *Journal of the American Chemical Society*.

The Raman spectra reported here were obtained with a Steinheil three-prism glass spectrograph having a dispersion of 6A/mm at 4000A. Photographs were taken on Agfa Super Plenachrome Press film with and without enough $NaNO_2$ solution in the light path to remove the mercury 4047A line as an exciter. Well-exposed unfiltered photographs were obtained in about six hours.

Data

In the following summaries the intensities given are visual estimates on a 0–10 scale. The exciting lines are designated by the Kohlrausch symbols. The letters *b* and *d* represent broad and diffuse, respectively.

$P(CH_3)_3$. 263 (5) ($\pm e, i, k$), 305 (2) ($\pm e, i, k$), 653 (9) ($\pm e, i, k$), 708 (5) (e, k), 948 (1) (e, k), 973 (0) (e, k), 1072 (0*d*) (e), 1293 (1) (e, k), 1312 (0) (e, k), 1421 (3*d*) (e, k), 2809 (2) (e, k), 2868 (2) (e, i, k), 2894 (10*b*) (e, i, k, p, q), 2954 (5*d*) (e, i, k), 2969 (5*d*) (e, i, k, q).

$As(CH_3)_3$. 223 (4) ($\pm e, k$), 239 (2*vd*) ($\pm e, k$), 568 (10) ($\pm e, i, k$), 583 (8) ($\pm e, k$), 884 (1) (e), 996 (0?) (e), 1242 (2*d*) (e, k), 1263 (3) (e, k), 1416 (1*vd*) (e, k), 2810 (2) (e, k), 2906 (10) (e, i, k, p, q), 2980 (5*b*) (e, k, p, q).

Polarization photographs were taken with a Wollaston prism polarizer and calcite wedge depolarizer in an arrangement similar to that of Reitz.[1] Because of the small volume of the samples and the low dispersion used the results were not very satisfactory. It can be seen from the photographs, however, that for $P(CH_3)_3$ the 653-cm^{-1} and the 2894-cm^{-1} lines are highly polarized. For $As(CH_3)_3$, the 2906-cm^{-1} line is highly polarized and either the 568-cm^{-1} line or the 583-cm^{-1} line (probably the former) is polarized.

[1] Reitz, Zeits. f. physik. Chemie **B33**, 368 (1936).

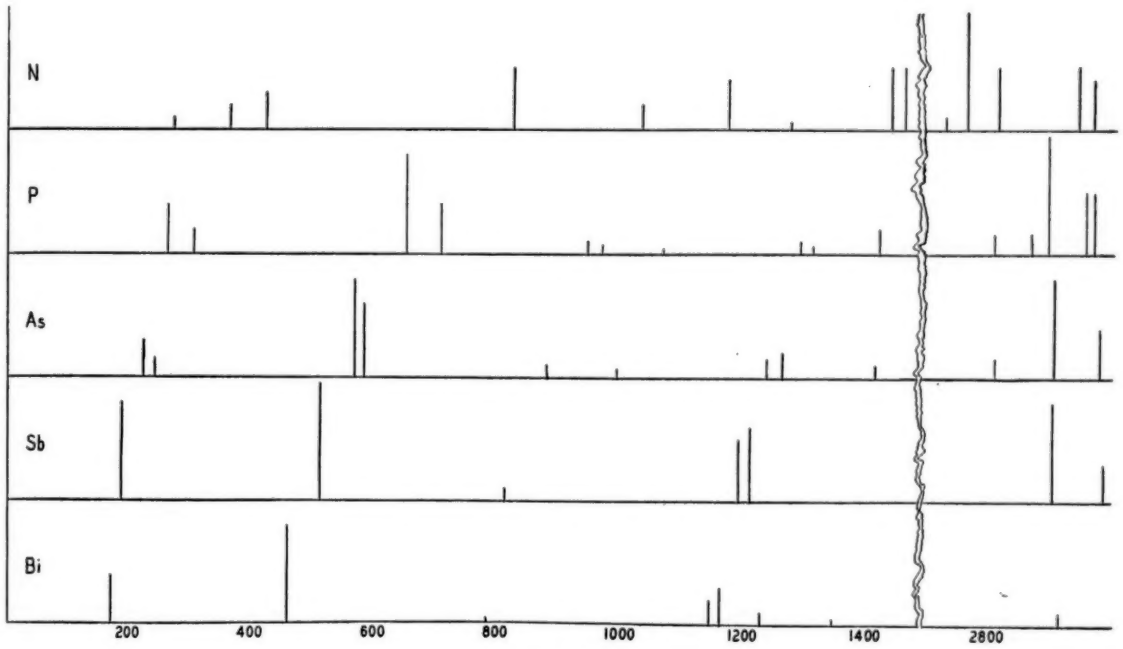

FIG. 1.

DISCUSSION

The Raman spectra of $N(CH_3)_3$,[2] $Sb(CH_3)_3$,[3] and $Bi(CH_3)_3$[4] have previously been reported. Fig. 1 offers a graphical survey of the fifth group methyls. The general similarity of these spectra is apparent.

The structures of three of these compounds, $N(CH_3)_3$,[5] $P(CH_3)_3$,[6] and $As(CH_3)_3$,[6] have been obtained by the method of electron diffraction. This work resulted in the conclusion that these molecules, like the corresponding halides, have the symmetry of a trigonal pyramid, C_{3v}. Such a molecule should have four distinct fundamental frequencies, two single and two doubly-degenerate, and all of them should be active in the Raman effect. It was therefore at first glance surprising that the low frequency region of the spectra of $Sb(CH_3)_3$ and of $Bi(CH_3)_3$ each consists of only two very strong, broad lines. A comparison with the spectra of $As(CH_3)_3$ and $P(CH_3)_3$ has led to a simple interpretation of this observation.

If, in the frequency equations obtained from a two-constant valence force potential function, the mass of the central atom is allowed to become infinite, these equations reduce to (Kohlrausch's notation[7]):

$$n_1^2+n_6^2=\frac{f}{m}+\frac{12d\cos^2\alpha}{m(1+3\cos^2\alpha)},$$

$$n_1^2\cdot n_6^2=\frac{12fd\cos^2\alpha}{m^2(1+3\cos^2\alpha)},$$

$$n_{2,4}^2+n_{3,5}^2=\frac{f}{m}+\frac{3d(1+\cos^2\alpha)}{m(1+3\cos^2\alpha)},$$

$$n_{2,4}^2\cdot n_{3,5}^2=\frac{3fd(1+\cos^2\alpha)}{m^2(1+3\cos^2\alpha)}.$$

The solutions of these equations are:

$$n_1^2=n_{2,4}^2=\frac{f}{m};\quad n_6^2=\frac{12d\cos^2\alpha}{m(1+3\cos^2\alpha)};$$

$$n_{3,5}^2=\frac{3d(1+\cos^2\alpha)}{m(1+3\cos^2\alpha)}.$$

[2] K. W. F. Kohlrausch, Monatsh. f. Chemie **68**, 349 (1936).
[3] E. J. Rosenbaum and T. A. Ashford, J. Chem. Phys. **7**, 554 (1939).
[4] N. G. Pai, Proc. Roy. Soc. **A149**, 29 (1935).
[5] L. O. Brockway and H. O. Jenkins, J. Am. Chem. Soc. **58**, 2036 (1936).
[6] H. D. Springall and L. O. Brockway, J. Am. Chem. Soc. **60**, 996 (1938).
[7] K. W. F. Kohlrausch, *Der Smekal-Raman-Effekt* (1938), p. 70.

TABLE I.

MOLECULE	α	ν_1	ν_6	$f\cdot10^5$	$d\cdot10^4$	$\nu_{2,4}$ CALC.	$\nu_{3,5}$ CALC.	$\nu_{2,4}$ OBS.	$\nu_{3,5}$ OBS.
$N(CH_3)_3$	69°	827	365	3.97	3.82	1078	380	1036	423
$P(CH_3)_3$	62°	653	263	2.78	2.14	710	256	708	305
$As(CH_3)_3$	59°	568	223	2.44	1.82	584	220	583	239
$Sb(CH_3)_3$	58°	513	188	2.09	1.36	517	185	513	188
$Bi(CH_3)_3$	57°	460	171	1.75	1.19	454	170	460	171

TABLE II.

R., R. AND S.	F. AND K.	R., R. AND S.	F. AND K.
223 (4)		1242 (2d)	1242 (m.)
239 (2vd)	239 (m.)	1263 (3)	1262 (st.)
568 (10)	576 (st.)	1416 (1vd)	1418 (st.)
583 (8)	585 (st.)	2810 (2)	2811 (m.)
	786 (m.)		2849 (sch.)
884 (1)	884 (m.)	2906 (10)	2902 (st.)
996 (0?)	988 (m.)	2980 (5b)	
	1036 (sch.)		3021 (s. st.)
	1135 (m.)		3051 (sch.)

This result indicates that two of the fundamentals (ν_1 and $\nu_{2,4}$) should pair off with increasing mass of the central atom. The other two frequencies should also approach each other when α, the angle between an edge of the pyramid and its symmetry axis, approaches 54°44′. For $Bi(CH_3)_3$ this angle is near 57° and for $Sb(CH_3)_3$ it is near 58°. It thus appears that the existence of only two low frequency lines of these molecules is the consequence of an accidental degeneracy leading to the superposition of pairs of lines. This degeneracy occurs without a splitting due to perturbation, because the normal modes of vibration concerned belong to different irreducible representations of the group C_{3v} and hence do not interact with each other.

This interpretation of the spectra is consistent with the outstanding intensity and width of the two lowest Raman lines of $Sb(CH_3)_3$ and with the gradual separation of corresponding lines in the series $As(CH_3)_3$, $P(CH_3)_3$, and $N(CH_3)_3$.

To learn how suitable a simple two-constant valence force potential function might be for these compounds, the corresponding frequency equations were evaluated. Two of the low lying frequencies were used to compute the stretching and bending force constants, and then these values were used to compute the other two frequencies. The angles for the two molecules whose electron diffraction patterns have not yet been studied were estimated from a consideration of the appropriate halides. When the nature of the approximations involved is considered, the results, as given in Table I, are surprisingly good. The regular variation of the two force constants is in accord with expectations.

Addendum. Since this work was completed a note by Feher and Kolb[8] on the Raman spectrum of $As(CH_3)_3$ has appeared. A comparison of the two sets of values is given in Table II.

Although many of these values are in excellent agreement, some of the discrepancies, both in position and intensity, are quite serious. We find it difficult to discuss them because Feher and Kolb give no information whatever about either the preparation and purity of their material or the spectroscopic equipment they used. We are quite certain that there is neither a strong line at 3021 cm^{-1} nor medium strong lines at 786 and 1135 cm^{-1}.

[8] Feher and Kolb, Naturwiss. **27**, 615 (1939).

The Vibration Spectra of Hydrazoic Acid, Methyl Azide, and Methyl Isocyanate

The Thermodynamic Functions of Hydrazoic Acid

EUGENE H. EYSTER,* *Department of Physics, University of Michigan, Ann Arbor, Michigan*

AND

R. H. GILLETTE, *Department of Chemistry, University of Michigan, Ann Arbor, Michigan*

(Received February 5, 1940)

The vibration spectra of hydrazoic acid, methyl azide, and methyl isocyanate have been investigated in the spectral region between 2 and 20μ. Correlation of the spectra of these structurally similar molecules has made possible the determination of all the fundamental frequencies of hydrazoic acid and all but the methyl torsion frequency in the methyl compounds. From these fundamental frequencies and the known rotational constants, the usual thermodynamic functions of hydrazoic acid have been calculated to the harmonic oscillator-rigid rotator approximation. Equilibrium constants for some characteristic reactions have also been obtained.

THE structures of hydrazoic acid[1] and of methyl azide[2] have now been determined by physical methods, and can be readily interpreted in the light of the modern structural theory. The vibration spectrum of the acid has also been investigated by Davies,[3] but he was unable to decide with certainty the magnitude of the two lowest frequencies. Since these two vibrations are confined essentially to the azide group, it was thought that a comparison of the spectra of hydrazoic acid and methyl azide would aid in deciding which of the low frequency bands are fundamentals. Since the structural theory predicts for methyl isocyanate a configuration approximating, though not identical with, that of methyl azide, the investigation of its spectrum was also felt appropriate. This compound is of special interest because Herzberg and Verleger,[4] from studies of the rotational structure of the third N—H harmonic of isocyanic acid, conclude that the structures of the covalent azide and isocyanate groups, at least in the free acids, are radically different.

The present paper describes the spectra of the three above-mentioned compounds, and presents a vibrational analysis which yields all the fundamental frequencies of hydrazoic acid, and all but the methyl torsion oscillations in the methyl compounds. From these results and the rotational constants of hydrazoic acid,[1] it has been possible to calculate the thermodynamic functions of the acid, and to conclude that the azide and isocyanate groups are structurally similar.

EXPERIMENTAL

Hydrazoic acid was prepared by the method of Dennis and Isham[5] from recrystallized sodium azide. The gas was swept from the reaction vessel through a calcium chloride drying tube, and was collected in a liquid-air trap from which a portion of the crude product was redistilled at low temperatures into a glass storage bulb where the substance was stored at reduced pressure until needed.

Methyl azide was prepared by the methylation of sodium azide as described by Dimroth and Wislicenus.[6] The crude sample was dried and redistilled before use.

Methyl isocyanate was prepared from potassium cyanate by the method of Slotta and Lorenz,[7] and was similarly dried and fractionally distilled. In no case were the strong water bands observed in samples of these compounds, nor did their spectra suggest the presence of other impurities.

* National Research Fellow in Chemistry.

[1] Eyster, J. Chem. Phys. **8**, 135 (1940).

[2] Pauling and Brockway, J. Am. Chem. Soc. **59**, 13 (1937).

[3] Davies, Trans. Faraday Soc. **35**, 1184 (1939).

[4] Herzberg and Verleger, Physik. Zeits. **37**, 444 (1937).

[5] Dennis and Isham, J. Am. Chem. Soc. **29**, 216 (1907).

[6] Dimroth and Wislicenus, Ber. **38**, 1573 (1905).

[7] Slotta and Lorenz, Ber. **58**, 1320 (1925).

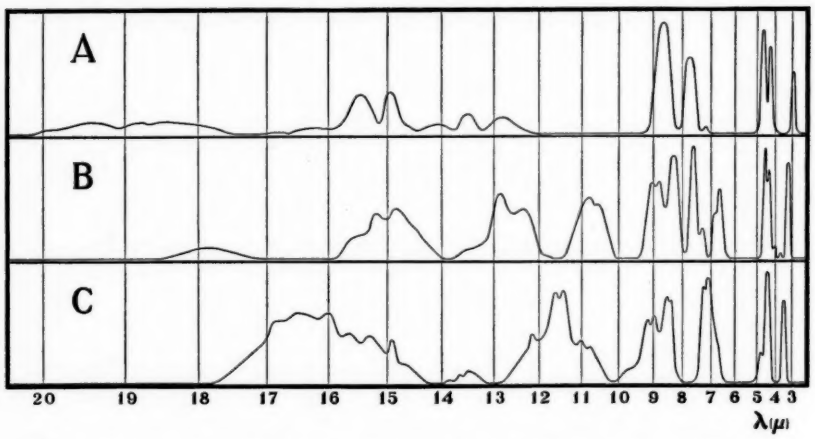

FIG. 1. Percent absorption (0 to 100 percent) as a function of wave-length for: *A*, Hydrazoic acid—13-cm cell—6 cm pressure. *B*, Methyl azide—11-cm cell—6 cm pressure. *C*, Methyl isocyanate—11-cm cell—8 cm pressure.

The absorption spectra of these three compounds have been studied between 2 and 20μ with the potassium bromide prism spectrometer described by Strong and Randall.[8] This instrument is now completely evacuable, and the thermocouple response, amplified by means of a periodic amplifier,[9] is automatically recorded. The gases were enclosed in glass absorption cells provided with potassium bromide windows. Hydrazoic acid was studied at pressures of 4 and 6 cm of Hg in a 13-cm cell, methyl azide at a pressure of 6 cm in an 11-cm cell, and methyl isocyanate at a pressure of 8 cm in an 11-cm cell. The wave-length calibration has been made by Professor Randall by the measurement of a large number of sharp absorption bands and emission lines whose wave-lengths are known from grating work. The prism spectra so determined are shown in Fig. 1, where the percent absorption is given as a function of wave-length. It has been felt best to present the spectra on the nonlinear wave-length scale which comes from the recorder, in order to show clearly the difficulties attending frequency measurements with an instrument of this type. At wave-lengths less than 4μ the dispersion has become regrettably small, and beyond 10μ it is often difficult to choose the center of a band whose envelope is complicated.

As a check on this instrument, three of the hydrazoic acid bands have also been mapped with a grating spectrometer described in essentially its present form by Barker and Meyer.[10] The apparent band centers, as determined by grating and prism instruments, proved to be in satisfactory agreement, especially below 4μ.

The spectra of hydrazoic acid and methyl azide have also been photographed by one of us (E. H. E.) between 7000 and 12,000A, in the spectroscopic laboratory of the Gates and Crellin Laboratories of Chemistry of the California Institute of Technology. The experimental procedure has already been described in connection with the rotational analysis of the two strong hydrazoic acid bands in this region.[1] In addition

TABLE I. *Infra-red bands and Raman frequencies of hydrazoic acid.*

INFRA-RED (GAS)			RAMAN (LIQUID)†	
λ_{VAC} (μ)	ν_{VAC} (CM^{-1})	INTENSITY	ν_{VAC} (CM^{-1})	INTENSITY
19.0	526	medium		
15.200	657.9	med. st.		
13.536	738.8	med. st.		
8.6768*	1152.5	very st.		
7.880	1269.0	strong	1300	weak
7.241	1381	very wk.		
4.6720*	2140.4	strong	2389 (?)	very wk.
4.342	2303	med. st.		
2.9980*	3335.6	med. st.		
1.1361	8802	ext. wk.		
1.047416*	9547.31	weak		
0.9353	10690	ext. wk.		
0.805660*	12412.19	very wk.		

* Grating measurements.
† Engler and Kohlrausch, Zeits. f. physik. Chemie **34B**, 214 (1936).

[8] Strong and Randall, Rev. Sci. Inst. **2**, 585 (1931).
[9] Firestone, Rev. Sci. Inst. **3**, 163 (1932).
[10] Barker and Meyer, Trans. Faraday Soc. **25**, 912 (1929).

to these strong bands, two weaker bands of hydrazoic acid and nine bands of methyl azide were photographed with the prism spectrograph.

The positions of the bands determined by these three methods are listed in Tables I–III. Whenever a band has been measured both with prism and grating instruments, the grating wavelengths are given, but it should be remembered that in only two cases—the 0.8057 and 1.0478μ bands of hydrazoic acid—have the band centers been located unambiguously by rotational analyses. These tables also give the Raman shifts observed in the liquid phase.

Vibrational Analysis

It now seems adequately demonstrated that both hydrazoic acid and methyl azide molecules contain linear asymmetric azide groups of essentially the same dimensions,[1,2] the hydrogen atom or methyl group being situated off the axis of the linear group. Although the interpretations of indirect physical evidence pertaining to the structure of the covalent isocyanate group are at present discordant,[4,11] the same structural theory which has been so well verified in the azides also predicts a linear structure for the covalent isocyanate group, and places the methyl group off the axis in the methyl derivative. If such be actually the case, the vibration spectra of these three compounds should reflect in their similarity the structural similarity of the molecules, allowance having been made, of course, for the difference between a hydrogen atom and a methyl group. Since these molecules probably all belong at best to the point group C_s, the usual process of making a vibrational analysis by comparing the Raman and infra-red spectra in the light of the symmetry selection rules is of little value here. Hence it was felt that to establish a definitive vibrational analysis the spectra of hydrazoic acid, methyl azide, and methyl isocyanate should be correlated in that order, and that these, then, should be correlated with the spectrum of a fourth suitable molecule of known structure whose spectrum has been analyzed. For this comparison molecule we have chosen methyl isocyanide.[12] It has therefore been our aim to discover series of bands in the spectra of these four molecules which might be associated with similar classical vibrations. The series of fundamental bands finally chosen are shown schematically in Fig. 2 and are tabulated in Table IV.

Table II. *Infra-red bands and Raman frequencies of methyl azide.*

Infra-red (gas)			Raman (liquid)*	
λ_{VAC} (μ)	ν_{VAC} (cm^{-1})	Intensity	ν_{VAC} (cm^{-1})	Intensity
			259	164
18.2	550	very wk.		
15.280	654	strong	668	35
12.660	790	strong		
10.910	914	strong	898	99
			1043	5
8.942	1118	med. st.	1116	8
8.375	1194	strong	1174	4
7.720	1295	very st.	1276	42
7.400	1351	weak	1324	6
6.972	1434	med. st.	1424	12
6.746	1482	med. st.	1461	16
4.666	2143	very st.	2104	28
4.484	2230	med. st.		
4.128	2420	very wk.		
3.786	2641	very wk.		
3.3	(3000)	strong	2939	54
1.1950	8369	extr. wk.		
1.1824	8457			
1.1620	8606			
1.1453	8731			
1.1341	8818			
0.9480	10,550			
0.9367	10,676			
0.9102	10,987			
0.8938	11,118			

* Kahovec, Kohlrausch, Reitz and Wagner, Zeits. f. phsyik. Chemie **39B**, 431 (1938).

Table III. *Infra-red bands and Raman frequencies of methyl isocyanate.*

Infra-red (gas)			Raman (liquid)*	
λ_{VAC} (μ)	ν_{VAC} (cm^{-1})	Intensity	ν_{VAC} (cm^{-1})	Intensity
			353	1b
16.480	607	strong		
15.356	651	med. st.		
13.466	743	very wk.		
11.492	870	strong	852	6
9.030	1107	med. st.		
8.471	1181	strong		
7.264	1377	med. st.		
7.084	1412	strong	1410	5
shelf	—	medium	1453	3b
4.840	2066	weak		
4.480	2232	strong		
3.4	(2900)	med. st.	2951	5
			2994	0

* Kopper and Pongratz, Monatshefte **62**, 78 (1933); see also Goubeau, Ber. **68**, 912 (1935) for data on the Raman spectrum of methyl isocyanate in solution.

[11] Goubeau, Ber. **68**, 912 (1935).
[12] Badger and Bauer, J. Am. Chem. Soc. **59**, 303 (1937).

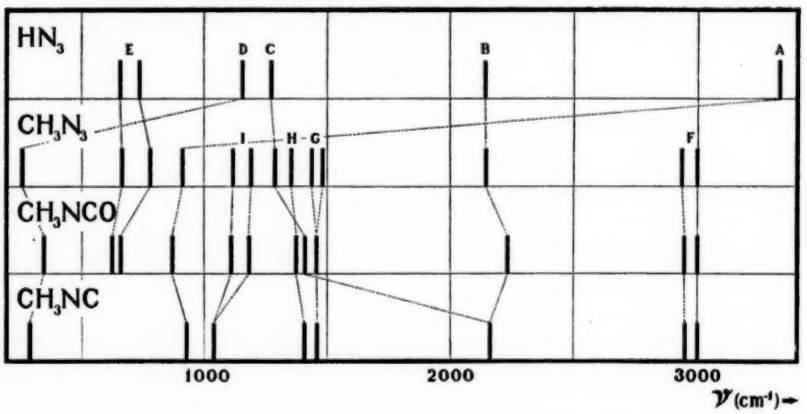

FIG. 2. The series of fundamental frequencies in the spectra of hydrazoic acid, methyl azide, methyl isocyanate, and methyl isocyanide. No attempt has been made to express the intensities.

Fundamental frequencies

The bands of series *A* correspond to the stretching of the N−H or N−CH_3 bond, and are strong in the infra-red. This series is also strong in the Raman spectra of the methyl compounds, but is not observed in the Raman spectrum of hydrazoic acid, possibly because of association in the liquid which involves the hydrogen atom.

The bands of series *B* and *C* correspond to stretching frequencies localized in the linear triatomic groups, degenerating in the isocyanide to a single N−C stretching frequency. The asymmetric frequencies of series *B* are all strong in the infra-red, and can be clearly differentiated from weaker combination and harmonic bands in the vicinity. Though this frequency is of medium intensity in the Raman spectrum of methyl azide, it does not appear in the isocyanate, a fact which we shall later consider. The series *C* lines are very strong in the Raman spectrum, and thus can be separated without confusion from the series *H* and *G* lines which are very much weaker.

Series *D* corresponds to the bending of the N−H or N−CH_3 bond against the linear group. The strong 1152.5 cm^{-1} band in the infra-red spectrum of hydrazoic acid is identified with this series by the fact that its second harmonic at 2303 cm^{-1} has been shown to vanish when the hydrogen is substituted with deuterium.[13] This series is determined by the Raman spectrum alone, in the case of the methyl compounds, as the frequencies are too low for the potassium bromide instrument.

Series *E* includes the bands arising from the deformation of the linear triatomic group; the twofold degeneracy of such a frequency seems to have been raised by the presence of the off-axis group, and two bands are found in the azides. In hydrazoic acid the band envelopes are well shown, and it appears quite certain that the doublet band with center at 657.9 cm^{-1} and doublet separation of 22.4 cm^{-1} is to be interpreted as the parallel component of the *A'* hybrid band. The wider band with the three apparent maxima appears to be the poorly resolved pure perpendicular *A''* band, whose very sharp ${}^{P}Q$ and ${}^{R}Q$ branches have been washed out by the wide slits, for the separation of the three maxima is in agreement with the envelopes of the ${}^{P}P$, ${}^{R}P$, ${}^{P}R$, and ${}^{R}R$ branches, as calculated from the known rotational constants of the molecule. The corresponding bands in methyl azide are strong and well separated in the infra-red. In methyl isocyanate these two bands have fused to one very wide band, the centers of whose components can only be estimated.

The bands of series *F* through *H* correspond to the well-known internal vibrations of the methyl group, and only series *G* needs any comment. This series corresponds to the doubly degenerate bending frequency of the free methyl group, and its degeneracy seems to be raised in methyl

[13] Buswell, McMillan, Rodebush and Wall, J. Am. Chem. Soc. **61**, 2809 (1939). These workers did not study the fundamental itself, but the evidence is clear from the effect on the harmonic.

azide. The series *G* bands in methyl isocyanate appear only as a shelf on the short wave-length side of the strong series *C* band, but the Raman line at 1453 cm^{-1} is said to be broad, perhaps indicating a slight raising of the degeneracy here also.

The series *I* bands, almost identical in appearance in both the azide and isocyanate, correspond to the rocking frequencies of the methyl group. The degeneracy of the frequency in methyl isocyanide is raised in the bent molecules to give two bands at somewhat higher frequencies. A final series, *J*, should occur in the bent methyl compounds, but has not been observed. It corresponds to the torsion oscillation of the methyl group.

Combination, harmonic, and difference bands

When the fundamental frequencies of a molecule have been correctly assigned, it should be possible to explain all other observed bands as difference transitions or transitions to harmonic and combination states. Actually, with the very high frequencies in the photographic region, it is often very difficult to do this uniquely, and even with the lower frequencies unique assignments are not easy to make when there are many fundamentals and low symmetry. Table V summarizes a suggested interpretation of the remainder of the observed spectra of these molecules in terms of the fundamentals of Table IV. Though the methyl torsion frequency is not known for the methyl compounds, it is, unfortunately, rarely involved in strong combination or harmonic bands. Though these assignments do not pretend to be unequivocal, it is interesting to note that no band or Raman line exists which cannot be correlated with the fundamentals of Table IV, with the single exception of the line at 2389 cm^{-1} in the Raman spectrum of liquid hydrazoic acid. However this line was found on but one plate, and it is stated that the exciting radiation appeared to produce so strong a photochemical reaction that crystals, presumably of some polymer, formed on the walls of the Raman tube toward the end of the exposure. Under such circumstances it is possible that this is not a hydrazoic acid line at all.

Structural Conclusions

Since it is already known that the structures of methyl azide and hydrazoic acid are similar, the close correspondence of their vibration spectra,

TABLE IV. *Series of fundamental frequencies in hydrazoic acid, methyl azide, methyl isocyanate, and methyl isocyanide.*

	HN_3		CH_3N_3		CH_3NCO		CH_3NC*	
Series	ν_{VAC} (cm^{-1})	I.R.	ν_{VAC} (cm^{-1})	I.R.	ν_{VAC} (cm^{-1})	I.R.	ν_{VAC} (cm^{-1})	I.R.
A	3335.6	*A'*	914	*A'*	870	*A'*	928	A_1
B	2140.4	*A'*	2143	*A'*	2232	*A'*	2161	A_1
C	1269.0	*A'*	1295	*A'*	1412	*A'*		
D	1152.5	*A'*	259	*A'*	353	*A'*	290	*E*
E	738.8 657.9	*A''* *A'*	790 654	*A''* *A'*	652 607	*A''* *A'*		
F			(3000) 2931	*A', A''* *A'*	2994 2951	*A', A''* *A'*	3003 2951	*E* A_1
G			1482 1434	*A'* *A''*	1453	*A', A''*	1456	*E*
H			1351	*A'*	1377	*A'*	1414	A_1
I			1194 1118	*A''* *A'*	1181 1107	*A''* *A'*	1041	*E*
J			—	*A''*	—	*A''*		

* Data from reference 12.

TABLE V. *Harmonic, combination, and difference bands of hydrazoic acid, methyl azide, and methyl isocyanate.*

COMPOUND	OBSERVED FREQUENCY	OBSERVED IN:	SUGGESTED ASSIGNMENT
HN_3	1381	Infra-red	(657.9+738.8) =1396.7
	2303	Infra-red	(2×1152.5) =2305.0
	8802	Infra-red	(2×3335.6+2×1152.5) =8827.3*
	9547.31	Infra-red	(3×3335.6)†
	10690	Infra-red	(3×3335.6+1152.5) = 10699.8*
	12412.19	Infra-red	(4×3335.6)†
	526	Infra-red	(1269.0−738.8) =530.2 (1152.5−657.9) =494.6
CH_3N_3	550	Infra-red	(2×259) =518
	1043	Raman	(1295−259) =1036
	2230	Infra-red	(2×1118) =2236
	2420	Infra-red	(1118+1295) =2413
	2641	Infra-red	(1351+1295) =2646
	8369	Infra-red	A complex of bands involving
	8457	Infra-red	3×*F* fundamentals and also such
	8606	Infra-red	series combinations as 2×*F*+2×*G*
	8731	Infra-red	etc. More specific assignments are
	8818	Infra-red	impossible.
	10550	Infra-red	
	10676	Infra-red	3×*F*+*B*
	10987	Infra-red	
	11118	Infra-red	4×*F*
CH_3NCO	743	Infra-red	(1107−353) =754
	2066	Infra-red	(1377+652) =2029
			(1453+606) =2059

* The anharmonicity in the 3335.6 frequency has been taken into account in evaluating the expressions in parentheses.
† These frequencies have already been discussed; see reference 1.

though gratifying, is only useful insofar as it makes possible the choice of low frequency fundamentals. It is, however, of more interest to note the close correspondence between the spectra of methyl azide and methyl isocyanate. From this similarity it seems safe to conclude that the N−C−O group, like the N−N−N group, is linear, and that the methyl group is attached off the axis. The increase in the *B* and *C* series frequencies on going from the azide to the isocyanate indicates a strengthening of the binding, and the absence of the series *B* band in the Raman spectrum of the isocyanate bespeaks a sort of pseudo-symmetry which might be achieved if the C−O bond were somewhat stronger than the N−C bond. It is probable that the ground state of a molecule *R*NCO is attained by resonance among the three electronic structures:

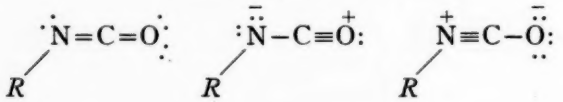

I II III

Each of these three structures, if realized alone, would lead to a linear N−C−O group; structure III alone would place the *R* group on the axis. Although it is difficult to predict how much each of these structures will contribute to the ground state, one might guess, in the absence of any other information, that they contribute equally since each contains the same number of covalent bonds. Upon this assumption, one may easily calculate the distances in the isocyanate group by Pauling's method.[14] This leads to the result: N−C=1.20A; C−O=1.16A. Thus one could predict (from Badger's rule, for example) that the C−O force constant will be greater than the N−C force constant; this difference in the force constants would tend to counteract the mass asymmetry and thus would produce the dynamical pseudo-symmetry mentioned above. Furthermore, the existence of three resonating structures in the isocyanate group as compared to two in the azide group would lead to increased binding energy in the isocyanate and hence to the observed increase in the series *B* and *C* frequencies. An electron diffraction study of methyl isocyanate is projected for the near future, and it is hoped that the results will lead to a more complete understanding of the structure of this molecule.

THERMODYNAMIC FUNCTIONS OF HYDRAZOIC ACID

The fundamental frequencies of hydrazoic acid, together with the known moments of inertia in the ground state,[1] provide sufficient data for the calculation of thermodynamic quantities in the rigid rotator-harmonic oscillator approximation. These are perhaps of special interest for this compound since its explosive nature renders calorimetric determinations difficult. The entropy, *S*, the free energy, *F*, and the heat capacity at constant pressure, C_p, have been calculated by methods adequately described in the literature. The fundamental frequencies are those of Table IV, while the moments of inertia were taken as $I_A^0=70.75$, $I_B^0=69.38$, and $I_C^0=1.3759$ (in units of 10^{-40} g cm²). Recent investigations have made it clear that the previously accepted values of the fundamental constants *e* (the electronic charge) and *h* (Planck's constant), and hence those constants derived from them, are in error. The magnitudes of the indicated changes are such as to introduce a

[14] Pauling, *The Nature of the Chemical Bond* (Cornell University Press, 1939), p. 180.

significant error into the values of thermodynamic functions derived from spectral data. We choose to employ the values: $h=6.6260\times10^{-27}$ erg sec., $e=4.8029\times10^{-10}$ abs. e.s.u., and the derived constants $N=6.0228\times10^{23}$, $k=1.3804\times10^{-16}$ erg deg.$^{-1}$, and $hc/k=1.4391$ cm deg.[15] Detailed calculations show that the rotational and translational entropy is decreased by about 0.07 unit by the introduction of these values, while the rotational and translational contribution to $-(F^0-H_0^0)/T$ is increased by about 0.06 unit. The change in the vibrational contributions is small in hydrazoic acid because there are no very low frequencies.

The results of the calculations are given in Table VI, where the usual conventions regarding symbols have been observed, except that E_0^0 has been replaced by H_0^0 in accord with more recent notation.[16] It was thought useless to carry the results above 600°K, since it is hard to see how HN_3 could be important in any equilibria above that temperature.

The main sources of uncertainty in the results of Table VI are (1) neglect of anharmonic terms in the vibrational energy, (2) use of the approximate rotational partition function $Q_R=\pi^{\frac{1}{2}}(8\pi^2kT)^{\frac{3}{2}}(I_AI_BI_C)^{\frac{1}{2}}/\sigma h^3$, and (3) neglect of rotational distortion terms in the rotational energy. The first of these will be negligible in the temperature region concerned, since the anharmonic hydrogen frequencies make very small contributions. The second approximation will become good at temperatures around 300°K, as shown by Gordon,[17] but may cause the low temperature results to be inaccurate. The most serious source of uncertainty is probably the third; these rotational distortion terms will cause the rotational levels to be drawn together, and hence our partition functions will be slightly small. It should be noted, however, that it has been necessary in this case neither to guess the moments of inertia nor to resort to the Raman spectrum of the liquid for any of the low frequency vibrations which contribute most to the vibrational partition functions.

Murphy has given analytic expressions for the various thermodynamic functions.[18] Although these have been extended by Linnett and Avery,[19] it was thought unnecessary to use the more complicated expression in this case since the vibrational contributions are relatively small. Hence an expression of the simpler form was fitted to the vibrational contributions to $-(F^0-H_0^0)/T$ of Table VI by the method of averages. This was then combined with the expression for the rotational and translational contributions to give the complete function. In principle, the entropy and other thermodynamic functions could be obtained from this equation by differentiation, but in practice the errors multiply so rapidly that the heat capacities so obtained are practi-

[15] These are either the base constants chosen by DuMond, or values derived with their aid, and we impute to them no more absolute significance than would he; they have been chosen for convenience, and because they are in essential agreement with "best values" chosen by others. See: DuMond, Phys. Rev. **56**, 153 (1939); Wensel, Nat. Bur. Stand. J. Research **22**, 375 (1939); and Skiba, Sci. Papers of the I. P. C. R., Tokyo, **34**, 1308 (1939).

[16] Giauque and Kemp, J. Chem. Phys. **6**, 40 (1938).

[17] Gordon, J. Chem. Phys. **2**, 65 (1934).

[18] Murphy, J. Chem. Phys. **5**, 637 (1937).

[19] Linnett and Avery, J. Chem. Phys. **6**, 686 (1938).

TABLE VI. *Thermodynamic functions of hydrazoic acid.*

T(°K)	$-\left(\frac{F^0-H_0^0}{T}\right)_{TR,ROT}$	$-\left(\frac{F^0-H_0^0}{T}\right)_{VIB}$	$-\left(\frac{F^0-H_0^0}{T}\right)_{TOTAL}$	$S_{TR}+S_{ROT}$	S_{VIB}	S_{TOTAL}	$C_{p\ VIB}$	$C_{p\ TOTAL}$
100	39.402	0.000	39.402	47.348	0.000	47.348	0.014	7.960
150	42.623	0.004	42.627	50.569	0.039	50.608	0.226	8.172
200	44.909	0.026	44.935	52.855	0.163	53.018	0.723	8.669
250	46.682	0.070	46.752	54.628	0.401	55.029	1.384	9.330
298.1	48.038	0.155	48.238	56.028	0.707	56.735	2.079	10.025
300	48.131	0.158	48.289	56.077	0.720	56.797	2.100	10.046
350	49.356	0.258	49.614	57.302	1.089	58.381	2.793	10.739
400	50.417	0.382	50.799	58.363	1.504	59.867	3.451	11.397
450	51.353	0.532	51.885	59.298	1.943	61.241	4.061	12.007
500	52.190	0.672	52.862	60.136	2.410	62.546	4.606	12.552
550	52.947	0.877	53.824	60.893	2.873	63.766	5.103	13.049
600	53.639	1.062	54.701	61.584	3.331	64.915	5.558	13.504

TABLE VII. *The standard free energy and equilibrium constants for the reaction* $\frac{1}{2}H_2+\frac{3}{2}N_2=HN_3$.

T(°K)	$\Delta(F^0-H_0^0)$	ΔF^0	K_p
298.1	6 627	78 525	2.655×10^{-58}
300	6 680	78 577	5.451×10^{-58}
400	9 494	81 392	3.258×10^{-45}
500	12 383	84 281	1.403×10^{-37}
600	15 280	87 178	1.713×10^{-32}

cally useless. The final equations are:

$$-(F^0-H_0^0)/T=250.933/T+23.444\log T-0.006917T+6.891\times10^{-6}T^2-9.1682$$

$$S^0=23.444\log T-0.0138T+2.097\times10^{-7}T^2+1.0135.$$

The maximum deviations of these expressions from the calculated points are 0.02 and 0.04, respectively. In order to obtain a reasonably accurate temperature function for C_p, a quadratic function was fitted to the data of Table VI by the method of least squares; the result is:

$$C_p=5.147+0.01896T-8.348\times10^{-6}T^2.$$

The maximum deviation from the tabular values is 0.04 cal./deg. above 250°K.

The thermodynamic functions calculated above may be combined with those of nitrogen[20] and hydrogen[21] to give the standard free energy of formation of HN_3. It is necessary, however, to evaluate ΔH_0^0, for which purpose accurate thermal data are very scarce. Meyer[22] has measured calorimetrically the heat of the reaction:

$$HN_3=\tfrac{1}{2}H_2+\tfrac{3}{2}N_2.$$

He gives $\Delta E=70900\pm500$ cal. at "room temperature." This value, when combined with the heat of solution, is in poor agreement with a value given by Berthelot[23] for the heat of formation of the aqueous solution. This latter value, however, is based on the heat of combustion of solid ammonium azide and hence may be open to question. If one assumes Meyer's value to apply at 298°K, one may calculate, from the well-known relation:

$$\Delta H_0^0=\Delta E^0+\Delta nRT-\Delta(F^0-H_0^0)-T\Delta S^0,$$

the value $\Delta H_0^0=71{,}898$ cal. for the formation of HN_3 from the gaseous elements. The values of ΔF^0 and K_p for this reaction given in Table VII have been obtained with the use of this value. Because of the uncertainty in ΔH_0^0 it was thought meaningless to correct the values of the thermodynamic functions of nitrogen and hydrogen for the change in fundamental constants.

The reaction $\frac{1}{3}NH_3+4/3N_2=HN_3$ is also of interest. ΔF^0 and K_p for this reaction may be obtained by combining the above data with those of Stephenson and McMahon[24] for ammonia. ΔH_0^0 may be calculated from the following reactions:

$\frac{1}{2}H_2+\frac{3}{2}N_2=HN_3$	$\Delta H_0^0=71{,}898$ cal.
$\frac{1}{3}NH_3=\frac{1}{6}N_2+\frac{1}{2}H_2$	$\Delta H_0^0=\ 3058$ cal.
$\frac{1}{3}NH_3+4/3N_2=HN_3$	$\Delta H_0^0=74{,}983$ cal.

The values of ΔF^0 and K_p for this reaction are given in Table VIII.

Since the errors in the partition functions for all substances involved in the reactions just discussed are known to be relatively small, by far the largest uncertainty in ΔF^0 and K_p is introduced by the uncertainty in the thermal data. For this reason the values of $\Delta(F^0-H_0^0)$ are included in Tables VII and VIII so that a more precise value of ΔH_0^0 could be easily included when it becomes available. It is interesting to note from the tables that at temperatures below about 450°K, the equilibrium favors decomposition into nitrogen and hydrogen, while above this temperature decomposition into nitrogen and ammonia might be expected to predominate. Meyer[22] has shown

TABLE VIII. *The standard free energy and equilibrium constants for the reaction* $\frac{1}{3}NH_3+4/3N_2=HN_3$.

T(°K)	$\Delta(F^0-H_0^0)$	ΔF^0	K_p
298.1	4 830	79 813	3.018×10^{-59}
300	4 868	79 851	6.414×10^{-59}
400	6 866	81 849	1.834×10^{-45}
500	8 899	83 882	2.097×10^{-37}
600	10 909	85 892	5.038×10^{-32}

[20] Giauque and Clayton, J. Am. Chem. Soc. **55**, 4875 (1933).
[21] Giauque, J. Am. Chem. Soc. **52**, 4816 (1930).
[22] Gunther, Meyer and Muller-Skold, Zeits. f. physik. Chemie **A175**, 154 (1935).
[23] Berthelot, *Thermochemie* (Paris, 1897), Vol. 2, p. 72.
[24] Stephenson and McMahon, J. Am. Chem. Soc. **61**, 437 (1939).

that in the vicinity of room temperature hydrazoic acid does in fact decompose quantitatively into nitrogen and hydrogen, although it is probable that equilibrium was not completely established.

The authors are very grateful to Professors H. M. Randall and E. F. Barker, of the Physics Department of the University of Michigan, for the use of the excellent spectroscopic equipment which made these results possible. One of us (E. H. E.) wishes to express his appreciation to Professor Richard M. Badger of the California Institute of Technology, in whose laboratory the photographic investigations were made, and is pleased to acknowledge his special indebtedness to the National Research Council.

MAY, 1940 JOURNAL OF CHEMICAL PHYSICS VOLUME 8

Electronic Absorption Spectra in Solution: with Special Reference to the Continuous Absorption of the Halogens

N. S. BAYLISS AND A. L. G. REES*
Department of Chemistry, University of Western Australia, Crawley, Western Australia

(Received February 23, 1940)

The cage theory of liquids has been applied to find the form of potential function that must be added to the $U(r)$ curves of gaseous molecules to give the $U(r)$ curves of dissolved molecules. It is possible to explain the slight displacement of the absorption maximum in halogens dissolved in nonassociated solvents, and also the change in the symmetry of the absorption curve. The large displacement of the maximum in associated solvents is due to a slight compression of the solute molecule by the quasi-crystalline structure of such solvents. The relaxation time of the solvent cage is such that band absorption should persist in solution when normal and excited states are of the same size; but that it should disappear when $r_e' > r_e''$.

THE chief experimental differences between electronic absorption spectra in the gaseous state and in solution[1] are as follows: (a) The total absorption intensity is altered, usually increased, in solution. (b) The absorption maximum is displaced to higher frequencies in solution. The displacement is small or zero in normal, nonassociated solvents; but it is considerable, of the order of magnitude 1000–2000 cm^{-1}, in associated solvents. (c) There is a change in the symmetry of the absorption curve about ν_{max}. (d) Band systems are modified in appearance, displaced in frequency, and often, as in the case of the halogens, disappear altogether in solution.

In this paper we shall be concerned only with those effects which can be discussed in terms of the $U(r)$ curves. Thus (a), which depends on the electronic part of the matrix component of the transition, will not be discussed. Furthermore, we shall deal mainly with the halogen continua; but the results are of more general application. The above effects have often been attributed rather vaguely to "solvation"; but it is evident that any real solvation in the chemical sense would result in more pronounced differences between gas and solution spectra than are generally observed. There are also two points which are worth noting. The displacement of the absorption maximum seems always to be to higher frequencies, and it is large only in associated solvents. Then there is the fact that band systems such as those of the halogens are not observed in solution, although Raman and infra-red data show that molecules possess vibrational quantization in the liquid state. Rotational quantization is, of course, broken down in the liquid; but it has been shown[2] that this is of no importance in discussing continuous spectra.

We shall attempt to express the differences between the potential energy curves of gaseous

* At present Beit Research Fellow, Imperial College of Science, London.

[1] For convenience, we shall use the term "solution" to include cases of absorption by pure liquids, where the absorbing molecule will be termed "solute," and the surrounding molecules "solvent."

[2] G. E. Gibson, O. K. Rice and N. S. Bayliss, Phys. Rev. **44**, 193 (1933).

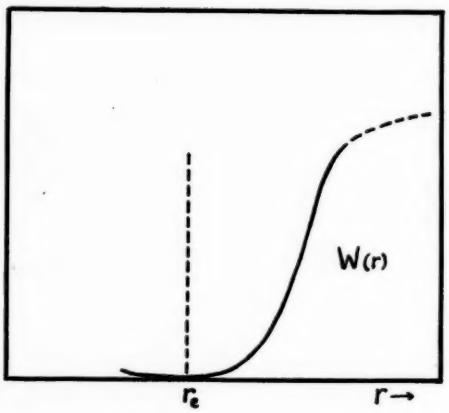

FIG. 1.

and dissolved molecules, $U_g(r)$ and $U_s(r)$, respectively, in terms of the modern cage theory of liquids. Rabinowitch and Wood[3] have applied similar ideas to the related problem of photo-dissociation in solution. Each solute molecule is surrounded by a cage of solvent molecules, from which it can escape only on receiving some kind of activation. Although the solute molecule and its cage are executing intramolecular vibration as well as a thermal jostling motion, we shall assume for simplicity that the cage has spherical symmetry. The cage is characterized by a relaxation time that Debye[4] has estimated to be of the order of 10^{-10} sec. Raman and Venkateswaran[5] find it to be 3.5×10^{-10} sec. for glycerol, and state that it is shorter for nonassociated liquids. In any case, the relaxation time is long compared with the period of molecular vibration (10^{-13} sec.), and therefore the cage must be regarded as rigid with respect to the vibration of the enclosed solute molecule, and to processes such as continuous absorption which occur within a single vibration period. We shall distinguish between cages formed by nonassociated and by associated solvents. In the former case, only the ordinary van der Waals and repulsive forces are in operation between the molecules, and we shall assume that the size of the cage is determined by the size of the solute molecule; i.e., in nonassociated solvents the normal solute molecule has the same nuclear separation as in the gas.

[3] E. Rabinowitch and W. C. Wood, Trans. Faraday Soc. **32**, 1381 (1936).
[4] P. Debye, Zeits. f. Elektrochem. **45**, 174 (1939).
[5] C. V. Raman and C. S. Venkateswaran, Nature **143**, 798 (1939).

CAGES IN NONASSOCIATED SOLVENTS

The potential energy function, $U_s''(r)$ of the dissolved molecule in its normal state will be derived from $U_g''(r)$ of the gaseous molecule by the addition of a potential energy function that expresses the effect of the surrounding cage on the vibration of the dissolved molecule. This function, which we call $W''(r)$, consists of two parts: (a) A part which includes the potential energy associated with the heat of solution and which is independent of the vibration of the solute molecule, but which depends on the size of the cage. (b) A part which depends on the nuclear separation of the solute molecule, whose nuclei at different stages in a complete vibration are at varying distances from the "wall" of the cage.

Apart from its dependence on the size of the cage, we assume that (a) is the same for both normal and excited solute molecules,[6] and that it can be neglected in the subsequent discussion. Part (b) is therefore what we call $W''(r)$, and it will be zero at $r''=r_e''$, increasing on both sides of this point as shown in Fig. 1, as the

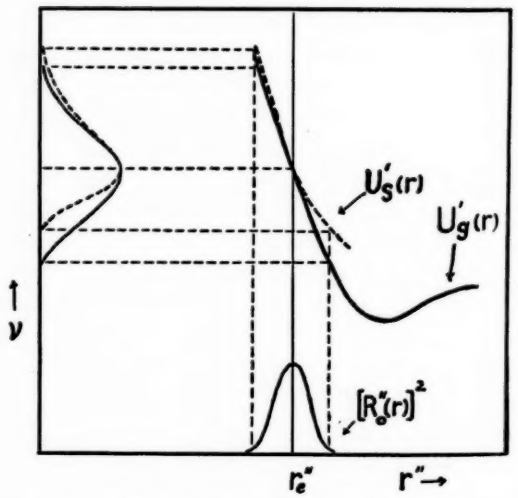

FIG. 2. Showing diagrammatically the relation of $U_s'(r)$ (broken curve) to $U_g'(r)$ (continuous curve). The reflection of the square of the lowest vibrational eigenfunction of the ground state, $R_0''(r)$, on to the frequency axis shows the relation between continuous absorption in gas (continuous curve) and in solution (broken curve).

[6] This is demanded by the experimental fact of practically no shift of ν_{max} in nonassociated solvents. Whatever the change in *absolute* potential energy, the $U(r)$ curves of normal and excited molecules must have the same *relative* energy separation in solution as in the gas.

nuclei in the course of a vibration are influenced by the attractive and repulsive forces of the cage. (At $r''=r_e''$, the attractive and repulsive forces of the cage are in equilibrium, since we have assumed that the solute molecule determines the size of the cage.) $W''(r)$ will rise much more steeply on the side of larger r'', since repulsive forces vary more rapidly with r than van der Waals attractive forces. As r'' increases, assuming that the cage does not relax, $W''(r)$ will rise steeply to a maximum which corresponds to the energy that is necessary for the separating atoms of the solute molecule to break through the cage. The height of this maximum does not concern us greatly; but owing to the rigidity of the cage for rapid processes, it will probably be rather greater than the activation energy for diffusion processes in nonassociated liquids,[7] which is about 3000–4000 calories per mole (0.13–0.17 ev).

The addition of $W''(r)$ to $U_g''(r)$ will increase the curvature at $r''=r_e''$, and should thus increase the vibration frequency of the solute molecule. Experimental evidence in general does not support this conclusion. Raman data for elements such as H_2, N_2, O_2 and Cl_2 show that the vibration frequency in the liquid is either equal to that in the gas, or else is slightly less by a few tenths of a percent.[8] The same is true for other molecules for which Raman and infra-red data are available.[9] In a few cases of strongly polar molecules such as HCl,[10] the liquid and dissolved states show a decrease of several percent in vibration frequency. However, another effect must be taken into account, which acts in the opposite direction to the effect under discussion. Electrical forces, according to Kirkwood,[11] cause an oscillating dipole to have a lower frequency in solution, thus counteracting our effect. For practical purposes we may conclude that $W''(r)$ is very flat in the immediate neighborhood of r_e'', leading to very little change in ω_e''.

However, since $W''(r)$ rises more steeply on the side of larger r'', it will also have the effect of making $U_s''(r)$ more symmetrical than $U_g''(r)$, and therefore the vibrating molecule in solution should approach more closely to the harmonic oscillator than in the gas. Evidence that the anharmonic nature of the oscillator is decreased

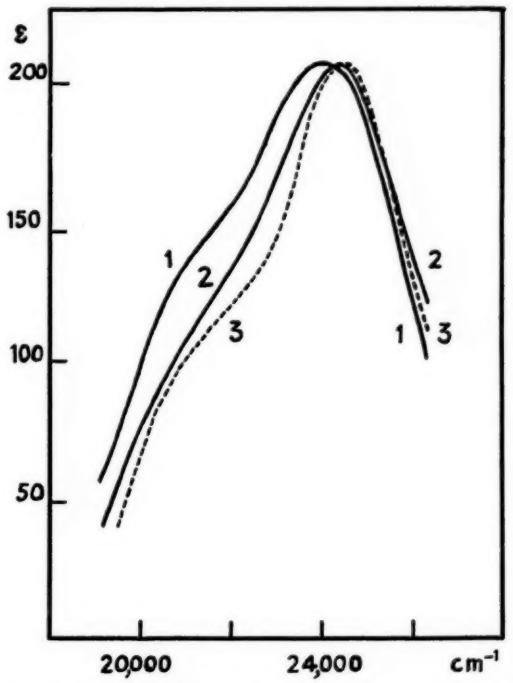

FIG. 4. Continuum of Br_2. 1, gas curve increased to have same maximum absorption as in solution. 2, Br_2 in chloroform. 3, Br_2 in solution calculated on assumptions in this paper (broken curve).

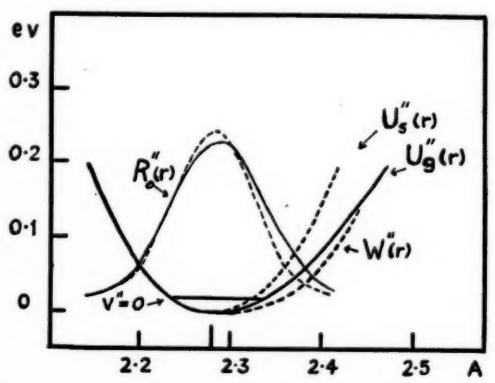

FIG. 3. Showing the addition of $W''(r)$ to $U_g''(r)$ to form $U_s''(r)$ on the simplifying assumption that $W''(r)$ is negligible at $r''<r_e''$, and that it makes $U_s''(r)$ symmetrical. The lowest vibrational eigenfunctions are shown for $U_g''(r)$ (anharmonic—continuous curve) and $U_s''(r)$ (Hermitian—broken curve). Data are for ground state of Br_2.

[7] R. M. Barrer, Trans. Faraday Soc. **35**, 644 (1939); M. J. Polissar, J. Chem. Phys. **6**, 833 (1938); H. S. Taylor, J. Chem. Phys. **6**, 331 (1938).

[8] *Landolt-Börnstein Tables*, third revised edition, Vol. 3.

[9] W. West and P. Arthur, J. Chem. Phys. **5**, 10 (1937).

[10] W. West, J. Chem. Phys. **7**, 795 (1939).

[11] See reference 10.

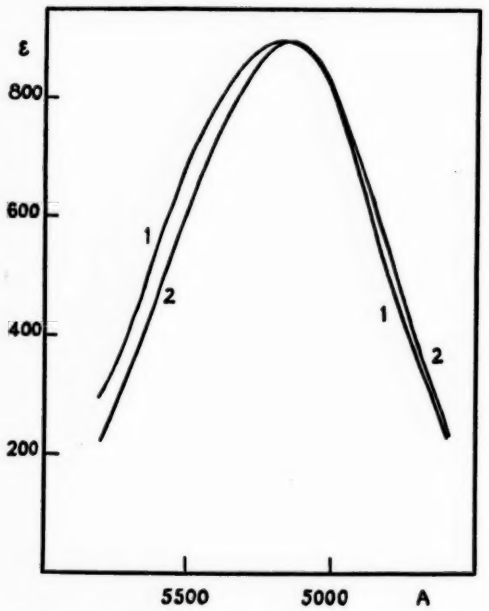

FIG. 5. Continuum of I_2. 1, gas curve increased to have same maximum absorption as in solution. 2, I_2 in carbon tetrachloride.

in solution is to be obtained from data quoted by West and Edwards.[12]

CONTINUOUS ABSORPTION IN NONASSOCIATED SOLVENTS

In terms of the Franck-Condon principle, the transition from normal to excited state is rapid compared with nuclear motions, and therefore also compared with the relaxation time of the cage. Thus, although continuous absorption occurs only when $r_e' > r_e''$, the excited molecule is formed in a cage whose size is appropriate to the normal molecule. Furthermore, this cage cannot relax within the time required for dissociation of the excited molecule. Thus for continuous absorption in solution, $U_s'(r)$ must be derived from $U_g'(r)$ by the addition of the *same* $W(r)$ as for the normal state; i.e., by adding $W''(r)$. This is shown in Fig. 2, where it is seen that the main effect is to raise $U'(r)$ at points where $r' > r_e''$. The effect of this on the continuous absorption can be derived by using the rule[13] that the absorption curve, except for a frequency factor, is obtained by reflecting the square of the vibrational eigenfunctions ($R''(r)$) of the normal state from $U'(r)$ on to the frequency axis, as shown in Fig. 2. It is found that the main effect is to "compress" the absorption curve on the low frequency side of the maximum and also to extend it slightly on the high frequency side. (See Figs. 4, 5.)

We have tested these ideas in a semi-quantitative way in the case of bromine, introducing the following simplifying assumptions to minimize the labor of calculation: (a) That $W''(r)$ is important only when $r'' > r_e''$. (b) That $W''(r)$ is such as to make $U_s''(r)$ symmetrical about r_e''. This makes it possible to use the simple Hermitian eigenfunctions of the harmonic oscillator.

In Fig. 3, we have shown $U_g''(r)$ for the normal state of Br_2, and also $W''(r)$ and $U_s''(r)$ on the assumption that the latter is symmetrical. The lowest anharmonic eigenfunction for $U_g''(r)$,[14] and the lowest Hermitian eigenfunction for $U_s''(r)$ are also shown. In Fig. 4, we show the result of calculating the continuous absorption of solutions of Br_2 on these assumptions. We have included the contributions of both the excited states concerned,[14] and we have also allowed for the contributions of the second and third vibrational levels of the ground state. The calculated curve is compared with the experimental data for bromine dissolved in chloroform,[15] and also with the absorption of the gas,[16] the absorption curve of the latter having been increased to have the same value at the maximum as the former. It is evident that the slight displacement of ν_{max} in nonassociated solvents can be attributed to the substitution of the Hermitian eigenfunction for the anharmonic, and the compression of the absorption curve on the low frequency side is also obvious. That this effect is general can be seen from the published curves for the absorption of bromine in other solvents,[17] and for the absorption of iodine in solution, which is compared with the adjusted gas curve in Fig. 5.[18]

[12] W. West and R. T. Edwards, J. Chem. Phys. **5**, 21 (1937).

[13] N. S. Bayliss, Proc. Roy. Soc. **A158**, 551 (1937); C. F. Goodeve and A. W. C. Taylor, Proc. Roy. Soc. **A152**, 221 (1935).

[14] N. S. Bayliss, reference 13.

[15] R. G. Aickin, N. S. Bayliss and A. L. G. Rees, Proc. Roy. Soc. **A169**, 234 (1938).

[16] A. P. Acton, R. G. Aickin and N. S. Bayliss, J. Chem. Phys. **4**, 474 (1936).

[17] Reference 13, also C. L. Child and O. J. Walker, Trans. Faraday Soc. **34**, 1506 (1938).

[18] I_2 gas: E. Rabinowitch and W. C. Wood, Trans. Faraday Soc. **32**, 540 (1936); I_2 in solution: O. J. Walker, Trans. Faraday Soc. **31**, 1432 (1935).

In spite of the simplifying assumptions, the theory gives a good qualitative account of the effect of nonassociated solvents. The choice of $W''(r)$ leads to an over-correction in the absorption; but in any case, it appears to rise rather too quickly to energies of the order of the activation energy for diffusion processes. A $U_e''(r)$ less anharmonic than the gas curve; but still not harmonic, would give a closer approximation.

Continuous Absorption in Associated Solvents

The main experimental feature in associated solvents is the marked displacement of the maximum to higher frequencies. We may assume that the general conclusions with regard to the solvent cage and $W''(r)$ are as described above, with one important difference. While in nonassociated liquids the molecules interact by ordinary attractive and repulsive forces, in associated liquids it is believed that hydrogen bonds help to give the liquid a quasi-crystalline structure such as that proposed for water by Bernal and Fowler.[19] As a result, the size of the cage in an associated solvent will be partly determined by the dimensions of the solvent molecule and the hydrogen bond. Cages of other than certain favored sizes will tend to cause distortion of the quasi-crystalline structure of the solvent and also some distortion of the solute molecule. The holes in the quartz-like structure of water are too small to accommodate a bromine molecule (diameter approximately 5A) without some compression of the latter or distortion of the structure. A decrease in r_e'' of the solute molecule will cause a marked shift of the absorption maximum to higher frequencies, in conformity with observation. The compression need not be great to account for the observed displacements (there is probably not enough energy available for any marked compression). In aqueous solutions of bromine, a decrease of 0.05A in r_e'', requiring an energy of about 450 calories per mole, is enough to account for the observed displacement of 1750 cm^{-1} in the maximum, and also makes it possible to account for the curious broadening and flattening of the bromine continuum in water.[20] Some such effect as this seems to be necessary to explain why the displacement of the maximum in associated solvents is *always* to higher frequencies. The argument against solvation is mainly in the small changes in molecular dimensions that are needed to produce quite large displacements.

Band Absorption in Solution

We conclude with some general suggestions regarding the appearance or nonappearance of band absorption in solution. It has been shown that, at the instant of its formation, the excited solute molecule is in a solvent cage of size appropriate to the normal molecule, and that the cage has a relaxation time of about 10^{-10} sec. If the excited molecule has the same size as the normal molecule, i.e., if $r_e' = r_e''$, no relaxation of the cage is needed to accommodate the excited molecule, and there should be no difficulty in establishing vibrational quantization in the excited state. In such cases, band absorption will be observed in solution as well as in the gas, subject to such displacements as are caused by the addition of $W''(r)$ to the potential energy curves of the two electronic states. It should be noted that benzene, which has a well-known band absorption in solution, has been shown to have normal and excited states of the same size.[21] On the other hand, if $r_e' > r_e''$, as in the halogens, the cage must relax to accommodate the excited molecule, a process that is not complete for more than 10^{-10} sec. It is not certain whether excited states in solution have as long a life (10^{-8} sec.) as in the gas; but in any case an appreciable fraction of that life is spent under the influence of the varying perturbation of a relaxing cage, and it is not surprising that the excited state does not establish sharp vibrational quantization. The result is that the gaseous band system will not be observed in solution.

[19] J. D. Bernal and R. Fowler, J. Chem. Phys. **1**, 515 (1933).

[20] N. S. Bayliss and A. L. G. Rees, J. Chem. Phys. **7**, 855 (1939).

[21] H. Sponer, G. Nordheim, A. L. Sklar and E. Teller, J. Chem. Phys. **7**, 207 (1939).

Intensities in Molecular Electronic Spectra

X. Calculations on Mixed-Halogen, Hydrogen Halide, Alkyl Halide, and Hydroxyl Spectra

ROBERT S. MULLIKEN
University of Chicago, Chicago, Illinois

(Received January 29, 1940)

The dipole strengths for certain perpendicular-type transitions $N \rightarrow Q$ in the mixed halogens, the hydrogen and monovalent metal halides, and the alkyl halides, are calculated theoretically by the LCAO and by the AO approximations. The scanty experimental absorption coefficient data on these halides (particularly the hydrogen and alkyl bromides and iodides) are critically examined, and acceptable experimental dipole strengths are obtained for the bromides. These show, very gratifyingly, the same kind of agreement with the calculated values as was found in IX of this series for the $N \rightarrow Q$ transitions in F_2, Cl_2, and Br_2. The iodides, however, just like I_2, show anomalously low strengths for the true $N \rightarrow Q$ part of the intensity ($N \rightarrow {}^3\Pi_1$ and $N \rightarrow {}^1\Pi$), together with high strength for $N \rightarrow {}^3\Pi_0{}^+$. These anomalies are ascribed here, as in I_2, to partial case c coupling (partial preservation of atomic J's). The comparison between theory and experiment *confirms the interpretation of the ultraviolet continua of the hydrogen and alkyl halides as $N \rightarrow Q$ transitions.* Dipole strength calculations for the well-known ${}^2\Sigma \rightarrow {}^2\Pi$ transition in OH have also been made. The agreement with Oldenberg and Rieke's experimental values for OH is of much the same kind as for the other molecules. A general equation for the $N \rightarrow Q$ dipole strength in AX or OH is obtained covering any degree of ionicity and of polarity. This includes the AO and LCAO approximations, with any degree of polarity, as special cases. It is found that the intensity is on the whole not especially sensitive to polarity. The magnitudes of overlapping and dipole strength integrals in relation to molecular stability and to principal quantum number of the valence orbital are discussed. The integrals are notably larger for molecules containing the heavier halogens ($3p$, $4p$, $5p$ orbitals) than for those containing fluorine ($2p$ orbital). They are also larger for hydrogen halides than for corresponding halogens.

I. MIXED HALOGENS: THEORY

IN IX of this series,[1] dipole strengths have been calculated for the perpendicular-type "$N \rightarrow Q$" long wave-length complex of transitions in the homopolar halogen molecules. Similar calculations are reported here for the related $N \rightarrow Q$ transitions in the mixed halogen molecules (e.g. ICl), the hydrogen, monovalent metal, and alkyl halides,[2-4] and for the well-known ${}^2\Pi \leftrightarrow {}^2\Sigma^+$ transition of the OH radical.

For each class of molecules, we first need electron configurations. For ICl, taken as an example of the mixed halogens, the configurations are analogous to those given in Eqs. (1) of IX for the homopolar halogens:

AO approximation, neglecting polarity:

$$\left.\begin{array}{l} N: (\sigma_{Cl}\cdot\sigma_I)(\pi_{Cl})^4(\pi_I)^4,\ {}^1\Sigma^+ \\ {}^{3,1}Q_a,\ {}^{3,1}Q_b: \left\{\begin{array}{l}\sigma_{Cl}\pi_{Cl}{}^4\sigma_I\ {}^2\pi_I{}^3, \\ \sigma_I\pi_I{}^4\sigma_{Cl}{}^2\pi_{Cl}{}^3\end{array}\right\},\ {}^{3,1}\Pi,\ {}^{3,1}\Pi. \end{array}\right\} \quad (1a)$$

MO approximation:

$$\left.\begin{array}{l} N: \sigma^2\pi^4\pi^{*4},\ {}^1\Sigma^+, \\ {}^{3,1}Q_a: \sigma^2\pi^4\pi^{*3}\sigma^*,\ {}^{3,1}\Pi, \\ {}^{3,1}Q_b: \sigma^2\pi^3\pi^{*4}\sigma^*,\ {}^{3,1}\Pi. \end{array}\right\} \quad (1b)$$

In (1a), σ_{Cl}, π_{Cl}, σ_I, π_I, stand for $3p\sigma_{Cl}$, $3p\pi_{Cl}$, $5p\sigma_I$, and $5p\pi_I$. In (1b), σ, σ^*, π, and π^* are, respectively, analogous to $\sigma_g np$, $\sigma_u np$, $\pi_u np$, and $\pi_g np$ of the homopolar halogens. The Q_a (lower energy) and Q_b (higher energy) Q complexes in (1) are, respectively, more or less analogous to Q_u and Q_g of the homopolar halogens. They differ from the latter in that transitions to *both* are now allowed by the selection rules.

The LCAO approximations to the MO's in (1b) now (cf. Eqs. (7) of IX) take the forms

$$\left.\begin{array}{l} \sigma \approx \alpha(3p\sigma_{Cl}) + \beta(5p\sigma_I), \\ \sigma^* \approx \alpha^*(5p\sigma_I) - \beta^*(3p\sigma_{Cl}), \\ \pi \approx \gamma(3p\pi_{Cl}) + \delta(5p\pi_I), \\ \pi^* \approx \gamma^*(5p\pi_I) - \delta^*(3p\pi_{Cl}). \end{array}\right\} \quad (2)$$

(Term symbols are here used to stand for wave

[1] R. S. Mulliken, J. Chem. Phys. **8**, 234 (1940).
[2] R. S. Mulliken, Phys. Rev. **46**, 550 (1934): halogens. For a correction, see reference 6 below.
[3] R. S. Mulliken. Phys. Rev. **50**, 1017 (1936); **51**, 310 (1937): hydrogen halides.
[4] R. S. Mulliken, Phys. Rev. **47**, 413 (1935): methyl iodide, and comparison with ClI; J. Chem. Phys. **3**, 513 (1935): alkyl halides.

functions.) Here $\alpha>\beta$, $\gamma>\delta$, since chlorine is more electronegative than iodine. To be consistent with this, the AO approximation wave functions corresponding to (1a) should receive some admixture of ionic functions.

Since, however, most of the mixed halogens are not strongly polar, we first make calculations neglecting polarity. For the two sets of Q states in AO approximation, it appears that the correct wave functions should be two nearly-50,50 linear combinations of the two AO configurations given in (1a), almost the same as in the truly homopolar halogens.[4a] If we neglect the difference in electronegativity between the two atoms,[4a] the linear combinations should be exactly 50,50, and Eqs. (23)–(26) of IX and the discussion following these becomes applicable here if we substitute σ_I, π_I, σ_{Cl}, π_{Cl} for σ, π, σ', π' in the equations there. On following through the type of analysis given in Section III of IX, one finds results essentially the same as there, namely:

$$Q_{NQ}=2/(1-S_{\sigma\sigma'}{}^4)^{\frac{1}{2}}[S_{\sigma\sigma'}(Q_{\pi_I\sigma Cl}\pm Q_{\pi Cl\sigma I}) -\tfrac{1}{2}(1+S_{\sigma\sigma'}{}^2)(Q_{\pi_I\sigma_I}\pm Q_{\pi Cl\sigma Cl})], \quad (3)$$

with the + signs for $N\rightarrow Q_a$, the − signs for $N\rightarrow Q_b$. In Eq. (3),

$$Q_{\pi_I\sigma Cl}=\int (5p\pi_y)_I y(3p\sigma)_{Cl}dv,$$

and so on. $Q_{\pi_I\sigma Cl}$ and $Q_{\pi Cl\sigma I}$ are analogous to $Q_{\pi\sigma'}$ of the truly homopolar halogen case, while $Q_{\pi_I\sigma_I}$ and $Q_{\pi Cl\sigma Cl}$ are examples of $Q_{\pi\sigma}$ of that case (cf. IX, Eqs. (10), (11)). As was noted in IX, $Q_{\pi\sigma}$ is zero unless one uses polarized AO's. Presumably $Q_{\pi_I\sigma Cl}$ and $Q_{\pi Cl\sigma I}$ in Eq. (3) are nearly equal. If so, $Q_{NQ}\approx 0$ for $N\rightarrow Q_b$ in Eq. (3), similar to $Q_{NQ}=0$ for $N\rightarrow {}^1Q_g$ in the truly homopolar case.

Now let us consider the LCAO MO approximation, *including polarity*. Proceeding along the lines followed in IX, we arrive first at the following equations analogous to Eqs. (6) of IX:

$$Q_{NQ_a}=2^{\frac{1}{2}}\int (\pi_y{}^*)y(\sigma^*)dv;$$
$$Q_{NQ_b}=2^{\frac{1}{2}}\int (\pi_y)y(\sigma^*)dv. \quad (4)$$

In Eq. (4), π^*, π, and σ^* are the MO's of Eqs. (1b), (2). For the general case with polarity, it is desirable to note the following:[5] (a) the magnitude and *sign* of the polarity can vary from one MO to another, while even for a single MO the magnitude of the polarity may differ somewhat in different molecular states; (b) the π^* or π MO in Eqs. (4) comes from the wave function of state N, the σ^* from that of state Q_a or Q_b, and the polarity coefficients should be taken accordingly.

Since it is not feasible to find general expressions for the polarity coefficients, it is best to obtain Q_{NQ} expressions in which these appear as parameters. By substituting Eqs. (2) into Eqs. (4), one obtains

$$-Q_{NQ_a}=2^{\frac{1}{2}}[\beta^*\gamma^*Q_{\pi_I\sigma Cl}+\alpha^*\delta^*Q_{\pi Cl\sigma I} +\alpha^*\gamma^*Q_{\pi_I\sigma_I}+\beta^*\delta^*Q_{\pi Cl\sigma Cl}],$$
$$Q_{NQ_b}=2^{\frac{1}{2}}[\alpha^*\gamma Q_{\pi Cl\sigma I}-\beta^*\delta Q_{\pi_I\sigma Cl} +\alpha^*\delta Q_{\pi_I\sigma_I}-\beta^*\gamma Q_{\pi Cl\sigma Cl}]. \quad (5)$$

For zero polarity, Eqs. (5) reduce to

$$-Q_{NQ}=[2(1\mp S_{\pi\pi'})(1-S_{\sigma\sigma'})]^{-\frac{1}{2}} \times[Q_{\pi_I\sigma Cl}\pm Q_{\pi Cl\sigma I}+\cdots], \quad (6)$$

with the upper signs for $N\rightarrow Q_a$, the lower for $N\rightarrow Q_b$. Here we find $Q_{NQ}\approx 0$ for $N\rightarrow Q_b$, just as in the AO nonpolar approximation.

As one sees from Eqs. (5), the effect of polarity is to increase $|Q_{NQ_b}|$ at the expense of $|Q_{NQ_a}|$. The most extreme possibility conceivable is $\alpha=\alpha^*=\gamma=\gamma^*=1$, $\beta=\beta^*=\delta=\delta^*=0$, for which *all* the intensity is transferred to $N\rightarrow Q_b$. It is difficult to estimate what values the polarity coefficients would actually have for the mixed-halogen $N\rightarrow Q$ transitions, but it seems likely

[4a] Consider for example the Q_a and Q_b $^1\Pi$ states of ICl. In getting the correct AO wave functions, one is first led to a quadratic secular equation between two initial $^1\Pi$ functions, say ψ_1 and ψ_2, corresponding to the two Π electron configurations given in (1a). Of the energy matrix elements appearing in this equation, H_{11} and H_{22} are apparently nearly but certainly not quite equal, and as a result the correct final wave functions are nearly but not quite 50, 50 linear combinations of the initial ones. [When the atoms are far apart, $H_{11}=H_{22}$, of course. At smaller distances, Coulomb energy terms occur, differing slightly for H_{11} and H_{22}.] In the case of equal electronegativities of the two atoms, we should have $H_{11}=H_{22}$.

[5] Cf. R. S. Mulliken, J. Chem. Phys. **3**, 583 (1935), Eq. (39). Taking for example the π MO of Eqs. (2), $\gamma^2-\delta^2$ serves as a measure of the polarity; similarly, $\gamma'^2-\delta'^2$ for the π^* MO, which is of opposite polarity to π.

that they are relatively near to the nonpolar case for most of the mixed halogens.

It seems possible, however, that the mixed halogens, for the $N\rightarrow Q$ transitions, tend more or less toward the case $\gamma^*\gg\delta^*$, $\gamma\gg\delta$, with $\alpha>\beta$.[6] This case is also of some interest in that it resembles one which is actually realized in the $N\rightarrow Q$ transition in the hydrogen and alkyl halides (see Eq. (12) below). Putting $\gamma'=\gamma=1$, $\delta'=\delta=0$, $\alpha=\beta$, for a simple approximation to this case, Eqs. (5) become

$$\begin{aligned} -Q_{NQ_a}&=(1-S_{\sigma\sigma'})^{-\frac{1}{2}}(Q_{\pi_I\sigma_{Cl}}-Q_{\pi_I\sigma_I}),\\ Q_{NQ_b}&=(1-S_{\sigma\sigma'})^{-\frac{1}{2}}(Q_{\pi_{Cl}\sigma_I}-Q_{\pi_{Cl}\sigma_{Cl}}). \end{aligned} \tag{7}$$

Here the intensity is almost equal for $N\rightarrow Q_a$ and $N\rightarrow Q_b$. The sum of dipole strengths $Q^2_{NQ_a}+Q^2_{NQ_b}$ is practically the same here as under the assumption of zero polarity; indeed, this sum is seen to be practically independent of the polarity.

Experimental measurements of dipole strengths for the two $N\rightarrow Q$ complexes in the mixed halogens would be of considerable interest, especially for the light they could throw on questions of polarity. Unfortunately no suitable data are available. In the case of ICl, to be sure, dipole strengths for both $N\rightarrow Q_a$ and a probable $N\rightarrow Q_b$ can be obtained from absorption coefficient measurements (cf. Table V). These cannot, however, be accepted as values of $Q^2_{NQ_a}$ and $Q^2_{NQ_b}$, since it is likely that most of the intensity (which, incidentally, is larger for $N\rightarrow Q_b$ than for $N\rightarrow Q_a$) belongs to the anomalous component $N\rightarrow Q_0$.[7]

II. Hydrogen and Univalent Metal Halides: Nonpolar Theory

In the hydrogen and the univalent metal halides, there is only one Q complex.[3] The electron configurations of the states N and Q in AX, where A = H, Ag, Na, or the like, are:

$$\textit{AO approximation (neglecting polarity)}: \left\{\begin{matrix} N: (s_A\cdot\sigma_X)\pi_X^4,\ {}^1\Sigma^+,\\ {}^{3,1}Q: s_A\sigma_X^2\pi_X^3,\ {}^{3,1}\Pi; \end{matrix}\right\} \tag{8}$$

$$\textit{MO approximation}: \left\{\begin{matrix} N: \sigma^2\pi_X^4,\ {}^1\Sigma^+\\ {}^{3,1}Q: \sigma^2\pi_X^3\sigma^*,\ {}^{3,1}\Pi \end{matrix}\right\} \tag{9}$$

where, in LCAO approximation,

$$\begin{aligned} \sigma&\approx\alpha(np\sigma_X)+\beta(ms_A),\\ \sigma^*&\approx\alpha^*(ms_A)-\beta^*(np\sigma_X) \end{aligned} \tag{10}$$

in (9), with $\alpha>\beta$, $\alpha^*>\beta^*$. The π MO's in (9) are nearly pure $np\pi$ AO's of the X atom, that is nearly the same as the π AO's in (8). The s_A AO's in (8) and (9) are $1s_H$ in the case of HX. For the metal halides, valence ms AO's of the metal atom may be used, but the approximation will be improved if one uses a mixture of ms and $mp\sigma$ instead of pure ms.

According to present views, the hydrogen halides except HF have small enough polarity so that calculations of Q_{NQ} made with the nonpolar approximation should be not much in error. Calculations will be made on this basis in the present section.

The general case with polar wave functions, needed for many of the monovalent metal halides and for HF, will be taken up in Sections IV and V.

For the MO approximation, following the same type of reasoning as in Section II of IX, we obtain, very nearly,

$$Q_{NQ}=2^{\frac{1}{2}}\int(np\pi_y)y(\sigma^*)dv. \tag{11}$$

In LCAO approximation, using Eq. (10) with $\alpha^*=\beta^*$, we then get

$$\text{LCAO MO:}\quad Q_{NQ}=(1-S_{s\sigma'})^{-\frac{1}{2}}(Q_{s\pi'}-Q_{\sigma\pi}), \tag{12}$$

where

$$\begin{aligned} S_{s\sigma'}&=\int(ms_A)(np\sigma_X)dv;\\ Q_{s\pi'}&=\int(ms_A)y(np\pi_y)_X dv;\\ Q_{\sigma\pi}&=\int(np\sigma_X)y(np\pi_y)_X dv. \end{aligned} \tag{13}$$

[6] For the two $^2\Pi$ states of $(ICl)^+$ obtained by removing the σ^* electron from either of the Q states in (1a), likewise for high energy $^{1,3}\Pi$ states of ICl where σ^* is replaced by a more excited σ orbital σ^*, it is sure that γ/δ and γ'/δ' greatly exceed unity (cf. reference 2). But for the Q states in (1b) this can hardly be true, as one sees by comparison with the AO approximation (1a),—cf. reference 4a,—even after making maximum allowance for admixture of ionic contributions in the latter. Reference 2, especially in Section 11 and Table V, where $\gamma\gg\delta$, $\gamma^*\gg\delta^*$ were assumed for the Q states, therefore needs some revision. For the N state of ICl, it may be that $\gamma\gg\delta$ and $\gamma^*\gg\delta^*$ should be assumed, but this is doubtful, and it is not clear how these coefficients could be determined there.

[7] R. S. Mulliken, Phys. Rev. **57**, 500 (1940). See Section V in regard to the mixed halogens.

TABLE I. *Parameters and coefficients in Eqs. (22) and (23). All A_{mn} and B_{mn} values not listed are zero.*

Molecule	k	C	D	A_{mn}							B_{mn}						
				n \ m	0	1	2	3	4	5	n \ m	0	1	2	3	4	5
HF	5	4	1	0			$-3T$	$-3T$			0			$3T$	$3T$		
				1			$3R$	$P+2R$			1			$-3R$	$-3R$		
				2	$3T$	$3T$		P			2	$-3T$	$-3T$		T		
				3	$-3R$	$-P-2R$	$-P$				3	$3R$	$3R$	R			
HCl	7	$(120)^{\frac{1}{2}}$	$(30)^{\frac{1}{2}}$	0				$-6T$	$-6T$		0				$15T$	$15T$	
				1			$-3T$	$3(P+R)$	$3(P+R)$		1			$+9T$	$-9P-6R$	$-3P-12R$	
				2		$3T$	$3Q$	$2P+R$	$3P$		2		$-9T$	$-9Q$	$-3P-6R$	$-3P+3T$	
				3	$6T$	$-3P+3T$	$-2P-R$		P		3	$-15T$	$9P-6T$	$3P+6R$	$2Q$	$-P$	
				4	$-6R$	$-3(P+R)$	$-3P$	$-P$			4	$15R$	$3P+12R$	$3P+3R$	P		
HI	9	$4(105)^{\frac{1}{2}}$	$2(105)^{\frac{1}{2}}$	0					$-15T$	$-15T$	0					$45T$	$45T$
				1				$-12T$	$12P+3R$	$9P+6R$	1				$45T$	$-45P$	$-15P-30R$
				2				$12R$	$9P+3R$	$9P$	2				$-45R$	$-21P-24R$	$-15P+6T$
				3		$12T$	$12T$		$4P$	$4P$	3		$-45T$	$-45T$		$-6P+9T$	$-6P$
				4	$15T$	$-12P+3T$	$-9P-3R$	$-4P$		P	4	$-45T$	$45P$	$21P+24R$	$6P+9R$		$-P$
				5	$-15R$	$-9P-6R$	$-9P$	$-4P$	$-P$		5	$45R$	$15P+30R$	$15P+6R$	$6P$	P	

It is of interest that Eq. (12) is exactly like either one of the two Eqs. (7) derived above for ICl assuming special (artificial) relations as to polarization in the latter.

For the AO nonpolar approximation, the wave functions are as follows:

$$\psi(N) = [n!2(1+S^2)]^{-\frac{1}{2}}(\psi_{\mathrm{I}}+\psi_{\mathrm{II}}), \tag{14}$$

$$\psi(^1Q_y) = [n!2(1-S^2)]^{-\frac{1}{2}}(\psi_{\mathrm{V}}+\psi_{\mathrm{VI}}), \tag{15}$$

where S means $S_{s\sigma'}$, and

$$\left.\begin{aligned}\psi_{\mathrm{I}} &\approx \sum_P \pm P s_\alpha(1)\sigma_\beta(2)\pi_{y\alpha}(3)\pi_{y\beta}(4)\cdots,\\ \psi_{\mathrm{II}} &\approx \sum_P \pm P \sigma_\alpha(1)s_\beta(2)\pi_{y\alpha}(3)\pi_{y\beta}(4)\cdots,\end{aligned}\right\} \tag{16}$$

$$\left.\begin{aligned}\psi_{\mathrm{V}} &\approx \sum_P \pm P s_\alpha(1)\pi_{y\beta}(2)\sigma_\alpha(3)\sigma_\beta(4)\cdots,\\ \psi_{\mathrm{VI}} &\approx \sum_P \pm P \pi_{y\alpha}(1)s_\beta(2)\sigma_\alpha(3)\sigma_\beta(4)\cdots.\end{aligned}\right\} \tag{17}$$

Following the same methods as in Section III of IX, we finally obtain

$$AO: Q_{NQ} \approx (1-S^4)^{-\frac{1}{2}}[2SQ_{s\pi'}-(1+S^2)Q_{\sigma\pi}]. \tag{18}$$

In order to make numerical computations for the hydrogen halides, we need first to evaluate S and $Q_{s\pi'}$ of Eqs. (13) for insertion in Eqs. (12), (18). (A similar procedure can be used for other monovalent metal halides, but will not be carried through here.) For $np\sigma_X$ and $np\pi_X$ we use the same Slater AO's as in IX (cf. Eqs. (12)–(13) there), while for $1s_{\mathrm{H}}$ we have

$$1s_{\mathrm{H}} = (h^3/\pi)^{\frac{1}{2}} \exp(-hr_{\mathrm{A}}). \tag{19}$$

In general, $h = Z^*/a_0 n^*$ (cf. Eq. (14) of IX); here $n^*=1$, $Z^*=1$. The integrals S and $Q_{s\sigma'}$ of Eqs. (13) are now set up like $S_{s\sigma'}$ and $Q_{\pi\sigma'}$ of IX, here calling the more positive atom A, the halogen atom B. The origin of coordinates is conveniently taken at the midpoint of the line of length r which joins the two nuclei.

The integrals are now transformed to confocal elliptic coordinates

$$\xi,\ \eta,\ \phi(\xi=(r_{\mathrm{A}}+r_{\mathrm{B}})/r,\ \eta=(r_{\mathrm{A}}-r_{\mathrm{B}})/r),$$

and can be evaluated with some labor. In each case the integrand contains a factor $\exp[-(h_{\mathrm{X}}+h_{\mathrm{H}})]$, which on transformation to elliptical coordinates becomes $\exp(-\gamma\xi+\delta\eta)$, where

$$\left.\begin{aligned}\gamma &= \tfrac{1}{2}r(h_{\mathrm{X}}+h_{\mathrm{H}}), \quad \delta = \tfrac{1}{2}r(h_{\mathrm{X}}-h_{\mathrm{H}}),\\ h &= Z^*/a_0 n^*.\end{aligned}\right\} \tag{20}$$

Slater's values for Z^* and n^* are to be used for the halogens (see IX). As an example, $Q_{s\pi'}$ for HF in elliptical coordinates is

$$Q_{s\pi'} = (r^5/32\pi)(h_{\mathrm{H}}{}^3 h_{\mathrm{F}}{}^5)^{\frac{1}{2}} \int (\xi^2-1)(1-\eta^2)(\xi^2-\eta^2)\sin^2\phi e^{-\gamma\xi}e^{\delta\eta}d\xi\,d\eta\,d\phi. \tag{20a}$$

Letting

$$P = 2e^{-\delta}, \quad Q = 2e^{\delta}, \quad R = e^{\delta}+e^{-\delta}, \quad T = e^{\delta}-e^{-\delta}, \tag{21}$$

the results for HF, HCl, and HI can all be expressed in the following forms,

$$S_{s\sigma'}=e^{-\gamma}[C^{-1}(\gamma+\delta)^{k/2}(\gamma-\delta)^{3/2}(\gamma\delta)^{-(k+3)/2}]\sum_m\sum_n A_{mn}\gamma^m\delta^n, \quad (22)$$

$$Q_{s\pi'}=\tfrac{1}{2}re^{-\gamma}[D^{-1}(\gamma+\delta)^{k/2}(\gamma-\delta)^{3/2}(\gamma\delta)^{-(k+5)/2}]\sum_m\sum_n B_{mn}\gamma^m\delta^n \quad (23)$$

with values of the quantities k, C, D, A_{mn}, B_{mn} as given in Table I.

III. Hydrogen and Univalent Metal Halides: Polar LCAO Approximation Theory

The LCAO MO equation (12) for nonpolar HX or AX is easily generalized to take care of polarity ($\alpha^*>\beta^*$ in Eq. (10)). It then becomes

$$Q_{NQ}=2^{\frac{1}{2}}(\alpha^*Q_{s\pi'}-\beta^*Q_{\sigma\pi}). \quad (24)$$

Let us apply this to the molecule HF. Pauling has suggested that this molecule is about 50 percent polar, that is, that the charge distribution in state N corresponds about to $H^{+\frac{1}{2}}F^{-\frac{1}{2}}$. Now it can easily be shown[5] that this would correspond in Eq. (10) to $\alpha^2-\beta^2=0.5$. Using also the normalization conditions

$$\alpha^2+\beta^2+2S\alpha\beta=1, \quad \alpha^{*2}+\beta^{*2}-2S\alpha^*\beta^*=1, \quad (25)$$

together with the computed value of S from Table IV below, and the requirement that σ and σ^* of Eq. (10) shall be mutually orthogonal,[8] one finds

$$\begin{aligned}\sigma&=0.814(2p\sigma_F)+0.404(1s_H),\\ \sigma^*&=0.955(1s_H)-0.641(2p\sigma_F).\end{aligned} \quad (26)$$

These may be compared with the following relations which hold for the assumption of zero polarity:

$$\begin{aligned}\sigma&=0.625(2p\sigma_F+1s_H),\\ \sigma^*&=0.823(1s_H-2p\sigma_F).\end{aligned} \quad (27)$$

That the N state configuration $\sigma^2\pi_F{}^4$ (cf. Eq. (9)) with σ given by Eqs. (26) corresponds to $H^{+\frac{1}{2}}F^{-\frac{1}{2}}$ is readily verified. The four π electrons belong entirely to the F atom; of the charge $-e$ of each of the two σ electrons the fraction $\alpha^2+S\alpha\beta$ must be alloted to the F atom, the fraction $\beta^2+S\alpha\beta$ to the H atom.[5] But with α and β as in Eq. (26), $\alpha^2+S\alpha\beta=0.75$, $\beta^2+S\alpha\beta=0.25$, so that of the charge of the σ^2 pair, $-1.5e$ belongs to F, $-0.5e$ to H. This corresponds to $H^{+\frac{1}{2}}F^{-\frac{1}{2}}$.

If we use the same values of α and β for state Q as for state N, and the corresponding values of α^* and β^* making σ and σ^* orthogonal, all as given by Eqs. (26), the charge distribution for state Q is found to correspond to $H^{-\frac{1}{2}}F^{+\frac{1}{2}}$. This result appears less strange when we note that using *nonpolar* LCAO MO's (Eqs. (9), (27)), state Q has a charge distribution $H^{-\frac{1}{2}}F^{+\frac{1}{2}}$.

Referring now to Eq. (24), and putting $Q_{\sigma\pi}=0$, we see that Q_{NQ} is increased by polarity in the MO's (of state Q) just in the ratio that α^* for the actual case with polarity exceeds α^* for the nonpolar case, that is (cf. Eqs. (26), (27)) in the ratio 0.955/0.823.

It is thus seen that in LCAO approximation, polarity has the effect of increasing the computed Q values for the hydrogen halides, but that the change is not great even for very strong polarity. Except for HF, the polarity correction using LCAO's is evidently entirely negligible.

IV. Hydrogen and Univalent Metal Halides: Theory of General Case with Any Degree of Ionicity and Polarity

In order to introduce polarity into the AO approximation wave function for state N of a molecule AX, one needs to mix some of a suitable A^+X^- wave function into the nonpolar A·X wave function which corresponds to Eq. (8). While doing this, we may as well bring in a further generalization which makes the treatment more satisfactory, by introducing *ionicity*.[9]

The wave function for state N of AX may then be written as

$$\psi(N)\approx a\psi(A\cdot X)+b\psi(A^+X^-)+c\psi(A^-X^+), \quad (28)$$

[8] Of course the requirement that σ and σ^* shall be orthogonal MO's holds only to the extent that they may be considered as belonging to the same field. Any error in this assumption is probably less than the error already involved in the LCAO approximation.

[9] For a discussion of ionicity (there called "ionicness") and polarity in AX and other types of molecules, cf. R. S. Mulliken, Phys. Rev. **50**, 1017 (1936).

where all terms in the equation correspond to $^1\Sigma^+$ functions, with the following electron configurations:

$$(A\cdot X),\ (s_A\cdot\sigma_X)\pi_X^4;\quad (A^+X^-),\ \sigma_X^2\pi_X^4;\quad (A^-X^+),\ s_A^2\pi_X^4. \tag{29}$$

Polarity is brought in through the relation $b>c$. Or by suitable adjustment of the coefficients a, b, c (approximately to $a=2^{\frac{1}{2}}b=2^{\frac{1}{2}}c$), Eq. (28) becomes identical with the nonpolar LCAO approximation wave function: the corresponding relation for H_2 is well known.

For the Q state of AX, the only possible important ionic term is one of A^-X^+ polarity:

$$\psi(Q)\approx d\psi(s_A\cdot\sigma_X^2\pi_X^3)+e\psi(s_A^2\cdot\sigma_X\pi_X^3). \tag{30}$$

The LCAO approximation for $\psi(Q)$ can be shown to correspond to Eq. (30) with $d=e$.

Using Eqs. (28) and (30) for the ψ's, we can calculate Q_{NQ} for a very general case. From the resulting general expression, special ones corresponding to various assumptions as to polarity and ionicity of states N and Q can then be obtained.

We first set up the antisymmetrical wave functions. $\psi(A\cdot X)$ in Eq. (28) is as given above by Eq. (14). $\psi_\nu(s_A\cdot\sigma_X^2\pi_X^3)$ in Eq. (30) is as given by Eq. (15). Further, in Eq. (28),

$$\left.\begin{aligned}\psi(A^+X^-)&=(n!)^{-\frac{1}{2}}\sum_P\pm P\sigma_\alpha(1)\sigma_\beta(2)\\&\qquad\times\pi_{\nu\alpha}(3)\pi_{\nu\beta}(4)\cdots,\\ \psi(A^-X^+)&=(n!)^{-\frac{1}{2}}\sum_P\pm Ps_\alpha(1)s_\beta(2)\\&\qquad\times\pi_{\nu\alpha}(3)\pi_{\nu\beta}(4)\cdots.\end{aligned}\right\}\tag{31}$$

In Eq. (30),

$$\psi(s_A^2\cdot\sigma_X\pi_X^3)=[n!2(1-S^2)]^{-\frac{1}{2}}(\psi_{VII}+\psi_{VIII}), \tag{32}$$

where

$$\left.\begin{aligned}\psi_{VII}&=\sum_P\pm Ps_\alpha(1)s_\beta(2)\sigma_\alpha(3)\pi_{\nu\beta}(4)\cdots,\\ \psi_{VIII}&=\sum_P\pm Ps_\alpha(1)s_\beta(2)\pi_{\nu\alpha}(3)\sigma_\beta(4)\cdots.\end{aligned}\right\}\tag{33}$$

Following the same methods as in Section III of IX, one finally obtains

$$\begin{aligned}(1-S^2)^{\frac{1}{2}}Q_{NQ}=&\{(1+S^2)^{-\frac{1}{2}}[2adS+ae(1+S^2)]+2^{\frac{1}{2}}[bd+cdS^2+beS+ceS]\}Q_{\sigma\pi'}\\&-\{(1+S^2)^{-\frac{1}{2}}[2aeS+ad(1+S^2)]+2^{\frac{1}{2}}[ce+beS^2+bdS+cdS]\}Q_{\sigma\pi}.\end{aligned}\tag{34}$$

It is readily verified that Eq. (34) reduces to the special equations already obtained for two special cases. Thus for $a=[(1+S^2)/2]^{\frac{1}{2}}/(1+S)$,

$$b=c=\tfrac{1}{2}(1+S),\ d=e=[2(1+S)]^{-\frac{1}{2}},$$

which corresponds to nonpolar LCAO MO's, Eq. (34) reduces to Eq. (12). For $a=d=1$, $b=c=e=0$, the pure homopolar AO case (Eq. (18)) is obtained. Table II shows the special forms which the coefficient of $Q_{\sigma\pi'}$ in Eq. (34) takes on for these and various other interesting cases. (Since $Q_{\sigma\pi}=0$ unless polarized AO's are used, the terms in $Q_{\sigma\pi}$ in Eq. (34) may ordinarily be dropped.) It also shows for these several cases

TABLE II. *Expressions and values for the coefficient of $Q_{\sigma\pi'}$ in Eq. (34) for various special cases.*

CASE	DESCRIPTION OF CASE	COEFFICIENTS IN EQS. (28), (30)	COEFFICIENT OF $Q_{\sigma\pi'}$ IN EQ. (34)	VALUES FOR $S=\frac{1}{4}$	VALUES FOR $S=\frac{1}{2}$
I	Pure homopolar AO (N and Q both pure A·X)	$a=d=1$, $b=c=e=0$	$2S/(1-S^4)^{\frac{1}{2}}$	0.50	1.03
II	State N half-ionic (25% A^+X^-, 25% A^-X^+), same as LCAO MO, state Q pure A·X	$a=[(1+S^2)/2]^{\frac{1}{2}}/(1+S)$, $b=c=1/2(1+S)$, $d=1$, $e=0$	$[(1+S)/2(1-S)]^{\frac{1}{2}}$	0.91	1.22
III	Homopolar-LCAO MO (state N 25% A^+X^-, 25% A^-X^+, state Q 50% A^-X^+)	a, b, c as in case II, $d=e=[2(1+S)]^{-\frac{1}{2}}$	$1/(1-S)^{\frac{1}{2}}$	1.15	1.42
IV	State N 50% A·X, 50% X^+A^-; state Q pure A·X	$a=b=2^{-\frac{1}{2}}[(1+S^2)^{\frac{1}{2}}/[(1+S^2)^{\frac{1}{2}}+2^{\frac{1}{2}}S]]^{\frac{1}{2}}$, $d=1$, $c=e=0$	$\{1+S[2/(1+S^2)]^{\frac{1}{2}}\}^{\frac{1}{2}}/(1-S^2)^{\frac{1}{2}}$	1.20	1.48
V	50%-polar-LCAO MO (state N 50% polar, state Q 25% A^-X^+)	(cf. Eq. (26))		1.33	
VI	State N pure A^+X^-, state Q pure A·X	$b=d=1$, $a=c=e=0$	$[2/(1-S^2)]^{\frac{1}{2}}$	1.46	1.63

the numerical values of the coefficient of $Q_{s\pi'}$ when S is set equal to the special values $\frac{1}{4}$ and $\frac{1}{2}$, approximately corresponding to HF and to HI (cf. Table IV below).

Comparing cases I and II in Table II, it is seen that strong ionicity in state N increases Q_{NQ} very considerably as compared with the homopolar AO approximation, especially if S is small. Ionicity in *both* states (which in state Q takes the form of reverse polarity) increases Q somewhat more (case III, homopolar-LCAO approximation). Strong polarity in state N (cf. cases IV, V, VI) is even more effective. Only in HF and the strongly polar metal halides, however, is the actual polarity large enough to be very important in calculating Q in the AO approximation. In the LCAO approximation, variations in polarity prove to be relatively unimportant for Q, because of the large ionicity which is always present.

Cases IV and VI in Table II should correspond fairly well to HF and CsF, respectively. In these molecules state Q should be nearly nonpolar.[3] State N can never be completely polar in the alkali halides, but should approach this most nearly in CsF.

V. The Alkyl Halides: Theory

In the spectrum of every alkyl halide, the longest wave-length electronic absorption region is an ultraviolet continuum. These continua are very similar to the $N\rightarrow Q$ spectra of the hydrogen halides, and there seems now to be little room for doubt that they are analogous to the latter. (Such an analogy has been intimated, but with hesitation, in earlier papers.[4])

The following electron configurations may then be assigned:[10]

$$\textit{AO approximation:}\quad \left\{\begin{matrix} N:(\sigma_C\cdot\sigma_X)\pi_X^4,\ ^1A_1 \\ {}^{3,1}Q:\ \sigma_C\sigma_X^2\pi_X^3,\ {}^{3,1}E \end{matrix}\right\} \tag{35}$$

$$\textit{MO approximation:}\quad \left\{\begin{matrix} N:[\sigma]^2\pi_X^4,\ ^1A_1 \\ {}^{3,1}Q\ \ [\sigma]^2\pi_X^3[\sigma^*],\ {}^{3,1}E \end{matrix}\right\} \tag{36}$$

Electrons not directly involved are omitted. The AO's σ_X and π_X are of course $np\sigma$ and $np\pi$. The simplest satisfactory AO approximation is probably that in which the σ_C AO's in (35) are the tetrahedral bond orbitals $t\sigma_C$ of Slater and Pauling, where

$$t\sigma_C=\tfrac{1}{2}(s_C+3^{\frac{1}{2}}p\sigma_C). \tag{37}$$

In (36), neglecting polarity,[10] the MO's $[\sigma]$ and $[\sigma^*]$ in LCAO approximation should be

$$[\sigma]=[2(1+S)]^{-\frac{1}{2}}(\sigma_X+[\sigma]_{CR_3}), \tag{38}$$

$$[\sigma^*]=[2(1-S)]^{-\frac{1}{2}}([\sigma]_{CR_3}-\sigma_X), \tag{39}$$

where $[\sigma]_{CR_3}$ can be taken without gross error to be $2p\sigma_C$.[11,12]

With the foregoing assumptions as to σ_C in (35), $[\sigma]$ in (38), and $[\sigma^*]$ in (39), we can proceed exactly as for HX in Section II, and arrive at equations the same as Eqs. (12), (18) there, except that $2p\sigma_C$ or $t\sigma_C$ here replaces ms_A there. Hence, putting $Q_{s\pi}=0$ and neglecting $(1-S^4)$ in the analogs of Eqs. (12), (18), and using Eq. (37), we have

$$\text{AO}:\ Q_{NQ}=2S_{t\sigma'}Q_{t\pi'}=\tfrac{1}{2}(S_{s\sigma'}+3^{\frac{1}{2}}S_{\sigma\sigma'})(Q_{s\pi'}+3^{\frac{1}{2}}Q_{\sigma\pi'}), \tag{40}$$

$$\text{LCAO MO}:\ Q_{NQ}=(1-S_{\sigma\sigma'})^{-\frac{1}{2}}Q_{\sigma\pi'}, \tag{41}$$

where

$$S_{s\sigma'}=\int(2s_C)(np\sigma_X)dv,\qquad Q_{s\pi'}=\int(2s_C)y(np\pi_X)dv,$$

$$S_{\sigma\sigma'}=\int(2p\sigma_C)(np\sigma_X)dv,\quad Q_{\sigma\pi'}=\int(2p\sigma_C)y(np\pi_X)dv, \tag{42}$$

$$S_{t\sigma'}=\int(2t\sigma_C)(np\sigma_X)dv,\quad Q_{t\pi'}=\int(2t\sigma_C)y(np\pi_X)dv.$$

[10] Polarity will not be considered here. Its effects should be closely analogous to those discussed above for HX, and should presumably not be so very important except for fluorides.

[11] Strictly, $[\sigma]_{CR_3}$ contains a considerable admixture of σ orbitals of the three R groups or atoms (cf. the type $[z]'$ in Eq. (6) of J. Chem. Phys. **1**, 498 (1933), taking $c'=[2(1+S)]^{-\frac{1}{2}}$, $d'=[8(1+S)]^{-\frac{1}{2}}$, which would correctly

In case one wishes to see how Q_{NQ} is affected by using $p\sigma_C$ or $s\sigma_C$ instead of $t\sigma_C$ for σ_C in (35), or[12] by using $t\sigma_C$ or $s\sigma_C$ instead of $p\sigma_C$ for $[\sigma]_{CR_3}$ in (38)–(39), it is only necessary to modify (40) and (41) in obvious ways.

In order to compute numerical values of Q_{NQ}, the first four integrals in Eqs. (42) must be evaluated. These integrals are similar to those for molecules AX and for mixed halogen molecules. As before, we use Slater AO's. The $np\sigma$ and $np\pi$ AO's are as given in Eqs. (12)–(13) of IX; the Z^*'s and n^*'s for halogen atoms are as given there; for carbon $2p\sigma$, $Z^*=3.25$, $n^*=2$. For carbon $2s$, taking carbon as atom A, X as atom B, the Slater AO is

$$2s_C=(h^5/3\pi)^{\frac{1}{2}}r_Ae^{-hr_A}, \tag{43}$$

with $h=Z^*/a_0n^*=3.25/2a_0$ here.

Because of the laboriousness of the calculation the integrals of Eqs. (41) have been evaluated here only for alkyl *chlorides*. Defining γ, δ, h, as in Eq. (20), except that h_C here replaces h_H there, the results can be expressed as follows,

$$S_{s\sigma'}=e^{-\gamma}[\mu/6]\sum_m\sum_n A_{mn}\gamma^m\delta^n, \tag{44}$$

$$S_{s\sigma'}=e^{-\gamma}[\mu/12^{\frac{1}{2}}]\sum_m\sum_n B_{mn}\gamma^m\delta^n, \tag{45}$$

$$Q_{s\pi'}=\tfrac{1}{2}re^{-\gamma}[\mu/\gamma\delta]\sum_m\sum_n C_{mn}\gamma^m\delta^n, \tag{46}$$

$$Q_{\sigma\pi'}=\tfrac{1}{2}re^{-\gamma}[3^{\frac{1}{2}}\mu/\gamma\delta]\sum_m\sum_n D_{mn}\gamma^m\delta^n, \tag{47}$$

where

$$\mu=10^{-\frac{1}{2}}(\gamma+\delta)^{7/2}(\gamma-\delta)^{5/2}\gamma^{-6}\delta^{-6}. \tag{48}$$

Expressions for the A's, B's, C's, and D's of Eqs. (44)–(47) have been evaluated in terms of the quantities P, Q, R, and T of Eq. (21), and tabulated as in Table I above; but to save space, this rather extensive tabulation will be omitted.

Instead of evaluating the integrals of Eqs. (44)–(47) exactly, one can make an approximation which is fairly good and which greatly simplifies the formulas and computations. This type of approximation should be especially useful for the iodides where the exact formulas would be very complex. The same kind of approximation could also have been used for the hydrogen halides, but the errors would be greater there.

Taking $Q_{\sigma\pi'}$ as an example, the exact integral, which was evaluated to give the results expressed in Eq. (47), is

$$Q_{\sigma\pi'}=\int(p\sigma)_C y(p\pi)_{Cl}d\tau=[2h_C{}^5h_{Cl}{}^7/15\pi^2]^{\frac{1}{2}}\int z_C y^2 r_{Cl}e^{-\gamma\xi}e^{\delta\eta}d\tau. \tag{49}$$

Here the exponential terms in the integrand have already been transformed to elliptical coordinates, the others not yet. The following expression is an approximation to Eq. (49):

$$Q_{\sigma\pi'}=(2/15)^{\frac{1}{2}}(\bar{h}^6/\pi)\int z_C y^2 r_{Cl}e^{-\gamma\xi}d\tau. \tag{50}$$

Here $\bar{h}$ is the average of h_C and h_{Cl}, and is equal (cf. Eq. (20)) to γ/r. Eq. (50) is obtained by replacing both h_C and h_{Cl} in Eq. (49) by their average. This (cf. Eq. (20)) causes the factor $e^{\delta\eta}$ to drop out, so that the work is greatly simplified. It can readily be verified that Eq. (50) still corresponds to the use of normalized AO's.

Using Eq. (50) and analogous simplified expressions for the other integrals, evaluation of the four integrals of Eqs. (44)–(47) for the alkyl chlorides now gives the following results:

$$S_{s\sigma'}=[e^{-\gamma}/10^{\frac{1}{2}}][\gamma^5/45+\gamma^4/9+4\gamma^3/9+\gamma^2+\gamma], \tag{51}$$

$$S_{s\sigma'}=[e^{-\gamma}/30^{\frac{1}{2}}][\gamma^5/15+\gamma^4/5+\gamma^3/15-8\gamma^2/5-5\gamma-5], \tag{52}$$

$$Q_{s\pi'}=[\tfrac{1}{2}re^{-\gamma}/10^{\frac{1}{2}}\gamma][2\gamma^5/105+23\gamma^4/105+6\gamma^3/5+68\gamma^2/15+10\gamma+10], \tag{53}$$

$$Q_{\sigma\pi'}=[\tfrac{1}{2}re^{-\gamma}/30^{\frac{1}{2}}\gamma][2\gamma^5/35+46\gamma^4/105+62\gamma^3/35+4\gamma^2+4\gamma]. \tag{54}$$

represent $[\sigma]_{CR_3}$ in LCAO approximation if all four bonds in R_3CX were equivalent and nonpolar), together with a little admixture of $2s_C$ entering because of the nonequivalence of the C–R and C–X bonds. The effect of the R admixture would be to *reduce* the calculated dipole strength of $N\rightarrow Q$ by a factor $\frac{3}{4}$. It can be shown that $2s_C$ admixture (whose amount is uncertain) *increases* the dipole strength provided its sign is such as to strengthen the C–X bonding power of $[\sigma]_{CH_3}$, as appears probably correct. Thus the net effect of both types of admixture should be roughly *nil*.

[12] One might also, using Hund's localized MO's, assume $[\sigma]_{CR_3}$ in (38) and (39) to be identical with the tetrahedral AO $t\sigma_C$ of (37). The writer believes, however, that this would make the MO approximation somewhat worse, at least for (39) and the Q state.

TABLE III. *Calculated and observed dipole strengths for $N \rightarrow Q$ transitions ($^2\Pi \rightarrow {}^2\Sigma^+$ in OH).*

Molecule	$r_e(A)$[1]	Parameters[2] γ	Parameters[2] δ	Integrals[3] Overlap	Integrals[3] Transition	Dipole Strength $D(A^2)$ Calculated D Assumptions as to bond-type[4]	Type of Approximation LCAO[5]	Type of Approximation AO[6]	Observed D[7]
HF	0.917	3.090	1.354	$0.305(S_{s\sigma'})$	$0.164(Q_{s\pi'})$	50% polar Nonpolar	{0.0524 {0.0389	{0.0421 {0.0102	——
HCl	1.275	3.657	1.248	0.456	0.224	Nonpolar	0.0924	0.0441	——
HBr	1.414					Nonpolar	[0.096]	[0.049]	0.029
HI	1.604	4.393	1.362	0.496	0.224	Nonpolar	0.0992	0.0529	Not exceeding 0.010, probably *much less*
OH	0.971	3.00	1.164	$0.346(S_{s\sigma'})$	$0.183(Q_{s\pi'})$	Nonpolar	0.0124	0.00167	Slightly more than 0.00078
CH_3Cl	1.77 ±.02	6.13	0.681	$0.324(S_{s\sigma'})$	$0.122(Q_{s\pi'})$	Nonpolar $p\sigma$ carbon valence	0.0219	0.0062	
				$0.308(S_{s\sigma'})$	$0.106(Q_{s\pi'})$	Nonpolar $s\sigma$ carbon valence	0.0161	0.0042	(0.005?)
				$0.434(S_{l\sigma'})$	$0.159(Q_{l\pi'})$	Nonpolar $l\sigma$ carbon valence	0.0445	0.0190	
CH_3Br	1.91 ±.06						Prob. sl. larger than for CH_3Cl		0.0053
CH_3I	2.12	7.07	0.548				Prob. sl. larger than for CH_3Br		0.0003

[1] The equilibrium internuclear distances r_e for the hydrogen halides and OH are from band spectra, for the methyl halides from electron diffraction.

[2] The parameters are: $\gamma = (r/2a_0)\,[(Z^*_X/n^*_X) + (Z^*_A/n^*_A)]$; $\delta = (r/2a_0)\,[(Z^*_X/n^*_X) - (Z^*_A/n^*_A)]$, where A refers to H or to C, X to the halogen atom. The numerical values of γ and δ in the tables correspond to $r = r_e$ and to $Z^* = 1, 3.25, 5.12, 6.1, 7.6, 7.6$, $n^* = 1, 2, 2, 3, 3.7, 4$ for H, C, F, Cl, Br, I, respectively.

[3] See Eqs. (21)–(23), (42), (44)–(48); also Eqs. (51)–(54) for an approximation to (44)–(47).

[4] In regard to the effects of polarity, see Sections III–IV and Table II. In regard to different possible assumptions as to the type of valence orbital used by the carbon atom in the methyl halides, see Sections V–VI.

[5] See Eqs. (12), (41); also Table II, Case V and Sections III, IV in regard to the 50% polar calculations for HF.

[6] See Eqs. (18), (40); also Table II, Case IV for the 50% polar calculation on HF.

[7] For HBr, HI, CH_3Br, CH_3I, see Table IV. For CH_3Cl, the rough qualitative information (reference 15) that the continuum is about equal in strength to that of CH_3Br has been used; it is assumed that practically the whole intensity is $N \rightarrow {}^1Q$. For OH the "observed" D value is based on Oldenberg and Rieke's observed $f = 2.80 \times 10^{-4}$ (see reference 21).

The extent to which Eqs. (51)–(54) approximate Eqs. (44)–(47) may be judged by the following numerical results computed for CH_3Cl. Using Eqs. (44)–(47) one obtains the respective values 0.324, 0.308, 0.122, 0.106 for $S_{\sigma\sigma'}$, $S_{s\sigma'}$, $Q_{\sigma\pi'}$, $Q_{s\pi'}$ (cf. Table III), while using Eqs. (51)–(54) one obtains 0.310, 0.341, 0.097, and 0.099. In judging these results, it should be kept in mind that absorption intensity involves the squares of these integrals. One sees that while the approximation here considered is not so very bad for the methyl halides, it would probably not be acceptable for the hydrogen halides, with their much larger δ/γ ratio (cf. Table III).

VI. Hydrogen and Alkyl Halides: Comparison with Experiment, and Interpretation of Ultraviolet Continua

Using Eq. (12) or (18) together with (20)–(23), or (40), (41) with (44)–(48), we can now compute numerical values of Q_{NQ} and its square D_{NQ} for the hydrogen and alkyl halides, in nonpolar LCAO and in AO approximations. The results of such computations, done in each case for the state N equilibrium separation of the nuclei, are given in Table III. For HBr, the results are interpolated between HCl and HI, while for CH_3Br and CH_3I, the results have not been calculated, but should be not far different from

those for CH_3Cl. For CH_3Cl, calculations are given not only corresponding to Eqs. (40), (41), but also for other choices of σ_C in (35) and of $[\sigma]_{CH_3}$ in (38)–(39).

The calculated D values in Table III are nearly all based on the nonpolar approximation. In the case of HF, however, calculated values for a molecule halfway between nonpolar HF and H^+F^- in structure are also given. This and other calculations (see Sections III, IV) indicate that D in the hydrogen and alkyl halides is not very sensitive to polarity in LCAO approximation, but somewhat sensitive (especially if S is small) in AO approximation. On the whole, neglect of polarity should occasion no serious error except in the fluorides.

Good experimental absorption coefficient measurements on the $N \rightarrow Q$ ultraviolet continua are available for the bromides and iodides from the work of Goodeve and collaborators.[13,14] More qualitative data exist also for the chlorides.[13,15] It appears that the $N \rightarrow Q$ spectra of the higher alkyl halides[14] are practically identical with those of the methyl halides, so we shall consider just the latter and the hydrogen halides.

Although technically the symmetry is lower in the methyl halides than in the hydrogen halides, it seems safe to assume that in the neighborhood of the carbon-halogen bond and especially in the halogen atom, the departure from cylindrical symmetry constitutes only a minor perturbation. The structure of the Q complex ($^3\Pi_2$, $^3\Pi_1$, $^3\Pi_{0^-}$, $^3\Pi_{0^+}$, and $^1\Pi$) and of the $N \rightarrow Q$ spectrum of the hydrogen halides may then be expected to recur essentially unchanged[16] in the methyl halides, since the excitation is from the halogen atom essentially into the carbon-halogen bond in MO approximation, or in AO approximation is confined to the halogen atom (cf. (35)–(36)). The close similarity of the spectra of different alkyl halides can also be understood on this basis.

It is also expected that the methyl halides should be like the hydrogen halides in dissociation behavior. Namely,[3] all components of the Q complex except Q_0 should dissociate to give a normal ($^2P_{1\frac{1}{2}}$) halogen atom, while Q_0 should give a $^2P_{\frac{1}{2}}$ halogen atom.

The observed continua for HBr, HI, CH_3Br, and CH_3I are all broad and very smooth, and all but that of CH_3I have defied any analysis into components. In HI and CH_3I, the long wave-length tail of the continuum extends far enough to indicate definitely that *at least* a small fraction of molecules dissociate to give a $^2P_{1\frac{1}{2}}$ iodine atom. It is of course not thereby excluded that part or all of the shorter wave-length region also corresponds to dissociation to give $^2P_{1\frac{1}{2}}$ iodine. In the bromides, the long wave-length tail does not extend far enough to give such information.

In the case of CH_3I, study of the distribution of intensity in the continuum by Porret and Goodeve[14] indicates the latter to be composite, with a very weak transition to a potential energy curve with lower (therefore $^2P_{1\frac{1}{2}}$) asymptote, and a strong transition to a curve with higher (hence $^2P_{\frac{1}{2}}$) asymptote. This seems to have only one possible interpretation: the very weak transition is $N \rightarrow {}^3Q_1$, the strong one $N \rightarrow Q_0$. From theory,[7] there must then also be a weak $N \rightarrow {}^1Q$ continuum, presumably concealed under that of $N \rightarrow Q_0$. This state of affairs is closely similar to that found in I_2, and we may attribute it, as there, to strong case c tendencies.

Its occurrence both in CH_3I and I_2 creates a presumption that it is characteristic of iodides, and that it probably exists also for HI. Presumably, then, it might be possible to find evidence in the HI continuum of complexity similar to that found in CH_3I. One cannot be sure, however, that the quantitative relations would be the same there. As already noted, it is sure that at least a small part of the HI con-

[13] Cf. reference 3 for review of data on hydrogen halides. Best quantitative data on HBr and HI, C. F. Goodeve and A. W. C. Taylor, Proc. Roy. Soc. **A152**, 221 (1935); **A154**, 181 (1936).

[14] Alkyl bromides and iodides: D. Porret and C. F. Goodeve, Trans. Faraday Soc. **A165**, 31 (1938). CH_3Br: P. Fink and C. F. Goodeve, Proc. Roy. Soc. **A163**, 592 (1937). Earlier literature is given in these papers.

[15] G. Herzberg and G. Scheibe, Zeits. f. physik. Chemie **7B**, 397–9 (1932): methyl halides, CH_3OH, CH_3CN, and others. A. Henrici, Zeits. f. Physik **77**, 49 (1932).

[16] Because of the trigonal symmetry in CH_3X, angular momenta are no longer strictly quantized. But further, the Jahn-Teller effect enters (H. A. Jahn and E. Teller, Proc. Roy. Soc. **A161**, 220, (1937); H. A. Jahn, Proc. Roy. Soc. **A164**, 117 (1938)), destroying the trigonal symmetry and splitting up the $^3Q_2$, $^3Q_1$, and ^1Q levels each into a double level. But because of the localization of the excitation near the X atom, it seems probable that both of these types of departure from the AX situation are relatively small in magnitude and unimportant for the present problem.

tinuum goes to a $^2P_{1\frac{1}{2}}$ asymptote, hence that $N\rightarrow{}^3Q_1$ and $N\rightarrow{}^1Q$ are at least weakly present.

In the cases of HBr and CH_3Br, no evidence of complexity has been found, although in Br_2 there is clear evidence of at least two components.[1,7] The difference may reasonably be explained by the fact that the Q state potential energy curves are much steeper in CH_3Br and HBr than in Br_2, making the separate continua of $N\rightarrow{}^3Q_1$, $N\rightarrow Q_0$, and $N\rightarrow{}^1Q$ broader so that they should overlap much more completely. Also, all the bromide are much broader than the iodide continua.

In order to obtain experimental D_{NQ} values to compare with those computed theoretically, it is necessary to eliminate from the observed intensity of each $N\rightarrow Q$ continuum that part which belongs to $N\rightarrow Q_0$. For the latter is due to case c perturbations, and does not belong to D_{NQ}.

In the absence of direct evidence in the bromides and in HI as to how much of the intensity belongs to $N\rightarrow Q_0$, we may be guided by general considerations and by analogy to what is known about Br_2, I_2, and CH_3I. The total dipole strength of the $N\rightarrow Q$ complex may be called $\Sigma G'D$, where $G'=1$ for $N\rightarrow Q_0$ but $G'=2$ for $N\rightarrow{}^3Q_1$ and for $N\rightarrow{}^1Q$.[7] D_{NQ}, which is the sum[1] of the D's for $N\rightarrow{}^3Q_1$ and $N\rightarrow{}^1Q$, is therefore given by $\frac{1}{2}(\Sigma G'D-D_{NQ_0})$. In Table IV is collected the available information on Cl_2, Br_2, and I_2 from a previous paper,[7] together with information obtainable from the work of Goodeve and co-workers on the halides.

In order to estimate D_{NQ_0} values for CH_3Br and HBr, it seems reasonable to assume that these are smaller than for CH_3I and HI roughly in the same ratio that D_{NQ_0} is smaller for Br_2 than for I_2, that is in a ratio of about 15 or about 30. (The two figures correspond to two alternative interpretations for Br_2, of which the first seems to be somewhat the more probable.[7]) For our purposes, an assumed ratio of 20 should be near enough to being correct. (The fact that the ratio of the D_{NQ_0}'s of Br_2 and Cl_2 is nearly equal to the corresponding ratio for I_2 and Br_2 gives some support to our choice.)

The probable rough correctness of our proposed procedure may be justified as follows. Since the occurrence of $N\rightarrow Q_0$ is a result of case c tendencies, we may confidently expect these to increase rapidly from CH_3Br to CH_3I, just as they do from Br_2 to I_2, and in much the same ratio. While the hydrogen halides, the methyl halides, and the halogen molecule corresponding to a given halogen atom might well differ considerably in extent of case c tendencies, it is much less likely that the *relative* strengths of these tendencies for different halogen atoms would differ greatly from hydrogen halides to methyl halide to halogen molecule.

TABLE IV. *$N\rightarrow Q$ Dipole strengths.*

MOLECULE	$\Sigma G'D\times10^3$†(A^2)	$D_{NQ_0}\times10^3(A^2)$	$2D_{NQ}\times10^3(A^2)$
Cl_2	5.7	0.1	5.6
Br_2	16.0	4, or 2	12, or 14
CH_3Br	11.2	[0.6]	[10.6]
HBr	58	[<1]	[57]
I_2	62	61	1.0 or 1.5? (very rough)
CH_3I	13	12.5	0.5‡
HI	20	[<20]	[<20]
ICl Q_a	8.6	8?	small?
ICl $Q_b(?)$	11.2	11?	small?

† The data on Cl_2, Br_2, I_2, and ICl are from Table I and Section V of reference 7. The $\Sigma G'D$ data for the other molecules are based on the absorption curves of Goodeve and co-workers. The high frequency portions of these curves have not been measured, but have been estimated by the writer, with probably no great resulting error in the $\Sigma G'D$ values.

‡ The rough value of $2D_{NQ}$ for CH_3I is obtained as follows. According to Porret and Goodeve's analysis (cf. reference 14), the part of the absorption here identified as $N\rightarrow{}^3Q_1$ corresponds to a peak absorption coefficient k_{max} of 0.3 at $\nu=35{,}000$, as compared with $k_{max}=33$ at $\nu=39{,}000$ for the main peak. Now the total dipole strength ($\Sigma G'D$) for the whole $N\rightarrow Q$ complex is found (see preceding note) to be 0.0130. That of $N\rightarrow{}^3Q_1$ is then $0.0130\times(0.3/33.3)\times(39/35)=1.3\times10^{-4}$. Since $G'=2$ for $N\rightarrow{}^3Q_1$, $D=0.65\times10^{-4}$ for the latter. This may be called D_1. Now we must estimate D_2, that is, D for $N\rightarrow{}^1Q$. For this purpose we may assume that X/a (cf. reference 7, Table II) is roughly the same as or a little larger than in I_2 (a is surely about the same, X probably somewhat larger). This leads (cf. reference 7, Table II) to an estimate of very roughly 3 for the ratio D_2/D_1, and so to the rough value 2.7×10^{-4} for $D_2+D_1=D_{NQ}$.

Using the assumed D_{NQ_0} ratio of 20 from iodide to bromide, the bracketed items in Table IV are secured. We see that, by a wide margin of safety, only a small fraction of the total intensity in HBr and CH_3Br can reasonably be attributed to $N\rightarrow Q_0$. (It should be noted that, assuming the ratio 20 to be correct, the *upper limits* for the D_{NQ_0} values for the bromides are independent of any assumptions as to the correctness for the iodides of anything but $\Sigma G'D$, and that these upper limit values are still small.) It appears, then, that we now have rather reliable D_{NQ} values for the bromides (see Tables III, IV), and for CH_3I.

The only remaining question is about HI. By analogy with I_2 and CH_3I, it is *likely* that D_{NQ} is

very small, and that nearly the whole of $\Sigma G'D$ belongs to $N \rightarrow Q_0$. There is, to be sure, no guarantee of this; but in any case, D_{NQ} is certainly much smaller for HI than for HBr (cf. Table IV). This empirical result does not at all correspond to the theoretical calculations (cf. Table III), but the same anomaly occurs in CH_3I and in I_2, in both cases associated with abnormally high $N \rightarrow Q_0$ intensity. It seems safe to attribute these associated anomalies in all three iodides to strong case *c* influences not allowed for in the theoretical calculation, just as we did previously for I_2.[7]

In HBr and CH_3Br (and CH_3Cl), where case *c* influence is of minor importance, there is a gratifying parallelism between observed and calculated values of D_{NQ}, of the same type found previously in F_2, Cl_2, and Br_2. Thus D_{NQ} is several times larger for HBr than for CH_3Br and Br_2, both by calculation and by experiment. In each case the observed values are somewhat smaller than the AO calculated values, and several times smaller than the LCAO calculated values, as also for F_2 and Cl_2. A similar kind of agreement is found for the $^2\Pi \rightarrow {}^2\Sigma^+$ transition of OH, as will be shown in Section VIII.

VII. General Remarks and Conclusions on $N \rightarrow Q$ Transition Moments and on Molecular Structure

The correctness of the statement made in Section VI that the agreement between theory and experiment is of the same kind for CH_3Br as for HBr, Br_2, Cl_2, F_2, and OH depends somewhat on whether one assumes an *s*, a $p\sigma$, or a tetrahedral valence orbital for the carbon atom in the C−Br bond. If a pure $p\sigma$ valence orbital is assumed, the agreements are *closer* than for HBr, Br_2 and the others. If a pure tetrahedral valence orbital is assumed, the agreements are less close than in the other cases. Something intermediate between a $p\sigma$ and a tetrahedral orbital (corresponding to a reasonable structure) leads to the same degree of agreement for CH_3Br as for HBr and the others.

By way of explanation of the larger D_{NQ} (both calculated and observed) for HBr than for Br_2, the greater stability of the molecule may be cited. This should increase the integrals which govern the value of *D*. The fact that the AO and LCAO calculated values are somewhat closer together for the hydrogen halides than for the halogens is presumably attributable to the same cause.

A striking fact shown by Table III is that the calculated *S*, $Q_{s\pi'}$, and Q_{NQ} are nearly alike for HCl and HI (and presumably HBr), and much smaller for HF. Further, the $S_{s\sigma'}$ values are strikingly large for HCl, HI. Similar relations between the calculated values for Cl_2, Br_2, and I_2 as compared with those for F_2 are shown in Table I of IX; and in that case are confirmed by a like behavior of the experimental D_{NQ} values. These calculations and observations suggest that np orbitals with $n>2$ are more effective than $2p$ orbitals in their overlapping with orbitals of other atoms. This appears reasonable when one considers how the shapes of the outer parts of np orbitals are altered when $n>2$. Such relative favorableness of overlapping for np when $n>2$ has bearings on the problem of the strengths of chemical bonds.

VIII. The $^2\Sigma^+ \rightleftarrows {}^2\Pi$ System of the Hydroxyl Radical

Of considerable chemical and astrophysical interest is the $^2\Sigma^+ \rightleftarrows {}^2\Pi$ transition in OH. This is conveniently treated here, since it involves the same integrals as $Q \leftarrow N$ of HF, although of course with different parameters.

The electron configurations are:

$$\textit{AO approximation neglecting polarity:} \quad \left\{ \begin{matrix} (1s_H \cdot \sigma_O)\pi_O{}^3, \ ^2\Pi \\ 1s_H\pi_O{}^4, \ ^2\Sigma^+ \end{matrix} \right\} \tag{55}$$

$$\textit{MO approximation:} \quad \left\{ \begin{matrix} \sigma^2\pi_O{}^3, \ ^2\Pi \\ \sigma\pi_O{}^4, \ ^2\Sigma^+ \end{matrix} \right\} \tag{56}$$

In LCAO approximation, the σ MO of (56) is

$$\sigma \approx k(2p\sigma_O) + l(1s_H). \tag{57}$$

The MO wave functions are

$$\left. \begin{aligned} \psi_\alpha(^2\Pi_y) &= (n!)^{-\frac{1}{2}} \sum_P \pm P\sigma_\alpha(1)\sigma_\beta(2)\pi_{y\alpha}(3)\cdots, \\ \psi_\alpha(^2\Sigma^+) &= (n!)^{-\frac{1}{2}} \sum_P \pm P\sigma_\alpha(1)\pi_{y\beta}(2)\pi_{y\alpha}(3)\cdots, \end{aligned} \right\} \tag{58}$$

with analogous expressions for $\psi_\beta(^2\Pi_y)$, $\psi_\beta(^2\Sigma^+)$,

$\psi_\alpha(^2\Pi_x)$, and $\psi_\beta(^2\Pi_x)$. Proceeding as usual, we find

$$Q=\int \psi_\alpha(\Pi_y)\Sigma_{y_i}\psi_\alpha(\Sigma)d\tau=\int(\sigma)y(2p\pi_y)dv. \quad (59)$$

In nonpolar LCAO approximation (using Eq. (57) for σ, with $k=l$), Eq. (59) yields

$$Q=[2(1+S_{s\sigma'})]^{-\frac{1}{2}}(Q_{s\pi'}+Q_{\sigma\pi}), \quad (60)$$

with $S_{s\sigma'}$, $Q_{s\pi'}$, $Q_{\sigma\pi}$ as in Eqs. (13); $Q_{\sigma\pi}=0$ unless polarized oxygen AO's are used. Eq. (60) is similar to Eq. (12) for the transition $N\rightarrow Q$ in AX, but differs in that plus signs appear here in place of minus signs there, also, more important, in the occurrence of an extra factor $2^{-\frac{1}{2}}$. Hence, in case $Q_{s\pi'}$ should be about the same as there, D would be reduced by approximately a factor $\frac{1}{2}$ compared with D_{NQ} of AX.[17]

The total absorption intensity or f value, which is proportional to $G'D$, is further reduced by a second factor $\frac{1}{2}$, because here $G'=1$, as compared with $G'=2$ for AX. This can be seen by reference to an earlier paper.[18] It must be kept in mind when experimental data are used to obtain an experimental D.

In nonpolar AO approximation,

$$\psi_\alpha(^2\Pi_y)=[2(1+S^2)n!]^{-\frac{1}{2}}\sum_P \pm P[s_\alpha(1)\sigma_\beta(2)\pi_{y\alpha}(3)\cdots+\sigma_\alpha(1)s_\beta(2)\pi_{y\alpha}(3)\cdots], \quad (61)$$

$$\psi_\alpha(^2\Sigma^+)=(n!)^{-\frac{1}{2}}\sum_P \pm P s_\alpha(1)\pi_{y\beta}(2)\pi_{y\alpha}(3)\cdots. \quad (62)$$

Using these equations, we obtain

$$Q=[2(1+S^2)]^{-\frac{1}{2}}(SQ_{s\pi'}+Q_{\sigma\pi}). \quad (63)$$

Comparing Eqs. (60), (63) with the corresponding Eqs. (12), (18) for Q_{NQ} of AX, and putting $Q_{\sigma\pi}=0$ in all, it is seen that Q^2 here is smaller than Q_{NQ}^2 there by a factor of about $\frac{1}{2}$ according to the LCAO equations (as already noted), but by a factor of about $\frac{1}{8}$ according to the AO equations. Thus the two approximations here diverge more than usual.

It is now of great interest that Oldenberg and Rieke[19] have obtained experimental measurements of absorption strengths for some of the OH band lines. Their results were reported in the form of f values. As has been pointed out previously,[18] a correct measure of the dipole strength for a molecular electronic transition is obtainable by summing the dipole strengths over *all* band lines arising from a common initial detailed level and going to various upper vibrational, rotational, and spin levels; and the result should be practically the same for *any* initial level under ordinary circumstances, regardless of the latter's vibrational, rotational, spin, or other fine-structure quantum numbers. Any degeneracy in an initial level needs to be considered only in respect to its effect on the population of that level. Hence we have,[20] for our case, in square angstroms,

$$D=(9.12\times10^4)(\Sigma f)/G'\nu, \quad (64)$$

with ν in cm^{-1} and $G'=1$ as noted in an earlier paragraph; the summation is to be taken over all lines of the band system which arise from any given initial level.

Using Oldenberg and Rieke's data for various initial levels,[21] an average experimental D as

[17] The reason for this factor $\frac{1}{2}$ here is to be found in the fact that in the absorption transition in OH, a σ electron of σ^2 jumps into a π shell containing initially only *one* vacancy, whereas in the transition $N\rightarrow Q$ in HX, a π_y electron of π_y^2 (*or*, a π_x electron of π_x^2) jumps into a σ^* shell initially empty and so containing *two* vacancies.

[18] R. S. Mulliken, J. Chem. Phys. **7**, 17–18 (1939). The real reason for $G'=2$ in HX is that the jump $\pi\rightarrow\sigma^*$ (cf. reference 17) is from a shell containing two full sub-shells (π_x^2 and π_y^2). From *each* of these, with equal probability corresponding to D_{NQ}, an electron can jump, so that the total probability of a jump is doubled. In OH, there is no such factor, since the jump is from a single (σ) shell.

[19] O. Oldenberg and F. F. Rieke, J. Chem. Phys. **6**, 439 (1938).

[20] See reference 12, Eq. (10).

[21] Referring to Oldenberg and Rieke's Table II, giving f values for individual lines, it is found that the necessary f's to form the desired Σf's are available only for six initial levels. These are levels from which should arise the lines $Q_1(J)$, $^QP_{21}(J)$, and $^SR_{21}(J)$. Now Oldenberg and Rieke give f values for $Q_1(J)$ and for $^QP_{21}(J)$ for J values ranging from 3/2 to 13/2, for the 0,0 band. Since the $^SR_{21}(J)$ branch is very much weaker than the others, the absence of data on its lines will not appreciably affect the desired Σf, which then becomes the sum of the f's for $Q_1(J)$ and $^QP_{21}(J)$ only, taken over all bands. Actually there are data only on the 0,0 band, but it is known that other bands are much weaker, so that their omission should not cause much error in Σf. Adding the f's of $Q_1(J)$ and $^QP_{21}(J)$ gives $\Sigma f=2.78$, 2.80, 2.76, 2.81, 2.82, 2.85, all times 10^{-4}, for $J=3/2$, 5/2, $\cdots$ 13/2. The average value is 2.80×10^{-4}. Possibly 3.0×10^{-4} would be better when allowance is made for bands other than the (0,0).

given in Table III is obtained. The corresponding theoretical values of D were obtained using Eqs. (60), (63) with $Q_{\sigma\pi}=0$, and employing Eqs. (22), (23) and Table I, with suitable values of r, γ, and δ as given in Table IV, in order to compute S and $Q_{s\pi'}$. The agreement between observed and computed D values is of much the same kind found for HBr, CH_3Br, F_2, Cl_2, and Br_2. This gives confidence as to the possibility of making valid predictions for $N\rightarrow Q$ and related transitions in the case of molecules where experimental data are not available. Such predictions would be of great value for a number of molecules of astrophysical importance.[22]

Before concluding, it is advisable to examine the effect of polarity on the calculation, since OH is probably rather strongly polar. Taking first the LCAO approximation, it is easily found that, for $k\neq l$ in Eq. (57), Eq. (60) is replaced by

$$Q=lQ_{s\pi'}+kQ_{\sigma\pi}. \tag{65}$$

Since l is decreased by polarity in OH, Q is thereby decreased. Thus the effect is opposite in sign to that in HF. In magnitude the effect is easily found to be of minor importance, as in HF.

In order to determine the effect of polarity in the AO approximation, we may as well first obtain the most general expression for the transition moment Q using wave functions having any degree of ionicity and polarity (cf. Section IV and Eq. (34) for AX). The wave functions are now

$$\psi(^2\Pi)=a\psi[(\sigma_O\cdot 1s_H)\pi_O{}^3]+b\psi(\sigma_O{}^2\pi_O{}^3)+c\psi(1s_H{}^2\pi_O{}^3), \tag{66}$$

$$\psi(^2\Sigma^+)=d\psi(1s_H\pi_O{}^4)+e\psi(\sigma_O\pi_O{}^4).$$

The corresponding Q expression is found to be

$$Q=\{[2(1+S^2)]^{-\frac{1}{2}}a(dS+e)+c(d+eS)\}Q_{s\pi'}+\{[2(1+S^2)]^{-\frac{1}{2}}a(d+eS)+b(dS+e)\}Q_{\sigma\pi} \tag{67}$$

On putting $a=d=1$, $b=c=e=0$, this reduces as it should to the nonpolar AO equation (63), and on putting $a=[(1+S^2)/2]^{\frac{1}{2}}/(1+S)$, $b=c=1/2(1+S)$, $d=e=1/[2(1+S)]^{\frac{1}{2}}$, it reduces to the nonpolar-LCAO equation (60).

Examination of Eq. (67), starting from the AO approximation, shows that polarity (increase in b and e) has little effect on the value of Q. For example, after putting $Q_{\sigma\pi}=0$, one calculates Q for OH to be 0.20 $Q_{s\pi'}$ if there is no polarity ($a=d=1$), while for the strong polarity corresponding to $a=b$, $c=0$, $d=e$, Q is again 0.20 $Q_{s\pi'}$, practically unchanged. On the other hand, ionicity greatly increases Q, as is seen by comparing the nonpolar AO and LCAO equations (63) and (60).

[22] Cf. F. E. Roach, Astrophys. J. **89**, 99 (1939); R. S. Mulliken, Astrophys. J. **89**, 283 (1939).

The Reactions of Ethyl Radicals

WALTER J. MOORE, JR., AND HUGH S. TAYLOR
Frick Chemical Laboratory, Princeton University, Princeton, New Jersey

(Received February 26, 1940)

The photochemical investigation of the decompositions of diethyl zinc and diethyl mercury has established that the products in each case consist principally of ethane, ethylene, and butane, with smaller amounts of hydrogen and butylene. The composition of the product varies with the alkyl, but does not change markedly with temperature from 45° to 250°. An examination of the effects of varying the concentration, intensity of radiation, packing of reaction vessel, and inert gas pressure leads to the conclusion that butane is formed by the combination of two ethyl radicals produced in the primary process, while ethane and ethylene arise from a reaction between ethyl radicals and metal alkyl molecules. The reaction between ethyl radicals and hydrogen becomes measurable at about 160°, and by analogy with the corresponding process with methyl radicals may be assigned an activation energy of 9 ± 2 kcal. The reaction $C_2H_5+H=2CH_3$ proceeds rapidly at 100°. The investigation of the photolysis of ethyl iodide in the presence of mercury vapor and the mercury photosensitized hydrogenation of ethylene supports the conclusions based on the metal alkyl studies.

THE reactions of methyl radicals derived from mercury dimethyl have recently been described by Cunningham, Smith and Taylor.[1,2] The present investigation represents an extension of these studies to ethyl radicals produced under nearly identical experimental conditions.

Earlier studies of the metal ethyls have been confined to pyrolyses at such high temperatures that secondary processes have obscured the ethyl radical reactions. If the free radicals are produced photochemically, however, it is possible to work in a temperature range where only processes having a low activation energy need be considered. Previous results obtained in this way are summarized subsequently (Table V) together with those obtained in the present investigation with mercury and zinc ethyls as the radical source. In addition to these latter, a few experiments on the mercury photosensitized hydrogenation of ethylene, and on the photolysis of ethyl iodide in presence of mercury vapor will be reported.

Thompson and Linnett[3] have made extensive studies of the absorption spectra of the metal alkyls. The spectra of the zinc and mercury ethyls are very similar, each consisting of a region of continuous absorption followed by a system of diffuse bands at lower wave-lengths. The long wave-length limits of the continua are found to be 2500A for diethyl mercury and 2800A for diethyl zinc.

Experimental Details

Apparatus

The apparatus used for these experiments was essentially similar to that designed by Cunningham and Taylor for the study of the dimethyl mercury decomposition.

The reaction vessel was a quartz cylinder of 30 mm diameter and about 125 cc volume. The remainder of the apparatus was of Pyrex glass. The metal alkyls were kept in glass tubes surrounded by a freezing mixture of solid carbon dioxide and acetone, and separated from the reaction vessel by a mercury cut-off in the case of the mercury diethyl or an all-metal valve in the case of zinc diethyl. In this way the alkyls were kept from all contact with stopcock grease in which they are extremely soluble.

At the beginning of each run the freezing trap was removed from the alkyl reservoir and the vapor allowed to expand into a bulb of volume appropriate to the amount needed for the run. This amount of vapor was cut off from the reservoir and condensed into the reaction vessel, which was then sealed off from the apparatus. Irradiation was carried out in a furnace fitted with a quartz window. After irradiation the reaction vessel was sealed back to the apparatus, and the product gases removed from the illumi-

[1] J. P. Cunningham, thesis, Princeton University, 1937; Taylor and Cunningham, J. Chem. Phys. **6**, 359 (1938).
[2] J. O. Smith, thesis, Princeton University, 1938; Smith and Taylor, J. Chem. Phys. **7**, 390 (1939).
[3] Thompson, Proc. Roy. Soc. **A150**, 603 (1935); Thompson and Linnett, *ibid.* **A156**, 108 (1936).

nation system after breaking an internal glass capillary in the exit tube of the vessel by means of a magnetically operated plunger.

The radiation source was an arc of the mercury in quartz type, operated hot at 50 volts and 3 amperes d.c. Under these conditions careful tests by Cunningham had demonstrated the complete reversal of the mercury resonance line at 2536.7A. When a source of resonance radiation was required a low pressure cold arc, of the type containing inert gas, was employed, which operating at 500 volts and 50 milliamp. a.c. furnished an intense resonance radiation.

The remainder of the apparatus consisted of a gas burette for measuring the pressure of gases at constant volume, a trap which when cooled with various freezing mixtures permitted successive fractions of the product hydrocarbons to be taken for analysis, a system of Toepler pumps for transferring the gases within the apparatus, and an arrangement for analyzing the products.

The method of analysis

The analytical method is based on the work of Trenner, Morikawa and Taylor[4] on the catalytic cracking of hydrocarbons to methane, which takes place on an active nickel catalyst and in the presence of an excess of hydrogen without any concomitant carbonization. If this method is applied, instead of the usual combustions, in order to find an average carbon number for an unknown hydrocarbon, or mixture of hydrocarbons, two checks are afforded of the accuracy of the determination, the amount of methane formed and the amount of hydrogen consumed. Unsaturates may be determined by hydrogenation on the same catalyst at 100°, the cracking reaction occurring at around 300°.

The total amount of gaseous products formed in these experiments averaged two to three cc. In the photolyses of mercury and zinc diethyls this might possibly consist of: hydrogen, methane, ethane, propane, propylene, butane, butylene, and small amounts of higher hydrocarbons. Actually, however, no propane or propylene and only traces of methane were ever found.

A fraction consisting of methane and hydrogen is pumped off from a trap chilled in liquid air, the hydrogen burned on cupric oxide at 300°, the water formed condensed in a trap at −78°, and the residual gas recorded as methane.

A second fraction is taken at −138°, the melting point of ethyl chloride, which should contain all of the ethylene, most of the ethane, considerable amounts of any C_3 hydrocarbon that might be present, and perhaps traces of butane and butylene carried over by the evolved gases. Using known mixtures of ethane, ethylene, and butane it was demonstrated that all of the ethylene, most of the ethane, and no detectable amount of butane were pumped off at −138°. The absence of C_3 hydrocarbons in the fraction was established by catalytic cracking, which always gave a value for the average carbon content of 2.00 ± 0.02. Unsaturates are determined by hydrogenation on nickel at 100°, the decrease in pressure being recorded as ethylene.

A third fraction, consisting of butane and butylene, plus residual ethane, is pumped off at −78°, and similarly hydrogenated to determine butylene. The mixture of ethane, butane, and excess hydrogen is then cracked at 300°, excess hydrogen burned over cupric oxide, and the amount of methane formed is measured. From the average carbon content of the cracked hydrocarbons thus obtained, and the unsaturate analyses, one may calculate the composition of the product gases. This procedure obviates any necessity of relying on the doubtful fractionation of ethane from butane. We believe that the determination of the average carbon number can be made with an accuracy of at least ±0.05, which is considerably better than is realized by the usual combustion methods.

Materials

Mercury diethyl was prepared by the method of Marvel and Gould[5] as modified by Gilman and Brown.[6] It was distilled from fused calcium chloride, and finally purified by repeated fractionations at low pressure. When kept cooled to −78° and shielded from light, it underwent no detectable decomposition.

[4] Trenner, Morikawa and Taylor, J. Am. Chem. Soc. **59**, 1103 (1937).

[5] Marvel and Gould, J. Am. Chem. Soc. **44**, 153 (1922).

[6] Gilman and Brown, J. Am. Chem. Soc. **52**, 3314 (1930).

TABLE I. *Zinc diethyl.*

RUN	TEMP.	MOLES PERCENT IN PRODUCT				
		H_2	C_2H_4	C_2H_6	C_4H_{10}	C_4H_8
C13	45	10	28	27	19	16
C15		9	31	28	23	9
C14	100	9	26	26	31	8
C24	160	9	19	32	31	9
C16		10	24	23	34	11
C27		10	24	22	34	12
C29		10	26	21	34	9
C19	200	8	19	29	35	9
C26		6	19	27	39	9
C18		9	16	30	38	7
C20	250	1	19	35	36	9
C22		1	12	41	35	11
C25		2	15	33	38	12
C28		2	10	38	39	11
C30		3	11	33	41	12
C17†	250	0	10	31	46	13
C23*	200		19	37	34	10
C31*			23	41	28	8
C21*	250		12	52	26	10
C32*			7	51	33	9

* Starred runs with addition of 200 mm hydrogen.
† Thermal decomposition.

Zinc diethyl was an Eastman product, purified by fractional distillation at low pressure and temperature.

Ethyl iodide, Merck's reagent grade, was purified by low pressure distillation.

Tank hydrogen which had been prepared electrolytically was passed over platinized asbestos at about 300°, then through a trap cooled in liquid air. A sample of the purified hydrogen left no residue volatile at −78° when burned on cupric oxide at 300°. Tank nitrogen was passed over freshly reduced copper at 450°, through a liquid-air trap, and was kept in a bulb coated with metallic calcium.

Ethylene, Ohio Chemical Company, was purified by condensing a sample in liquid air, pumping away about one-third and retaining a middle third for use. On hydrogenation it was found to contain 100.1 percent unsaturates, and cracked to give av. *C.* 1.99.

Ethane was prepared by hydrogenation of the purified ethylene, repeatedly pumping off excess hydrogen from liquid air. Butane, 99 percent pure, Ohio Chemical Company, was purified as outlined for ethylene, cracked to av. *C.* 3.97.

The nickel catalyst was similar to that used in the experiments of Morikawa, Benedict and Taylor[7] where it is described as follows: "The nickel catalyst was a very active nickel-*kieselguhr* preparation, made by precipitation of the carbonate on *kieselguhr*, ignition, and reduction in hydrogen at progressively increasing temperature to 450°. It contained 15 percent nickel."

EXPERIMENTAL RESULTS

Diethyl zinc

The results of the photolysis of diethyl zinc are recorded in Table I. In each run a pressure of diethyl zinc equivalent to 25 mm in the volume of the reaction vessel was taken, and observations were carried out over a range of temperature from 45 to 250°. Even at the highest temperature the thermal decomposition was negligible compared with the photochemical. During the course of the reaction a film of zinc was deposited on the walls of the quartz vessel, so that reproducible rate measurements were not possible.

At 250° in the presence of 200 mm hydrogen only a trace of methane was found in the reaction products, amounting to less than 1 percent of the total; in the runs without added hydrogen no methane was detected. Besides the lower hydrocarbons reported in Table I, there was

TABLE II. *Mercury diethyl.*

RUN	TEMP.	MOLES PERCENT IN PRODUCT					RATE MM/MIN.
		H_2	C_2H_4	C_2H_6	C_4H_{10}	C_4H_8	
22	45	1	25	29	38	7	0.70
23		2	25	27	38	8	0.72
24	100	1	21	33	37	8	1.25
25		1	22	30	38	10	1.26
26		1	21	30	41	7	0.96
28	160	4	20	31	34	11	1.55
29		2	22	30	37	9	1.52
30	200	1	20	41	30	9	1.89
31		2	15	40	34	9	1.87
37		1	21	36	33	9	1.89
34	250	1	20	42	28	9	2.26
35		1	19	37	34	9	2.43
36		2	19	37	33	9	2.35

[7] Morikawa, Benedict and Taylor, J. Am. Chem. Soc. **58**, 1445 (1936).

also formed a small amount of higher hydrocarbons. At lower temperatures this amounted to about 1 percent of the products, increasing to 2–3 percent at 250°. The higher hydrocarbons were presumably mostly hexane, octane, and perhaps polymerized ethylene C_nH_{2n}.

At lower temperatures the products are seen to be (1) ethane and ethylene in amounts equal within the experimental accuracy of the analyses except for a possible slight deficit of ethylene that may have polymerized, (2) equivalent amounts of butylene and hydrogen, and (3) a considerable amount of butane. As the temperature is raised the proportion of butane increases at the expense of the ethane and ethylene. Beginning at about 160° the hydrogen formation is diminished by some process with a marked temperature dependence, for, at 250°, hydrogen has practically disappeared from the reaction products. This disappearance is not, however, paralleled by a disappearance of butylene which is formed in constant quantity over the whole temperature range. The ratio of hydrogen to carbon in the products is maintained as 2.5 by an increased formation of ethane and decreased formation of ethylene at the higher temperatures.

The addition of 200 mm of hydrogen leads to an increase in ethane production, which first becomes apparent at around 200° and appreciable at 250°. The reaction of added hydrogen is thus similar to that of the small amounts produced endogenously in the same temperature range.

TABLE III. *Mercury diethyl in presence of hydrogen.*

Run	Temp.	mm H_2	Moles percent in Product				Rate mm/min.
			C_2H_4	C_2H_6	C_4H_{10}	C_4H_8	
47	100	200	21	38	38	3	1.33
46	160	200	15	47	33	5	1.60
44							1.98
45	200	200	16	51	30	3	2.47
42			16	56	23	5	2.06
38			9	50	38	3	2.38
55	250	700	1	90	9	0	—
41		200	8	64	23	5	4.06
40			9	60	27	4	4.22
39			8	61	24	7	3.94
48		100	12	56	25	7	2.63
49		50	14	48	33	5	2.90

TABLE IV. *Variation of conditions of mercury diethyl photolysis.*

Run	Temp.	Remarks	Moles percent in Product					
				H_2	C_2H_4	C_2H_6	C_4H_{10}	C_4H_8
27	100	+10% H_2		11	—	—	—	—
58	160	10X concentration 1/10 intensity		0.5	21.5	45	23	10+higher hydrocarbons
59	160	15X concentration normal intensity		1	25	33	37	4
60	160	+500 mm N_2		—	20	27	47	6
61	160	Packed vessel		6	20	20	48	6
62	160	Normal concentration and intensity. Unpacked vessel		3.5	22	26.5	38	10
63	100	Packed vessel		7	23	20	42	8
			CH_4	C_2H_4	$C_2H_6+C_3H_8$		C_4H_{10}	C_4H_8
57	100	+200 mm H_2 and mercury resonance radiation	28	3	50		17	2

Diethyl mercury

The mercury diethyl results are recorded in Tables II, III and IV.

In the runs in Table II, the alkyl pressure was 25 mm. The striking difference between these and the zinc ethyl results is the lesser amount of hydrogen and greater amount of ethane formed from the mercury compound. That this is not due to some reaction leading to removal of hydrogen after it has been formed is shown by run 27. Ten percent of hydrogen was added before photolysis, eleven percent being recovered from the reaction products. As with zinc diethyl the thermal decomposition is unimportant even at 250°.

There appears in this case to be a slight decrease, rather than an increase, in butane production with temperature. The proportions of ethylene, butylene, and hydrogen remain sensibly constant over the temperature range; that of ethane shows a slight but definite increase.

The over-all rate of reaction exhibits a threefold increase in the two hundred-degree range covered by these experiments, suggesting that the quantum yield of the photolysis rises with temperature, as is the case with dimethyl mercury.[8] On adding hydrogen, an increased rate of decomposition is noted, with an increased formation at lower temperature of both ethane and butane. The quantity of hydrogen reacting and of ethane formed increases rapidly with increasing temperature. The effect of added

[8] Linnett and Thompson, Trans. Faraday Soc. **33**, 501, 874 (1937).

TABLE V. *The products from ethyl radicals prepared from various sources.*

Source of Ethyls	Temp.	Moles percent in Product of					
		H_2	CH_4	C_2H_4	C_2H_6	C_4H_{10}	C_4H_8
EtBr+Na, EtCl+Na (Bawn and Dunning)[1]	350°	0	0	0	0	100	0
Et_2CO photolysis (Noyes and Ells)[2]	30	0	0	10	10	80	0
Mercury photosensitized hydrogenation of ethylene	25	—	4	—	16	80	0
Mercury diethyl photolysis	45	2	0	25	29	38	7
Zinc diethyl photolysis	45	10	0	25	22	34	9
Lead tetraethyl pyrolysis (Meinert)[3]	150	1	0	38	46	14	2
Ethyl iodide+Hg vapor photolysis	100	1	0	29	43	15	12
Ethyl iodide photolysis (West and Schlessinger)[4]	25	0	0	50	50	0	0

[1] Trans. Faraday Soc. **35**, 898 (1939).
[2] J. Am. Chem. Soc. **61**, 2492 (1939).
[3] J. Am. Chem. Soc. **55**, 979 (1933).
[4] J. Am. Chem. Soc. **60**, 961 (1938).

hydrogen is much more prominent here than with diethyl zinc, and even at 100° there is a definite change in the character of the decomposition products. The effect of varying hydrogen pressure is shown in the series of runs at 250°; with 700 mm of hydrogen, 90 percent of the product is ethane, compared with 48 percent with 50 mm of hydrogen.

In Table IV are the results of varying the conditions under which the photolyses were carried out. When the mercury diethyl pressure is increased, and when the light intensity is simultaneously decreased, there is a considerable increase in ethane formation together with the formation of considerable higher hydrocarbon, presumably polymerized ethylene.

The addition of 500 mm of nitrogen or packing of the reaction vessel increases the proportion of butane in the products.

In run 57 is reported an experiment in which mercury diethyl and 200 mm of hydrogen at 100° were illuminated with mercury resonance radiation. At this temperature reaction with molecular hydrogen is inappreciable. Methane accounts for 28 percent of the product.

Discussion of Results

The primary photolytic process which follows light absorption by the metal alkyls in the continuum around 2500A has been postulated as a dissociation of the molecule with free radical formation, according to one or both of the mechanisms[1,9]

$$R_2M+h\nu=R+RM$$
$$\text{or } R+R+M.$$

In Table V are summarized the final fates of ethyl radicals obtained in the present investigation, together with certain pertinent results of earlier workers. The products vary from 100 percent butane, in the case of the Polanyi type experiments, to 100 percent of ethane and ethylene in the case of ethyl iodide.

The rapid removal of metallic mirrors by free radicals emphasizes the possibility that recombinations of ethyls with zinc or mercury to reform the original metal alkyl may be an important secondary process. The formation of mercury diethyl in the mercury photosensitized hydrogenation of ethylene was detected by the faint but unmistakable odor of the alkyl on opening the reaction vessel, after pumping off the more volatile products.

The increased quantum yield at higher temperatures may be ascribed, as in the dimethyl mercury case, to a chain mechanism

$$C_2H_5+(C_2H_5)_2M=C_4H_{10}+C_2H_5+M$$
$$\text{or } C_2H_6+C_2H_4+C_2H_5+M.$$

The formation of butane may also occur by combination of two ethyl radicals either bimolecularly or as three-body process in the gas phase or at the wall. It has been stated that the bimolecular formation of ethane from two methyls is a very rare occurrence,[10] but the greater complexity of the ethyl, as compared with the methyl radical should facilitate the process of internal stabilization following a collision between the two radicals. The increased formation of butane on packing the reaction vessel or adding an inert gas indicates, however, that the three-body recombination is still a factor of some importance.

The temperature dependence of the proportion of butane from diethyl zinc might be ascribed to a slightly higher activation energy for the combination of two ethyls on zinc as compared

[9] Linnett and Thompson, Trans. Faraday Soc. **33**, 874 (1937).
[10] Kassel, J. Chem. Phys. **5**, 922 (1937).

with quartz. It is also probable that the reaction

$$C_2H_5+Zn(C_2H_5)_2=C_4H_{10}+ZnC_2H_5$$

has a higher activation energy than the corresponding reaction with mercury diethyl, due to the greater strength of the Zn−C bond.[11,12]

The disproportionation reaction

If the disproportionation of two ethyl radicals to ethane and ethylene occurs bimolecularly in the gas phase, the activation energy, E, in order to account for the results of Bawn and Dunning, must be at least four kcal. greater than that for the combination of the radicals. It is possible, however, that some of the butane formation observed by Bawn and Dunning occurs through the intermediacy of sodium ethyl at the walls of the reaction vessel. Although we do not believe that disproportionation is an important process at the low temperatures of the present investigations, it may be of much greater significance at the higher temperatures prevailing in the pyrolyses of hydrocarbons.

The large formation of ethane and ethylene observed in the photolysis of ethyl iodide, the considerable formation from the metal alkyls, and the small quantity formed from diethyl ketone must all be ascribed to reactions of the type

$$C_2H_5+(C_2H_5)_nX = C_2H_6+C_2H_4+(C_2H_5)_{n-1}X. \quad I$$

The activation energy for this reaction will be at most two to three kcal. greater than that for combination of ethyls to form butane. The ethane-ethylene fraction from mercury diethyl increases with increase in pressure of the alkyl and decrease in light intensity, which is to be expected if it depends on a reaction such as I, while butane is formed by the combination of two ethyl radicals.

The most important of the factors responsible for the large variation in products between, e.g., ethyl iodide and diethyl ketone as a source of ethyl radicals is the correspondingly large variation in the ethyl radical concentrations from these compounds. An ethyl radical will combine with an iodine atom much more efficiently than with another ethyl or with a propionyl radical. This is because of the greater probability of formation of the activated state in a reaction involving an atom and a radical as compared wih a reaction between two complex radicals. Thus Bawn[13] has estimated that the steric factor for $C_2H_5+I=C_2H_5I$ is unity, compared with a value of around 10^{-4} for $C_2H_5+C_2H_5=C_4H_{10}$. Since the formation of butane depends on the square of the ethyl radical concentration, while the reaction equivalent to disproportionation depends only on the first power, any decrease in the radical concentration will favor the formation of ethane and ethylene.

However, even when a large proportion of the iodine atoms are removed during the photolysis of ethyl iodide by the addition of mercury vapor to the system, the butane formation is still small (around 20 percent), and factors other than the variation in radical concentration must also be considered to explain the variation in products between diethyl ketone, the metal ethyls, and ethyl iodide. One may reasonably expect slight differences in the energy of activation of I due to the influence of the different C−X bonds on the adjacent C−H bonds, and such small differences in activation energy may lead to considerable differences in the composition of the products.

The formation of butylene and hydrogen

These are minor products of the reaction process amounting to 15 percent of the diethyl decomposed. It appears that they are produced by surface reactions but the mechanism must be different in the two cases of zinc and mercury. On the former hydrogen equivalent to the butylene is formed. In the case of mercury where the surface should be predominantly the quartz of the container two molecules of ethane appear to be formed simultaneously with the butylene.

It might be suggested that on the zinc surface a dehydrogenation reaction of ethyls was occurring: $2C_2H_5=C_4H_8+H_2$. This would be in accord with the known activity of zinc in pro-

[11] Bichowsky and Rossini, *Thermochemistry of Chemical Substances* (Reinhold, New York, 1936), p. 271. Guntz, Comptes rendus **105**, 673 (1887). Berthelot, Comptes rendus **129**, 918 (1899).

[12] Frankland and Duppa, Trans. Chem. Soc. **17**, 29 (1864).

[13] Bawn, Trans. Faraday Soc. **31**, 1536 (1935).

moting hydrogen atom recombination; it would leave, however, the problem of why hydrogenation of the resulting butylene to butane did not occur. There are conflicting reports on the efficiency of metallic zinc as a catalyst for the hydrogenation of ethylene.[14] We have shown by special test that zinc surfaces produced by this photolysis process are inactive catalytically in the hydrogenation of alkenes.

The deficiency of hydrogen in the case of the mercury alkyls would on this basis be attributed to the lower activity of quartz in promoting recombination of hydrogen atoms. The occurrence of ethane in place of hydrogen would suggest that such uncombined atomic hydrogen reacted with ethyl radicals or ethylene molecule striking the hydrogen covered areas to form ethane or ethyl, respectively, and giving in either case an over-all reaction

$$4C_2H_5=2C_2H_6+C_4H_8.$$

Packing the reaction vessel with quartz tubing increased the hydrogen yield from mercury diethyl which then approached that of the zinc diethyl experiments. Added hydrogen (200 mm) diminished butylene formation in the case of the mercury but not in the case of the zinc compound. These results would also be in harmony with quartz surfaces containing adsorbed atomic hydrogen and zinc surfaces free from this gas.

It may be noted, however, that the photolysis of dimethyl zinc resulted in no hydrogen formation, so that even in the presence of a zinc wall the reaction $2CH_3=C_2H_4+H_2$ does not occur.

Another sequence of reactions leading to butylene formation has also been considered:

$$C_2H_5+C_2H_4=C_4H_9$$
$$C_4H_9+C_2H_5=C_4H_8+C_2H_6.$$

This sequence would not account for the simultaneous appearance of butylene and hydrogen. It employs the disproportionation reaction which the other evidence seems to minimize in importance. Also, the deliberate addition of small amounts of ethylene did not appear to increase the butylene formation, so that there seems to be little polymerization of ethylene, present in low concentration, to butylene by the ethyl radicals. The actual presence of butyl radicals in low concentrations is suggested, however, by the occurrence of small amounts of volatile hydrocarbon products, which increase in amount when a small proportion of ethylene is added before photolysis. These may arise by such reactions as

$$C_2H_5+C_4H_9=C_6H_{14}$$
$$C_4H_9+C_4H_9=C_8H_{18}.$$

Reaction with hydrogen atoms

The large formation of methane when mercury diethyl and hydrogen are irradiated with resonance radiation at 100°, a temperature at which no reaction of ethyl with molecular hydrogen can be detected, confirms earlier suggestions[15,16] that the reaction $C_2H_5+H=2CH_3$ has a low energy of activation. A reasonable maximum value would appear to be $E=5$ kcal.

Reaction with hydrogen molecules

Reaction of ethyl radicals with hydrogen becomes evident at around 160°, the same temperature at which the corresponding reaction of methyl radicals is observed.[1] We may therefore conclude that the activation energies of these processes are about the same, and assign to the reaction $C_2H_5+H_2=C_2H_6+H$, an activation energy of around 9 kcal. The great increase in the rate of decomposition of mercury diethyl produced by added hydrogen at temperatures upwards of 160° is explained by a chain process analogous to that proposed for the similar effect with mercury dimethyl

$$H+Et_2Hg=C_2H_6+C_2H_5+Hg.$$

In the case of diethyl zinc this acceleration is not so marked, since the zinc wall arising in the course of the photolysis is an efficient catalyst for the removal of hydrogen atoms.

H. A. Taylor and M. Burton[17] have suggested that the reaction of free radicals with hydrogen takes place as a three-body process (e.g., $2CH_3+H_2=2CH_4$) without the formation of hydrogen atoms. They point out that in order to account for the observed rate of reaction of methyl and hydrogen by a bimolecular process

[14] Schmidt, Chem. Rev. **12**, 374 (1933).

[15] Eyring, Gorin, Kauzmann and Walter, J. Chem. Phys. **7**, 633 (1939).

[16] Steacie and Phillips, J. Chem. Phys. **5**, 203 (1937); Steacie and Parlee, Trans. Faraday Soc. **35**, 854 (1939).

[17] H. A. Taylor and M. Burton, J. Chem. Phys. **7**, 675 (1939),

it is necessary to introduce a steric factor of 10^{-4} if $E=8$ kcal., and state that this small steric factor would be unnecessary if the trimolecular process were assumed. Such a steric factor is, however, a logical consequence of the small probability of the activated state in reactions between complex radicals and molecules on the basis of the activated complex theory of Eyring. The problem is, therefore, not how to explain an anomalous steric factor but whether the steric factor for the trimolecular process may reasonably be expected to be any smaller than 10^{-4}. The present comparison of the effects of added hydrogen on zinc and mercury diethyls affords further evidence of the existence of a chain reaction initiated by hydrogen atoms formed by the bimolecular mechanism.

The activation energies for the reaction of methyl radicals with hydrocarbons as determined by Smith and Taylor[2] will probably be approximately valid for the corresponding ethyl radical reaction and although the entropy of activation may be somewhat less for the ethyl radical reaction, in general the reactivity of ethyl may be expected to be not appreciably inferior to that of methyl.

MAY, 1940 JOURNAL OF CHEMICAL PHYSICS VOLUME 8

Hindered Rotation

I. The Configuration of the Cyclohexane Molecule

A. LANGSETH AND B. BAK
Universitetets Kemiske Laboratorium, Copenhagen, Denmark

(Received March 15, 1940)

A restriction of the free rotation about the carbon-carbon single bond will play an important role in the potential function of the cyclohexane molecule. Any force whose nature is such that it will produce a hindrance to the free rotation about the C−C bond must also give rise to different potential energies for the "chair" and "tub" forms of cyclohexane even if these forms are "strainless" in the Baeyer theory sense. According to the nature of the rotational restriction (stabilizing "staggered" or "opposed" configurations) either the "chair," the "tub," or even the hexagonally symmetrical form with a plane carbon ring could be the most stable form. From considerations of the obtained Raman spectra of cyclohexane, cyclohexane-d_1, and cyclohexane-d_{12} it is shown that the only form present in measurable quantities is the form with a D_{6h} symmetry, i.e., the form with the plane of the carbon ring as a reflection plane for the hydrogen atoms. The rotational restriction about the C−C single bond, therefore, is of such a nature that it stabilizes this D_{6h} configuration, in which the H atoms are in "opposed" positions.

INTRODUCTION

AS first pointed out by H. Sachse[1] it is possible to construct two different nonplanar models for the cyclohexane molecule without deforming the tetrahedral angles of the carbon atoms (Fig. 1). Of these two forms I (the "chair") has a high symmetry, D_{3d}, and is rigid in the sense that it cannot be deformed without altering the C−C−C angles in the ring. The symmetry of II (the "tub") is not defined because of a certain flexibility of the model. Without any alteration of the tetrahedral angles it is possible by simple rotation about the C−C bonds to bring any one of the six carbon atoms up in the ends of the "tub." During this operation the symmetry changes between C_{2v} (for the "tub"), C_2, and D_2. On the basis of the simple valence force picture the two forms, I and II, should have the same potential energy because they are both strainless. In ordinary cyclohexane they should therefore both be present in the ratio of their statistical weights 1 : 3. If this proportion is found experimentally to be shifted towards one side or the other it is necessary to introduce a new restriction upon the potential function in order to explain the difference in potential energy of the

[1] H. Sachse, Ber. Deutsch. Chem. Ges. **23**, 1363 (1890); Zeits. f. physik. Chemie **10**, 203 (1892).

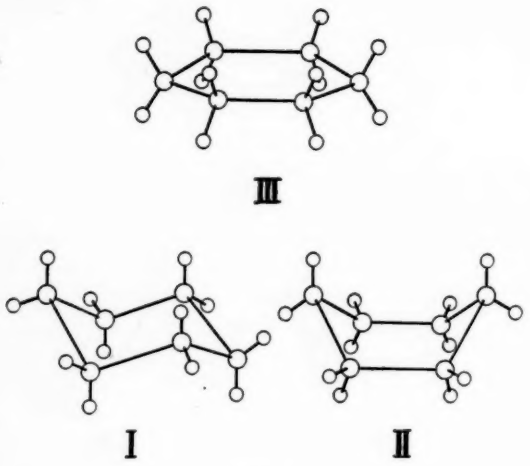

FIG. 1.

two forms. It is easily seen (from a model) that *any restriction having the required properties will be equivalent to a restriction of the internal rotation about the carbon-carbon single bond.*

As for the qualitative nature of the rotational restriction there are two possibilities to be considered. In the first case each methylene group in cyclohexane will have a tendency to place its H atoms in a staggered position with respect to the H atoms of the neighboring CH_2 groups (as in the centro-symmetrical D_{3d} form of ethane). This will stabilize the puckered D_{3d} form of cyclohexane. If, in the second case, the rotational restriction for the C−C single bond is of such a nature that it will tend to place the H atoms of the different CH_2 groups in opposed positions with respect to each other (as in the D_{3h} form of ethane), this will make the less symmetrical "tub" forms—C_{2v}, C_2, and D_2—more stable than the "chair" form—D_{3d}—and tend to produce the most stable plane D_{6h} form (III, Fig. 1). It is important to note that in the last case the rotational restriction will be opposed to the restriction due to the angular restoring force, i.e., *the C−C−C-angles will be deformed in tending to make the ring plane.* It depends on the nature as well as on the order of magnitude of the competing restrictions whether the cyclohexane molecule reaches the plane D_{6h} configuration in which the potential energy due to internal rotation has its minimum. Thus the determination of the configuration of cyclohexane will give valuable information concerning the nature of the rotational restriction about the carbon-carbon single bond.

EXPERIMENTAL

The *cyclohexane* used was a commercial product carefully purified by rectification through a 1.0-meter high column: $bp_{760}=80.6$°C. Even a strongly exposed Raman spectrum showed no trace of lines due to the presence of benzene, the impurity most likely to be present.

The *cyclohexane-d_1*, $C_6H_{11}D$, was prepared from pure bromocyclohexane, $C_6H_{11}Br$, by a Grignard reaction carried out in such a way (which will be described in detail elsewhere) that neither cyclohexane nor cyclohexene could be present as impurities. In order to check the method, a sample of C_6H_{12} was prepared in exactly the same way, using ordinary water instead of D_2O for decomposition of the Grignard compound. Its Raman spectrum was absolutely identical with that of the commercial product purified in the way mentioned above.

Cyclohexane-d_{12} was prepared by deuterating benzene-d_6 at 180°C in the presence of a Ni-catalyst:

$$C_6D_6+3D_2\rightleftharpoons C_6D_{12}.$$

The equilibrium mixture thus obtained was purified by treatment with bromine and a small quantity of iron powder in the dark. Under these conditions the benzene-d_6 is rapidly brominated, whereas the cyclohexane-d_{12} is scarcely attacked. After washing and drying it was rectified: bp_{760}77.8°–78.0°C.

The Raman spectra were obtained with a newly-built spectrograph. The dispersion at 4500A is 7A per mm and the resolving power

TABLE I. *Raman spectrum of cyclohexane.*

RAMAN FREQUENCY IN CM^{-1}	INTENSITY	STATE OF POLARIZATION	RAMAN FREQUENCY CM^{-1}	INTENSITY
384.1	1	*D*	2630.0	1
427.0	2	*D*	2665.4	2
762	0	—	2701.9	1
801.7	10	*P*	2853.8	10
1028.6	5	*D*	2888.3	2
1158.3	3	*P*	2896.7	2
1267.0	5	*D*	2908.1	1
1347.6	2	*D*	2924.0	8
1426.5	½	—	2934.7	8
1445.1	5	*D*		
1465.6	½	—		

sufficiently high to separate lines 1 cm^{-1} apart. The Raman apparatus is of a new construction using six mercury lamps and having a high light gathering power. Raman spectra were taken both without and with filter (sat. $NaNO_2$-solution) cutting off the violet lines.

The complete Raman spectra of cyclohexane, cyclohexane-d_1 and cyclohexane-d_{12} are given in the Tables I, II and III. The frequencies of the lines were measured from photographic enlargements by interpolation between standard lines of the iron arc. The positions of the polarized lines may be considered accurate to ± 0.2 cm^{-1}. The frequencies of the depolarized lines may usually be trusted to ± 0.5 cm^{-1}.

In Tables I and III the state of polarization for the low frequency lines are given. These estimations are based upon the observed shape of the lines.[2] It is well known that the state of polarization of a Raman line is intimately connected with the rotational structure of the "line," which is really an unresolved vibration-rotation band. If therefore the Raman spectrum is taken with a high dispersion instrument the strongly polarized lines appear as sharp lines (intense Q branch) and the depolarized as bands with no well-defined intensity maximum. Partially polarized lines have shapes in between these two limits with more or less sharp maxima according to their total polarization factor.

TABLE II. *Raman spectrum of cyclohexane-d_1*

Raman Frequency cm^{-1}	Intensity	Raman Frequency cm^{-1}	Intensity	Raman Frequency cm^{-1}	Intensity
321	0	1034.1	4	2114.9	1
370.7	1	1052.8	2	2144.1	2
375.9	1	1076.5	1	2164.7	2
423.2	2	1106.5	0	2171.8	2
427.4	2	1133.6	2	2180.7	0
566	0	1147.8	1	2192	0
589	0	1151.8	1		
(699?	0)	1162.4	1	2631.6	0
725.8	3	1168.5	0	2656.0	0
745	0	1199.8	1	2669.3	0
778.3	½	1255.1	1	2688.3	0
798.7	2	1264.7	4	2697.6	0
801.2	10	1301.0	2		
811	0				
821.3	½	1348	2	2853.8	10
852	0	1441.3	5	2882.4	2
940.5	1	1447.1	4	2922.1	7
963.1	½	1464.1	1	2936.6	8
1027.1	5				

[2] Cf. Langseth and Walles, Zeits. f. physik. Chemie **B27**, 214 (1934).

TABLE III. *Raman spectrum of cyclohexane-d_{12}*

Raman Frequency cm^{-1}	Intensity	State of Polarization	Raman Frequency cm^{-1}	Intensity
298.2	1	*D*	2064.3	1
373.2	2	*D*	2082.8	10
385	0	—	2097.6	4
593	0	—	2106.6	5
637	0	—	2127.0	1
696	0	—	2154.6	6
715.9	0	—	2173.8	1
723.8	10	*P*	2199.7	6
746.2	1	*P*	2239.3	1
795.6	5	*D*	2298.1	½
931	3	*D*	2320.9	1
937.2	5	*P*	2390.9	½
1014.8	1	*P*		
1070.6	3	*D*		
1119.8	2	*P*		
1214.1	2	*D*		
1305	0	—		

Our measurements of the Raman frequencies of cyclohexane agree—except for a couple of faint lines—with previous investigations.[3] Discrepancies between our estimation of the state of polarization of certain lines in the spectrum of cyclohexane and previous measurements will be discussed later on.

Discussion

1. Cyclohexane

As already mentioned it is necessary to consider D_{6h}, D_{3d}, D_2, C_{2v}, and C_2 as possible symmetries for the cyclohexane molecule. According to the selection rules for the symmetries D_2, C_{2v}, and C_2 all 48 vibrational frequencies are Raman active. Hence the presence of molecules of these symmetries in the cyclohexane should give rise to a very complicated spectrum. As Table I shows this is far from being the case. In fact the spectrum is surprisingly simple for a vibrational system of 18 atoms and immediately indicates a high symmetry of the molecule. Although the Raman spectrum of C_6D_{12} may appear more complicated than that of C_6H_{12}, it is still indicative of a higher symmetry than D_2, C_{2v}, or C_2 for the molecule.[4] Also, it is immediately evident, on comparison of the complexity of the spectra of C_6H_{12} (or C_6D_{12}) and $C_6H_{11}D$ (Table II) that a change from a high to a low symmetry has been

[3] For literature see Kohlrausch, *Smekal-Raman-Effekt*, Ergänzbd., p. 229.

[4] The spectrum of C_6D_{12} will be discussed in detail in the latter part of the article.

affected. We feel therefore justified in excluding the possibility of symmetries as low as D_2, C_{2v}, and C_2 for the cyclohexane molecule as well as the possibility of cyclohexane being a mixture of different stero-isomers. The remaining question is to decide between the only possible symmetries: D_{6h} and D_{3d}.

In Table IV the selection rules for the D_{6h} and D_{3d} symmetries are summarized. It is a well-known fact that Raman spectra of molecules containing several hydrogen atoms show a very complicated structure in the 3000-cm^{-1} region because of the high probability for accidental degeneracy between overtones (and combination tones) of hydrogen deformation frequencies and hydrogen stretching frequencies.[5] For this reason in Table IV the fundamentals corresponding to hydrogen stretching frequencies 2800–3000 cm^{-1} are separated out, and in the following only the region below *ca.* 1500 cm^{-1} will be considered.

From Table IV, the principal difference between the two symmetries is that the D_{6h} symmetry allows only 2 totally symmetric fundamentals, whereas the D_{3d} symmetry allows 4 totally symmetric frequencies, all of which should appear in the Raman spectrum as polarized lines. According to our observations the spectrum of cyclohexane contains 2 strongly polarized, and 6 depolarized lines corresponding to fundamentals with frequencies below 1500 cm^{-1}.[6] The 3 additional lines observed in this region are weak and can plausibly be explained as overtones and combination tones. The low frequency part of the Raman spectrum is therefore in perfect accordance with the selection rules for a D_{6h} structure of the cyclohexane molecule.

Furthermore, the D_{6h} symmetry is strongly supported by the following argument. From

TABLE IV.

Symmetry of the Molecule	Vibrational Symmetry Class	Number of Raman Active Fundamentals with Frequencies	
		<1500 cm^{-1}	>1500 cm^{-1}
D_{6h}	A_{1g}	2 non-deg. (P)	1 non-deg. (P)
	E_g^+	4 deg. (D)	1 deg. (D)
	E_g^-	2 deg. (D)	1 deg. (D)
D_{3d}	A_{1g}	4 non-deg. (P)	2 non-deg. (P)
	E_g	6 deg. (D)	2 deg. (D)

Table I it is seen that the two fundamentals with the lowest frequencies must have a combination tone whose frequency happens to fall close to the strongest Raman active fundamental, which must be assigned to a totally symmetrical (A_{1g}) vibration:

$$384.1+427.0=811.1 \text{ cm}^{-1}\sim 801.7 \text{ cm}^{-1}.$$

Because of the closeness of this accidental degeneracy an interaction may be expected to occur *if the combination tone has totally symmetrical properties*. Even if this interaction for some special reason was weak, we still might expect the combination frequency (which in itself must be allowed in Raman effect) to take up enough intensity from the very strong totally symmetrical fundamental to make it appear on a strongly exposed Raman plate. We have, however, *not* been able to detect any line which could be assigned to this combination tone, although the corresponding interaction in the spectrum of cyclohexane-d_1, where it must be allowed, is observed very distinctly.[7] From this we conclude that the said combination frequency in cyclohexane is *not allowed* to interact with the totally symmetrical vibration, and therefore has too low an intensity to be observed, as is usually the case for combination frequencies.

If cyclohexane had D_{3d} symmetry, fundamentals belonging to two different symmetry classes only would be Raman active, namely A_{1g} and E_g (cf. Table IV). A combination tone between any two frequencies from these symmetry classes will have totally symmetrical properties (A_{1g} or $A_{1g}+E_g$) and therefore will always be allowed to interact with the A_{1g} frequency.

[5] The same applies to the corresponding deuterium frequencies. This is illustrated most strikingly by the spectrum of $C_6H_{11}D$. For this molecule only one deuterium stretching frequency around 2200 cm^{-1} is to be expected. Five out of the six lines observed in this region must therefore be due to overtones and combination tones taking up intensity by interaction with the active fundamental.

[6] In a discussion of the structure of the cyclohexane molecule Kohlrausch and Stockmair (Zeits. f. physik. Chemie **B31**, 382 (1936)) decided in favor of the D_{3d} symmetry on the basis of previous polarization measurements, which seemed to indicate that 4 of the low frequency lines were polarized. According to Hanle and Heidenreich (Zeits. f. Physik **97**, 277 (1935)) the two rather faint lines, 384.1 cm^{-1} and 1347.6 cm^{-1}, seem to be polarized, whereas the shape of these lines on our plates definitely indicates a depolarization factor very close to 6/7. The following discussion of the spectrum confirms our estimation of $\rho=6/7$ for these two lines.

[7] The fact that the interaction in the cyclohexane-d_1 spectrum is observed to cause an *intensification* of the combination tone indicates that we should expect the same effect in the spectrum of C_6H_{12} even if a *weakening* theoretically might be the result of an interaction.

However, since no interaction has been observed cyclohexane cannot have D_{3d} symmetry. If on the other hand we assume D_{6h} symmetry for the molecule the Raman active frequencies belong to three different symmetry classes: A_{1g}, E_g^+, and E_g^-. A combination tone between an E_g^+ and an E_g^- frequency will have the symmetry $(B_{1g}+E_g^-)$ and is therefore not allowed to interact with a totally symmetrical frequency. This supports the assignment in Table V of the Raman lines 381.1 and 427.0 cm^{-1} to $E_g^-(\nu_{10})$ and $E_g^+(\nu_6)$, respectively, on the basis of a D_{6h} symmetry.

The first overtones of both of the degenerate frequencies ($2\nu_{10}=768.2$ cm^{-1} and $2\nu_6=854.0$ cm^{-1}) are allowed in Raman effect and might be expected to appear as weak lines in the spectrum. The theoretically possible interaction with the totally symmetrical vibration ($\nu_1=801.7$ cm^{-1}) is not likely to play any important role because of the large separation. We have in fact only been able to find the first as an extremely weak line at 762 cm^{-1}.

Without intending to give a detailed discussion of the observed spectra at the present stage of the investigation we have in Table V given an assignment of the observed low frequency lines in cyclohexane. This assignment is fairly certain as it is based on the knowledge we have of the corresponding modes of vibration in the benzene molecule.[8] For the sake of comparison the assignment of the cyclohexane-d_{12} spectrum is also given in Table V. This assignment will be discussed in some detail in the latter part of this article. We have numbered the modes of vibration in such a way that their relation to the corresponding normal frequencies in the benzene molecule is obvious.[9] A schematical diagram of the modes of vibration discussed in this article is given in Fig. 2.

2. Cyclohexane-d_1

The cyclohexane-d_1 molecule cannot have any symmetry higher than C_s (i.e., one plane of symmetry only). All the degenerate vibrations will therefore split up into two components and all frequencies forbidden in the Raman spectrum of cyclohexane (because of its high symmetry) are now allowed. As already mentioned, this is confirmed by the experiment insofar as there is a very considerable increase in the number of lines observed in the Raman spectrum of $C_6H_{11}D$ as compared with that of C_6H_{12}. Also the predicted release of degeneracy is observed for the two frequencies ν_{10} and ν_6. The two components of each of these close doublets correspond in the cyclohexane-d_1 molecule to nondegenerate vibrations, one of which is symmetrical (A') and the other antisymmetrical (A'') to the plane of symmetry which is now the only symmetry-element of the molecule.

It is of interest to consider the overtones and combination tones of the frequencies 10a, 10b, 6a, and 6b also in cyclohexane-d_1. They are all allowed in Raman effect and are also observed as will be seen from Table VI. But the important point is that the interaction to be expected between the totally symmetrical fundamental ν_1 and the combination frequencies $(\nu_{10a}+\nu_{6a})$ and $(\nu_{10b}+\nu_{6b})$, respectively—both of which are totally symmetrical—is observed as a spreading of the two lines to both sides of ν_1. For the same reason the two lines are more intense than unperturbed combination tones usually are. As already emphasized, the observation of this interaction in cyclohexane-d_1 strengthens our conclusion, that the reason why we did not find the corresponding interaction in the spectrum of cyclohexane is the fact that it is forbidden because of the D_{6h} symmetry of the molecule. The antisymmetrical combination frequencies $(\nu_{10a}+\nu_{6b})$ and $(\nu_{10b}+\nu_{6a})$ —which are not allowed to interact with ν_1—are found almost exactly at the calculated frequency

TABLE V. *Assignment of frequencies below 1500 cm^{-1}.*

C_6H_{12} Freq. cm^{-1}	Symmetry Class	Mode of Vibration	C_6D_{12} Freq. cm^{-1}
384.1	E_g^-	ν_{10}	*298.2*
427.0	E_g^+	ν_6	*373.2*
—	—	?	385
762	$(A_{1g}+E_g^+)$	$2\nu_{10}$	593
—	A_{1g}	$(\nu_1+\nu_{10})-\nu_{10}$	637
—	A_{1g}	$(\nu_1+\nu_6)-\nu_6$	696
—	A_{1g}	$(\nu_1+\nu_{10})-\nu_{10}$	715.9
801.7	A_{1g}	ν_1	*723.8*
—	A_{1g}	$(\nu_1+\nu_6)-\nu_6$	746.2
1028.6	E_g^+	ν_9	*795.6*
1158.3	A_{1g}	ν_{2x}	*937.2*
1347.6	E_g^-	ν_{10y} Inter-	*931*
—	$(A_{1g}+E_g^-)$	$\nu_1+\nu_{10}$ action	1014.8
1267.0	E_g^+	ν_{7x} Inter-	*1070.6*
—	$(A_{1g}+E_g^+)$	$\nu_1+\nu_6$ action	1119.8
1445.1	E_g^+	ν_8	*1214.1*
—	$(A_{1g}+E_g^+)$	$\nu_{2x}+\nu_8$	1305
1465.6	$(A_{1g}+E_g^+)$	$\nu_6+\nu_9$	—

[8] Cf. A. Langseth and R. C. Lord, Jr., Kgl. Danske Vidsk. Selsk. math.-fys. Medd. XVI, p. 6 (1938).

[9] Langseth and Lord, reference 8, p. 10. This notation is except for a few minor alterations—identical with that given by Wilson, Phys. Rev. **45**, 706 (1934).

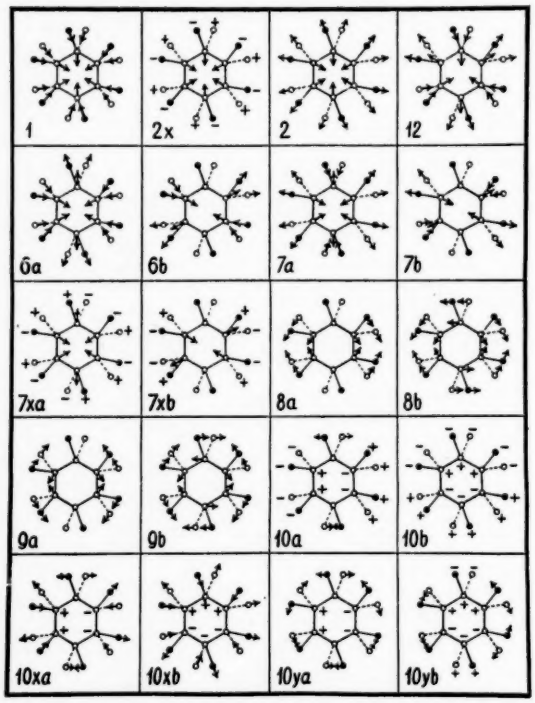

FIG. 2.

close to the strong ν_1 where they are overlapping a sharp line due to $C_5{}^{12}C^{13}H_{11}D$ molecules. This accounts for the intensity of this line being a little higher than one would expect for a pure carbon isotopic line.

3. Cyclohexane-d_{12}

As already mentioned the Raman spectrum of the heavy cyclohexane is more complicated than that of the light compound. This arises from two cases of accidental degeneracy between fundamentals and combination tones. The resulting interaction causes an increase in the number of Raman lines in the low frequency region of the C_6D_{12}-spectrum and thus complicates the simple structure of the spectrum which is found for C_6H_{12}. The assignment of the fundamentals given in Table V explains the strongest of the observed lines in the spectrum of C_6D_{12} and is supported by the "product rule." Although the use of the product rule is to some extent limited in this case because of the uncertainty in the assignment of hydrogen and deuterium stretching frequencies[10] it shows nevertheless that the given assignment, on the basis of a D_{6h} symmetry, is the only one plausible. In Table VII the theoretical[11] and the observed products (τ's) are given for the three Raman active symmetry classes. The agreement is satisfactory when the anharmonicity of the observed frequencies is taken into account.

The strongest of the interactions mentioned above is that between the combination frequency $\nu_1+\nu_6(A_{1g}+E_g{}^+)$ observed at 1119.8 cm^{-1} (calc.: 723.8+373.2=1097.0 cm^{-1}) and the fundamental, $\nu_{7x}(E_g{}^+)$ observed at 1070.6 cm^{-1}. Because of this interaction the combination tone appears as a rather strong line shifted towards higher frequencies. As the wave functions for ν_{7x} and $(\nu_1+\nu_6)$ are mixed because of the interaction, we should expect two other lines in the spectrum corresponding to transitions from the first excited level of ν_6 (which is densely populated at ordinary temperatures) up to the two resonance levels. These transitions correspond to an excitation of the strongly Raman active ν_1. The two difference tones should therefore be present in the spectrum if the given interpretation is correct. In fact, they are both observed at their calculated positions. As the frequencies of the starting level as well as of both end levels are observed in the spectrum, the frequencies of the expected lines are given accurately by the differences: 1070.6−373.2 =697.4 cm^{-1}, obs. 696 cm^{-1}, and 1119.8−373.2 =746.6 cm^{-1}, obs. 746.2 cm^{-1}.

The fortuitous degeneracy between $(\nu_1+\nu_6)$

TABLE VI. *Combination frequencies in cyclohexane-d_1.*

Symmetry Class	Assignment	Frequency in cm^{-1} Calc.	Obs.
A' A'' A'	$2\nu_{10a}$ $\nu_{10a}+\nu_{10b}$ $2\nu_{10b}$	742 747 752	745
A' A'' A'	$2\nu_{6a}$ $\nu_{6a}+\nu_{6b}$ $2\nu_{6b}$	846 850 854	852
A'' A''	$\nu_{10a}+\nu_{5b}$ $\nu_{10b}+\nu_{6a}$	798 799	799
A' A' A'	$\nu_{10a}+\nu_{6a}$ ν_1 $\nu_{10b}+\nu_{6b}$	794 *801.2* 803	Interaction 778 821

[10] The complexity of the spectra in these regions is caused by the chaotic mixture of interacting fundamentals, overtones and combination tones.

[11] The moments of inertia contained in the theoretical τ for the $E_g{}^-$ class are calculated on assumption of the C−C distance as 1.51A and the C−H distance as 1.08A.

and ν_{7x} cannot be complete because the two Raman lines have different intensities and states of polarization. As the 1119.8-line is weaker and more polarized than the 1070.6-line, the wave function for the 1119.8 cm^{-1} resonance level must contain the greater part of the $(\nu_1+\nu_6)$ wave function. Therefore, according to expectation the 746.2 cm^{-1} line is the stronger of the two difference tones.[12]

Another case of interaction is observed in the cyclohexane-d_{12} spectrum between the combination frequency $\nu_1+\nu_{10}(A_{1g}+E_g^-)$ and the two almost coinciding fundamentals $\nu_{2x}(A_{1g})=937.2$ cm^{-1} and $\nu_{10y}(E_g^-)=931$ cm^{-1}. Here the resonance is weaker (because of the larger separation of the interacting levels) and is responsible only for an intensification of the combination tone, which is observed at 1014.8 cm^{-1} almost at the calculated position: $\nu_1+\nu_{10}=1022.0$ cm^{-1}. This assignment is verified by the observation of the expected difference tone: 715.9 cm^{-1}, calculated $1014.8-298.2=716.6$ cm^{-1}. A slight mixing of the $(\nu_1+\nu_{10})$ with the ν_{2x} and ν_{10y} wave functions is also indicated by the very faint and broad line observed at 637 cm^{-1} which can be explained as the unresolved difference tones: $937.2-298.2=639.0$ cm^{-1} and $931-298.2=633$ cm^{-1}.

The Absence of C^{13}-isotopic Line in Cyclohexane

Finally we want to call attention to a very puzzling feature in the Raman spectrum of cyclohexane, even if this has no close relation to the problem we are discussing. It is the fact (which has been bothering one of us ever since he took his first Raman spectrum of cyclohexane in 1931) *that no C^{13}-isotopic satellite is to be found close to the strong 801.7 cm^{-1} line in cyclohexane.* The spectrum of $C_6H_{11}D$ reveals the mystery. The explanation is the same as the one which accounts for the surprisingly small shift in the frequency of ν_1 from 801.7 cm^{-1} in C_6H_{12} to 801.2 cm^{-1} in $C_6H_{11}D$. In cyclohexane as well as in benzene the trigonally symmetrical frequency ν_{12} (see Fig. 2) has a value in the neighborhood of the totally symmetrical ν_1.[13] In benzene ν_{12} has a somewhat higher frequency but in cyclohexane its frequency is a little lower than ν_1. In cyclohexane itself ν_{12} is inactive and not allowed to interact with ν_1. As soon, however, as the symmetry of the molecule is destroyed—e.g. by introduction of one deuterium atom or of one C^{13} atom—ν_{12} becomes a totally symmetrical vibration and a strong interaction with ν_1 springs into being. The result of this interaction is firstly, a transfer of intensity from ν_1 to ν_{12}, which causes ν_{12} to show up in the spectrum of cyclohexane-d_1 as a fairly strong and polarized line at 725.8 cm^{-1}, and secondly, that the two frequencies are pressed apart: ν_{12} towards lower and ν_1 towards higher frequencies. Now it happens that the increase in frequency for ν_1 due to the interaction cancels almost exactly the decrease in frequency due to the greater mass of the D or the C^{13} atom. For this reason ν_1 has almost exactly the same frequency in $C_6H_{11}D$ or in $C_5{}^{12}C^{13}H_{12}$ as in C_6H_{12}. However, if the mass of the molecule is increased further, as it is in $C_5{}^{12}C^{13}H_{11}D$, then a slight decrease in the frequency of ν_1 is observed as a C^{13}-isotopic satellite at 798.7 cm^{-1} in the spectrum of cyclohexane-d_1.

Table VII.

τ	A_{1g}	E_g^+	E_g^-
Theoretical	2.00	2.83	2.50
Calculated	1.9	2.7	2.4

Apparently, the same conditions as in C_6H_{12} are prevailing also in C_6D_{12} as we have been unable to find a C^{13}-isotopic line in its spectrum.

Summary

The Raman spectra of cyclohexane, cyclohexane-d_1 and cyclohexane-d_{12} have been obtained.

From considerations of: (1) number and state of polarization of fundamentals observed, (2) selection rules, in particular for cases of interaction between fundamentals and overtones or combination tones, and (3) Teller's product rule, the configuration of the cyclohexane molecule has been assigned a D_{6h} symmetry.

[12] Unfortunately the weak overtone of ν_6 (calc. 746.4 cm^{-1}) falls very close to the difference tone which it is partly overlapping. It served therefore no useful purpose to make quantitative measurements of the relative intensities of the two difference tones. Cf., the discussion of an exactly corresponding interaction, observed in the Raman spectrum of benzene; Langseth and Lord, J. Chem. Phys. **6**, 203 (1938); Kgl. Danske Vidsk. Selsk. Medd. XVI, p. 51 (1938).

[13] Cf. A. Klit and A. Langseth, J. Chem. Phys. **5**, 925 (1937); Langseth and Lord, reference 12, p. 25.

Hindered Rotation

II. The Hindered Rotation About the C−C Single Bond in Tetrachloroethane

A. LANGSETH AND H. J. BERNSTEIN*
Universitetets Kemiske Laboratorium, Copenhagen, Denmark

(Received March 15, 1940)

Because of the restriction to internal rotation, tetrachloroethane might consist of several rotational isomers: a *cis*-(C_{2v}) form, a *trans*-(C_{2h}) form, or forms intermediate to *cis* and *trans* with C_2 symmetry. From the Raman spectrum of $C_2D_2Cl_4$ and the spectrum of $C_2H_2Cl_4$ at different temperatures experimental evidence has been obtained which shows that the equilibrium mixture consists of two rotational isomers, the *cis*-C_{2v} form and the C_2 form. The C_{2v} form was found to be the more stable, with a potential energy 1100 cal. per mole lower than the potential energy of the C_2 form.

INTRODUCTION

RECENT investigations[1] have shown that there exists a considerable discrepancy between the values of the specific heat of ethane calculated at different temperatures from spectral data, and the values obtained experimentally. In order to overcome this disagreement a potential barrier (restricting the free rotation of one methyl group with respect to the other about the C−C axis) of about 3000 cal. per mole was introduced.[2] The presence of this potential barrier and the fact that the C−C axis is also a threefold axis of symmetry necessarily leads to a potential energy curve for ethane which has 3 identical minima as one methyl group is rotated through 360° with respect to the other.

Similarly for the substituted ethanes a potential energy curve of the 3 minima type is to be expected. However, because of the lower symmetry (the threefold axis being destroyed) and the nature of the substituted atoms, the ethane type curve will be deformed and the three minima will not be identical. In such a case one should expect isomers with different potential energies to exist.

Considering the possible isomers of substituted ethane $CXY_2 \cdot CXY_2$ it is evident that there are 4 cases to be discussed which fall into the following two classes. First, the class in which the potential energy curve has 3 minima in a complete revolution of one-half of the molecule with respect to the other half about the C−C axis, and second, the class in which the potential energy curve has 2 minima in a complete revolution.

In the first class one of the isomers has a plane of symmetry (the symmetry of the isomer being C_{2v} or C_{2h}) corresponding to the minimum at 0° (see Fig. 1). The other two identical minima on the potential energy curve correspond to the two isomers with an axis of symmetry only (symmetry C_2) which are mirror images of one another. Spectroscopically (Raman effect) these isomers are identical and will be considered as one configuration (C_2) with a statistical weight of 2. To this class belong the following two cases: (I) in which the isomer with the plane of symmetry is the more stable (C_{2v} or C_{2h}) and (II) in which the isomer with the axis of symmetry only (C_2) is the more stable. The energy curves for these two cases are given in Fig. 1.

In the second class there are two isomers corresponding to the two minima at 0° and 180° (see Fig. 2). They possess *cis*- and *trans*-configurations, that is C_{2v} and C_{2h} symmetries, respectively. To this class belong the following two cases; (i) where the *cis*-form is the more stable and (ii) where the *trans*-form is the more stable.

For all the cases represented in Figs. 1 and 2 changing the temperature of the substituted ethane will upset the equilibrium between the isomers present and affect a change in the concentrations of these isomers, so that a Raman

* 1851 Exhibition Research Scholar.

[1] Kistiakowsky and Nazmi, J. Chem. Phys. **6**, 18 (1938); Hunsman, Zeits. f. physik. Chemie **B39**, 23 (1938); Wilson, J. Chem. Phys. **6**, 740 (1938).

[2] Teller and Topley, J. Chem. Soc. 876 (1935); Kemp and Pitzer, J. Am. Chem. Soc. **59**, 276 (1937).

spectrum at one temperature will show marked intensity differences from a spectrum at another temperature. Since the lines in the spectrum due to the more stable isomer lose intensity when the temperature is increased and the lines of the less stable isomer gain intensity when the temperature is increased, a separation of the spectrum into the spectra of the two isomers present can be accomplished.

It was the purpose of this investigation to determine the number and configuration of the isomers of the substituted ethane $CHCl_2 \cdot CHCl_2$ (tetrachloroethane) i.e., to determine which of the cases in Table I was represented in tetrachloroethane.

Tetrachloroethane was chosen for the following reasons.

(1) Previous Raman frequency measurements yield a spectrum too rich in fundamentals to be explained in terms of one configuration only.

(2) Since there are so many heavy atoms in the molecule, the distribution of the lines in the spectrum is most dense in the region 100–800 cm^{-1} and the lines have a large separation. This region can be used then for identifying configurations.

(3) The high boiling point of tetrachloroethane permits a large temperature interval in which to obtain Raman spectra.

Experimental

Heavy tetrachloroethane was prepared in the following manner:

(1) $$CaC_2+D_2O+CO_2=C_2D_2+CaCO_3$$

(2) $$C_2D_2+2Cl_2=C_2D_2Cl_4$$

The second reaction was carried out by bubbling heavy acetylene and chlorine into a flask containing CCl_4 and finely divided $AlCl_3$. The heavy tetrachloroethane was separated from the CCl_4 by distillation, redistilled through a column one meter high, and its Raman spectrum taken.

Table I.

Possible Isomers Present	More Stable Isomer
C_{2v}, C_2	C_{2v}
C_{2v}, C_2	C_2
C_{2h}, C_2	C_{2h}
C_{2h}, C_2	C_2
C_{2h}, C_{2v}	C_{2v}
C_{2h}, C_{2v}	C_{2h}

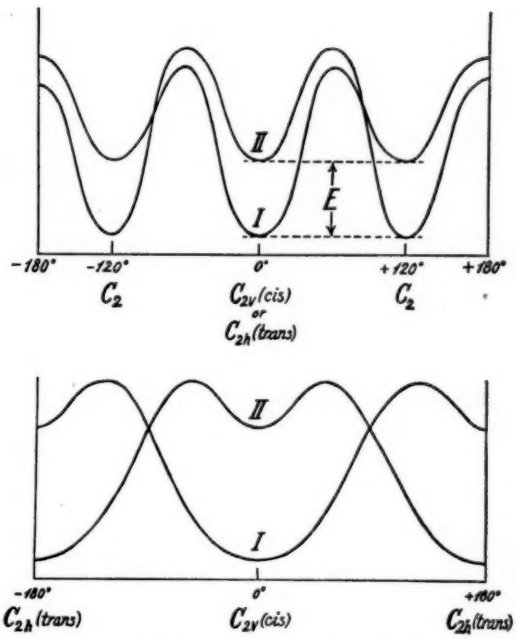

Fig. 1. (above) and Fig. 2. (below).

Tetrachloroethane (tech.) was distilled through a one-meter column, the middle portion of a constant boiling fraction (146.0–146.5°C) being taken for the Raman experiments.

The apparatus for obtaining the Raman spectra was of high light gathering power, high dispersion, and good resolution. A strong complete spectrum of benzene was obtained after five minutes exposure. The dispersion at 4500A was about 8A per mm and the resolving power sufficiently high to separate lines one cm^{-1} apart.

The spectra of $C_2H_2Cl_4$ and $C_2D_2Cl_4$ were obtained with and without a $NaNO_2$ (saturated solution in aqua) filter after two to three hours exposure. Enlarged prints of the Raman spectra and comparison iron arc spectrum were made, from which the frequencies were obtained by interpolation between the nearest known iron arc lines.

To obtain spectra at different temperatures a sealed Raman tube was prepared containing the pure $C_2H_2Cl_4$ and calibrated so that the expansion of the liquid indicated the temperature. The tube was wound with a high resistance wire, the turns being approx. 1 mm apart. A current

of 0.12 amp. was sufficient to maintain the liquid at a constant temperature of 125±1°C.

A spectrum of $C_2H_2Cl_4$ was obtained at two different temperatures on the same photographic plate and under identical experimental conditions. A density wedge was also photographed on the same plate. All times of exposure for the two spectra and the wedge were the same (60 minutes ±0.1 minute). The intensities of the lines in the spectra at the two temperatures were obtained from tracings recorded by a Moll microphotometer.**

Two such plates were obtained for two different temperature intervals.

Results

In Table II are given the complete spectra of $C_2H_2Cl_4$ and $C_2D_2Cl_4$.

In Table III only the lines from 100–800 cm^{-1} are given. Since these were the most distinct and most intense lines on the plate, intensity measurements were obtained. From the temperature effect on the intensity of the lines the spectrum of tetrachloroethane was separated into two spectra, one, for the more stable isomer and the other, for the less stable isomer. The frequencies for the light and heavy isomers are given in columns 1, 2, 7, and 8. The intensities for the two separate experiments (plate I and II) at four different temperatures are given in columns 3, 4, 5, and 6.

TABLE II.* *Raman frequencies in* cm^{-1}.

	$C_2H_2Cl_4$	INTENSITY	$C_2D_2Cl_4$	INTENSITY	ASSIGNMENT†
1	88.2	7	88.2	6	
2	173.0	6	172.6	3	
3	183.6	3	180.4	1	
4	226.0	2	226.2	2	
5	241.7	5	239.8	5	
6	288.8	5	287.1	5	ν_{8a} or ν_2
7	294.6	3	295.1	2	ω_{8a} or ω_2
8	352.9	8	350.2	7	ν_{7a}
9	366.7	4	362.1	3	ω_{7a}
10	546.4	3	531.2	2	
11	648.1	7	628.0	7	ν_{6a} or ν_1
12	765.1	2	703.1	2	ω_{6a} or ω_1
13	801.6	8	741.0	8	ν_3
14	812.1	2	758.1	2	ω_3
15	1018.1	3	772.1	1	
16	1028.1	1	829.8	2	
17	1118 ‡		886.3	1	
18	1171 ‡		938.0	1	
19	1203.1	1			
20	1217.0	3	950.6	2	ν_2 or ν_{8a}
21	1245.2	2	1006.6	1	
22	1278.8	1	1100.0	1	
23	1307.3	1			
24			2233.1	2	ω_1 or ω_{6a}
25	2989.1	3	2240.9	6	ν_1 or ν_{6a}

* The frequencies, No. 1–14 inclusive, 20 and 25, are corresponding frequencies for the light and heavy compound. The others have not been paired.

† The frequencies ν_1, ν_2, etc. refer to the modes of vibration (shown in Fig. 3) of the *cis*-form. The frequencies ω_1, ω_2, etc. are the corresponding modes in the form with C_2 symmetry. These frequencies were assigned on the basis of Teller's product rule (see Angus *et al.* J. Chem. Soc. London, 971 (1936)) with which they conform.

‡ These lines were very faint; the frequencies are given to within ±10 cm^{-1}.

** Within the accuracy of the technique for obtaining intensities it was found that peak intensities could be used instead of areas. As a result the intensities given in Table III are all peak intensities.

Discussion of the Results

In Fig. 3 is given a schematical diagram of the modes of vibration for an ethane molecule with D_{3h} symmetry ("opposed" configuration). For the sake of convenience the modes are numbered 1 to 12, the two components of each degenerate vibration being labelled "*a*" and "*b*" (i.e., symmetric or antisymmetric to the twofold axis of symmetry). If 4 opposed hydrogen atoms are substituted by chlorine atoms (in Fig. 3 marked as black dots) the diagram will serve as a convenient guide to the general nature and symmetry of the modes of vibration of the $C_2H_2Cl_4$ isomer with the *cis*-C_{2v} configuration. There are 18 modes of vibration, all allowed to appear in the Raman spectrum. Of these, only the chlorine deformation vibrations (2 or 8*a*), (7*a*), (10*a*), (7*b*), (10*b*), and (5 or 11*b*) could be expected to

TABLE III.*

RAMAN FREQUENCIES FOR $C_2H_2Cl_4$ ISOMERS IN CM^{-1}		$C_2H_2Cl_4$ PLATE I INTENSITIES AT		$C_2H_2Cl_4$ PLATE II INTENSITIES AT		RAMAN FREQUENCIES FOR $C_2D_2Cl_4$ ISOMERS IN CM^{-1}	
MORE STABLE ISOMER	LESS STABLE ISOMER	38°C	124°C	66°C	126°C	MORE STABLE ISOMER	LESS STABLE ISOMER
88.2	88.2					88.2	88.2
173.0	183.6					172.6	180.4
241.7	226.0	0.0407 .0100	0.0349 .0125	0.0327 .0113	0.0267 .0120	239.8	226.2
288.8	294.6	.0623 .0211	.0517 .0345	.0391 .0216	.0370 .0226	287.1	295.1
352.9	366.7	.2070 .0700	.1860 .0945	.1210 .0490	.1135 .0580	350.2	362.1
546.4	546.4	.0236	.0166	.0163	.0152	531.2	531.2
648.1	765.1	.0920 .0293	.0850 .0408	.0682 .0244	.0584 .0269	628.0	703.1
801.6	812.1					741.0	758.1

* All intensities less than 0.04 were very difficult to measure so that it is impossible to obtain a quantitative value for *E* from them. They are good enough, however, to indicate a rise or fall in intensity with increasing temperature.

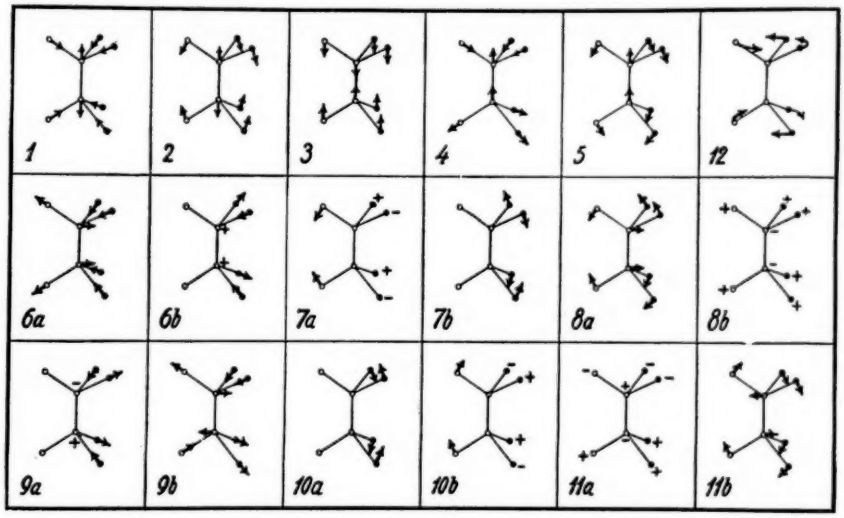

FIG. 3.

have frequencies lower than *ca.* 400 cm^{-1}. Similarly for a molecule with a C_2 configuration there are six frequencies, corresponding to the above modes, lower than 400 cm^{-1}. For a *trans*-(C_{2h}) configuration, however, the selection rules allow only the 9 fundamentals which are preserving the center of symmetry. In Fig. 3 if one-half of the molecule is rotated through 180° with respect to the other half, the modes of vibration of the *trans*-form are obtained. It is then easily seen that the modes allowed to appear in the Raman effect only 3 will have frequencies less than 400 cm^{-1}, namely (2 or 8*a*), (7*a*), and (7*b*).

From Table II it is evident that there are 5 observed fundamental vibrations in the spectrum of each isomer, with frequencies less than 400 cm^{-1}. It follows then that neither isomer possesses a *trans*-(C_{2h}) configuration. Hence one of the isomers is a *cis*-(C_{2v}) form, and the other, possesses a configuration intermediate to *cis* and *trans* with an axis of symmetry (C_2) only. Since neither of the isomers have a C_{2h} configuration, the class in which the potential energy curve has 2 minima only (Fig. 2) is ruled out and the energy curve must be of the 3 minima type (Fig. 1).

Since it has been shown that the spectrum of $C_2H_2Cl_4$ can be separated into the spectra of its isomers, and that neither of the two isomers possesses a *trans* configuration, it follows that the two isomers have C_{2v} and C_2 configurations. Of these, only the *cis*-(C_{2v}) isomer has a plane of symmetry, so that it corresponds to the minimum at 0° on the energy curve (Fig. 1). The other minima correspond to the two spectroscopically identical C_2 configurations.

It remains now to determine which of these isomers, C_{2v} or C_2 is the more stable. This was accomplished in the manner outlined below.

In curve I (Fig. 1) the ratio of the number of molecules with C_{2v} configuration to the number with C_2 configuration, is given by the relation

$$\frac{N_{C_{2v}}}{N_{C_2}}=\frac{1}{S}\cdot\epsilon^{E/RT},$$

where E is the difference in potential energy between the two isomers, and S is the statistical factor due to the number and positions of the minima for the C_2 form. The contribution to the statistical weight due to the number is 2, whereas the contribution due to the position of the minima is proportional to the width of the potential minimum hollow.

The intensity of a Raman line from the C_{2v} form is

$$I_{C_{2v}}=N_{C_{2v}}\cdot a_{C_{2v}},$$

where $a_{C_{2v}}$ is the intensity contributed by one C_{2v} molecule vibrating in a particular mode. The intensity of a line from the C_2 form is similarly $I_{C_2}=N_{C_2}\cdot a_{C_2}$ where a_{C_2} is the intensity of a C_2 molecule vibrating in a corresponding

mode. Then

$$\frac{Ic_{2v}}{Ic_2}=\frac{Nc_{2v}}{Nc_2}\cdot\frac{a_{c_{2v}}}{a_{c_2}}=\frac{Nc_{2v}}{Nc_2}\cdot A=\frac{A}{S}\cdot e^{E/RT}.$$

So that for curve I, in which the C_{2v} form is the more stable isomer,

$$\frac{I_{\text{more stable isomer}}}{I_{\text{less stable isomer}}}=\frac{Ic_{2v}}{Ic_2}=\frac{A}{S}\cdot e^{E/RT}.$$

In curve II (Fig. 1), however, the C_2 form is the more stable isomer so that;

$$\frac{I_{\text{more stable isomer}}}{I_{\text{less stable isomer}}}=\frac{Ic_2}{Ic_{2v}}=\frac{S}{A}\cdot e^{E/RT}.$$

It is possible then to distinguish between the two curves I and II since the ratio of the intensity of a line from the more stable isomer to the intensity of a corresponding line from the less stable, is either

$$\frac{A}{S}\cdot e^{E/RT} \quad \text{or} \quad \frac{S}{A}\cdot e^{E/RT},$$

respectively. This ratio can be evaluated once the value of E is known.

Irrespective of the actual energy curve for the molecule, or which isomer is the more stable, E is given by the following relation;

$$\left(\frac{I_{\text{more stable isomer}}}{I_{\text{less stable isomer}}}\right)_{T_1}\Big/\left(\frac{I_{\text{more stable isomer}}}{I_{\text{less stable isomer}}}\right)_{T_2}=\exp\left[\frac{E}{R}\left(\frac{1}{T_1}-\frac{1}{T_2}\right)\right].$$

To determine E experimentally, the lines of the doublet at 352.9 cm^{-1} and 366.7 cm^{-1} at temperatures T_1 and T_2 were measured microphotometrically. This pair was chosen because firstly, the lines are very intense and most easily measured, and secondly, they are corresponding lines i.e., they are both chlorine deformation vibrations, the line at 352.9 being mode 7*a* in Fig. 3 and 366.7 being the corresponding vibration for the C_2 isomer.

From Table III,

$$\left(\frac{I_{352.9}}{I_{366.7}}\right)_{38^\circ}\Big/\left(\frac{I_{352.9}}{I_{366.7}}\right)_{124^\circ}=\frac{2.96}{1.975}=\exp\left[\frac{E}{R}\left(\frac{1}{311}-\frac{1}{397}\right)\right],$$

whence $E=1150$ calories per mole (from plate I).

From the intensity measurements of the same lines at 66° and 126° (plate II), $E=1050$ cal. per mole.

The value of E adopted was 1100 cal. per mole.

Now $\left(\frac{I_{352.9}}{I_{366.7}}\right)_{38^\circ C}=2.96=\frac{I_{\text{more stable isomer}}}{I_{\text{less stable isomer}}}$,

so that $2.96=Q.\ \epsilon^{1100/1.98\times311}$ where Q is A/S or S/A depending on whether curve I or II obtains, respectively. Experimentally then $Q=0.497$ and

$$A/S=0.497 \text{ for curve I or}$$
$$A/S=2.01 \text{ for curve II.}$$

where A and S are as defined above. Since the angles in tetrachloroethane are nearly tetrahedral the minima representing the C_2 forms on the potential energy curve would be expected at ±120° (Fig. 1), but since there is an interaction energy due to dipoles the maxima are shifted towards the ordinate at 0° (Fig. 1). In other words the statistical weight of the isomer with C_2 symmetry is greater than, but not less than 2, i.e., $S\geq2$. So that if curve I obtains, $A\geq1.0$ and if curve II obtains, $A\geq4.0$.

Of these two choices the first is more reasonable since this would mean that the intensity contributed to the line at 352.9 cm^{-1} by one of the C_{2v} molecules is nearly equal to the intensity contributed to the line at 366.7 cm^{-1} by one of the C_2 molecules. It is indeed highly improbable that the ratio of the intensity contributions from a C_{2v} and C_2 molecule vibrating in similar modes (i.e., both chlorine deformation vibrations) can be as high as 4 : 1. In fact, within the experimental error of the intensity measurements it is possible to distinguish between the two values for A although it is not possible to determine A with any great degree of accuracy. Obviously the loss in intensity of a C_{2v} line divided by the gain in intensity of a corresponding C_2 line gives the

value of A. From Table III, this ratio for the lines 352.9 and 366.7 cm^{-1} is about 0.85 which undoubtedly indicates the value $A \backsimeq 1$ as the value to be chosen for A.

Since the experiments have distinguished between the values of $A=1$ or 4 and have shown that A has the lesser value, it follows that case I (curve I in Fig. 1) obtains, i.e., the more stable isomer has a *cis*-(C_{2v}) configuration and the less stable a C_2 configuration.

If the statistical factor is taken as 2 (i.e., a small dipole effect on the potential curve for the internal rotation and therefore $S=2$) the concentration of the *cis*-(C_{2v}) isomer at 20°C is 76.5 percent (a maximum value).

Conclusion

It has been shown that sym-tetrachloroethane, $CHCl_2 \cdot CHCl_2$, is an equilibrium mixture of two rotational isomers, a *cis*-form (C_{2v} symmetry) and a form intermediate to *cis* and *trans* with a C_2 configuration. Furthermore it has been shown that the *cis* is the more stable having about 1100 cal. per mole lower potential energy than the C_2 form.

From these data it is to be concluded that there must be a more important form of interaction present than that due to dipole interaction. The forces due to dipole interaction tend to make the molecule take up a *trans*-(C_{2h}) configuration, whereas the net effect of the forces acting in the molecule produces a stable *cis*-C_{2v} isomer and two less stable, spectroscopically identical C_2 isomers. Apparently there is another kind of interaction present, acting in opposite sense of the dipole interaction, and restricting the internal rotation about the C−C bond, producing a 3-minima potential curve corresponding to stable isomeric forms in which the atoms on the two carbon atoms are in opposed positions.

MAY, 1940 JOURNAL OF CHEMICAL PHYSICS VOLUME 8

Hindered Rotation

III. The Qualitative Nature of the Interactions Hindering Internal Rotation

A. Langseth, H. J. Bernstein* and B. Bak
Universitetets Kemiske Laboratorium, Copenhagen, Denmark
(Received March 15, 1940)

Experimental evidence shows that an important contribution to the potential barrier hindering internal rotation, is an interaction stabilizing "opposed" configurations. A qualitative picture of this interaction which is considered as arising in the bond connecting the two halves of a molecule, is presented, based on the symmetry properties of the molecule and the ideas associated with overlapping of wave functions. This interaction seems to be of chief importance in hydrocarbons where dipole and steric effects are small, such as ethane, propylene, toluene, cyclohexane, dimethylacetylene. Even in compounds where the dipole effect is great, such as tetrachloroethane and dichloroethylene, this interaction plays the most important role.

THE results of the preceding investigations on cyclohexane[1] and tetrachloroethane[2] show that the most stable configurations attained by the molecules is that in which the atoms are in the "opposed" position, i.e., the configuration with the carbon ring as a plane of symmetry and a mirror plane for the hydrogen atoms for cyclohexane (D_{6h} symmetry), and the configuration with a plane of symmetry perpendicular to the C−C axis for tetrachloroethane (C_{2v} symmetry).

These experiments indicate the necessity of introducing an interaction which stabilizes "opposed" configurations, when describing the occurrence of rotational isomers and their relative stability, which may be (as in the case of the molecules mentioned above) of greater magnitude than the other types of interaction

* 1851 Exhibition Research Scholar.
[1] A. Langseth and B. Bak, this journal, p. 403.
[2] A. Langseth, H. J. Bernstein, this journal, p. 410.

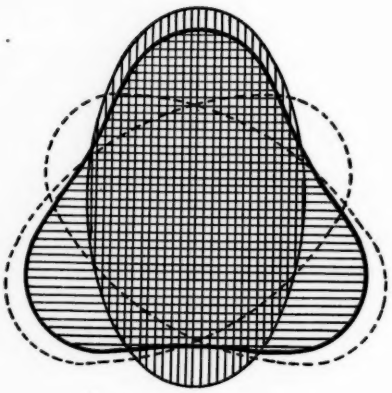

FIG. 1.

present, such as that due to dipoles and steric hindrance (which tend to stabilize "staggered" configurations). As a result, the most important contributions to the potential barrier restricting rotation are considered as arising from: (i) the interactions stabilizing "staggered" forms, such as those due to dipoles and steric effects, and (ii) the interactions stabilizing "opposed" forms. Furthermore, all the interactions of the second class mentioned above are considered as acting through the C−C bond and arising because of the lack of rotational symmetry of this bond.

We propose here a physical picture based on the symmetry properties of the molecule and the notions associated with overlapping of wave functions, to account for these interactions acting through the C−C bond and tending to stabilize "opposed" configurations.

(I) The actual symmetry of the C−C bond may be obtained by superposition of the individual symmetries of the single carbon bonds which are considered together to give the C−C bond. The symmetry of a single carbon bond is obtained by considering the distortion of the rotationally symmetrical carbon bond function due to the presence of the other bonds and atoms on the *C* atom.[3] For example, the rotational symmetry of a single carbon bond function is distorted by the presence of the C−H bonds and H atoms in a methyl group and assumes the trigonal symmetry of the group. A section of this trigonally symmetrical bond function in a plane perpendicular to the direction of the bond, has D_{3h} symmetry. When two methyl groups are considered together as an ethane molecule, the two identical carbon bond sections of the two methyl groups will overlap completely for the "opposed" configuration (D_{3h}) and least for the "staggered" configuration (D_{3d}).

(II) Assuming that the greatest exchange energy and therefore a minimum of potential energy is coincident with the maximum overlapping of these bond sections, the configuration of the ethane molecule is obtained as the "opposed" (D_{3h}) form. The difference in overlapping of the bond sections for the two forms (D_{3h} and D_{3d}) is a measure of the potential barrier arising from this interaction.

Since the previous investigation[1] has yielded the "opposed" form as the most stable for cyclohexane and since the dipole effect must be of the same order of magnitude for cyclohexane and ethane[4] while the steric effects are probably greater for cyclohexane,[5] it is reasonable to conclude that the stable form of ethane is the "opposed" (D_{3h}) configuration.

Apparently the most important interaction for molecules in which the interactions stabilizing "staggered" configurations are commensurable with those prevalent in ethane and cyclohexane, is the interaction acting through the C−C bond. So that, for such molecules as dimethylacetylene, toluene, and propylene, the above physical picture should adequately account for the internal rotational problems.

In dimethylacetylene ($CH_3-C\equiv C-CH_3$) the trigonally symmetrical C−C single bonds from the methyl groups interact through the C≡C triple bond, so that the resulting potential curve with 3 minima will arise as a second-order effect.

[3] Eyring *et al.*, J. Am. Chem. Soc. **61**, 1876 (1939), have shown that of the two interactions stabilizing the "opposed" form of ethane, namely, the interaction due to forms resonating between a single and double C−C bond structure, and the interaction between atoms on the C atom with the hybridized carbon orbitals, that the former accounts for the greater part of the potential barrier. These effects, however, take place in the C−C bond and are probably a quantitative estimate of the actual distortion from rotational symmetry. Since these interactions act through the C−C bond they must be included in our qualitative representation of all interactions stabilizing "opposed" forms.

[4] Eyring *et al.*, reference 3, have calculated the dipole interaction in ethane to be about 300 cal. per mole.

[5] The energy necessary to distort the normal tetrahedral C−C−C angle to 120° in the plane configuration has been estimated from the C−C−C deformation frequency in cyclohexane as *ca.* 1200 cal.

Accordingly, the potential barrier would be low and one would expect free or practically free internal rotation. This is in agreement with the experimental evidence.[6]

For toluene, overlapping of the D_{3h} bond section of the methyl group with the D_{2h} bond section of the phenyl group, must be considered. As can be seen from Fig. 1 this gives rise to a potential curve with 6 identical minima corresponding to the molecular configuration with a plane of symmetry. The difference in overlapping for rotational positions 30° apart, may be considerably less than the difference in overlapping in ethane where two identical trigonally symmetric sections are compared, so that the height of the potential barrier would be lower than that in ethane.

In propylene, overlapping of the D_{3h} bond section of the methyl group with the C_{2v} section

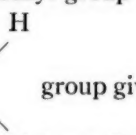

of the $CH_2=C$ group gives a potential curve with 6 minima which are divided into 2 sets of 3 identical minima corresponding to two possible isomers. For this molecule, however, the distortion of the bond sections must be of the same order of magnitude, so that for the same reason as mentioned above for toluene, the value of the potential barrier would be considerably less than that obtained for ethane. This is in agreement with the value of 800 cal. per mole given by Pitzer[7] and Kistiakowsky[8] for the barrier in propylene, as compared with 3000 cal. per mole for ethane. This value, however, was calculated on the basis of a 3 minimum potential curve, which fitted the experimental data better than a 6 minimum curve.[8] Also, the Raman spectrum of propylene[9] seems to indicate the presence of one configuration only. It seems then that there is a considerable energy difference between the two isomers and on account of this and the low height of the potential barriers the potential hollows corresponding to the less stable isomer are shallow and ill-defined so that the potential curve approximates a three minimum curve.

In the cases considered above, the steric and dipole effects were considerably less than the opposing interaction through the C−C bond. For molecules such as the long chain hydrocarbons (4 or more C atoms) important interactions due to steric hindrance arise and may be sufficiently great to stabilize the "staggered" or zig-zag form.

Also when the dipole effect is great, as in the dihalogen substituted ethanes, the "staggered" form may be stabilized as in $C_2H_4Cl_2$ and $C_2H_4Br_2$, where spectroscopic evidence has been obtained[10] indicating a greater stability of the *trans*-C_{2h} than of the *cis*-C_{2v} form. On the other hand, for tetrachloroethane our results[2] show the *cis*-(C_{2v}) form to be the more stable isomer and that the other isomer present has a C_2 configuration. These results can be satisfactorily interpreted on the basis of the overlapping theory in the following way. The free carbon bond section of the $CHCl_2$-group has C_{2v} symmetry. When two such groups are considered

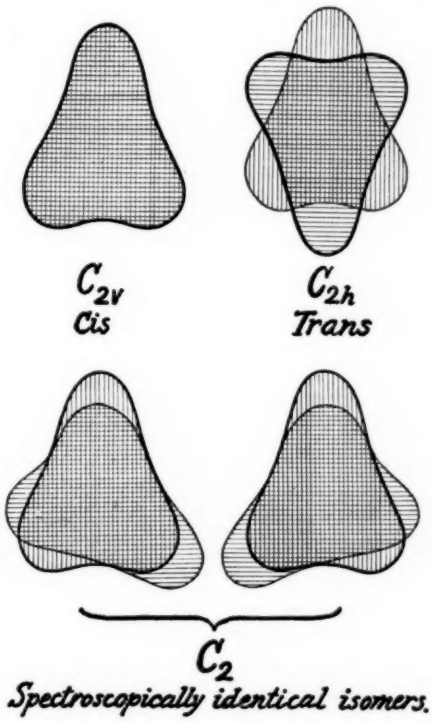

FIG. 2.

[6] B. L. Crawford, J. Chem. Phys. **7**, 437 (1939).
[7] K. Pitzer, J. Chem. Phys. **5**, 473 (1937).
[8] Kistiakowsky, Lacher and Ransom, J. Chem. Phys. **6**, 900 (1937).
[9] R. Ananthakrishnan, Proc. Ind. Acad. Sciences **3**, 527 (1936).
[10] Mizushima and Morino, Bull Chem. Soc. Jap. **13**, 182 (1938); Proc. Ind. Acad. Sci. Raman Jubilee Vol., p. 315.

together as a tetrachloroethane molecule, the maximum overlapping of the bond sections is obtained when the H atoms and Cl atoms are opposed to each other i.e., for a *cis*-C_{2v} configuration. A minimum overlapping is attained in the *trans*-C_{2h} configuration, but there are two rotational positions of maximum overlapping intermediate to the C_{2v} and C_{2h} configurations, *viz.* Fig. 2. It is readily seen that the *trans*-form corresponds to a maximum on the potential energy curve and is not present as an isomer.[2] The isomers present in an equilibrium mixture are the more stable *cis*-(C_{2v}) form and the less stable isomers with C_2 symmetry.

To account for the greater stability of the *trans*-isomer in dichloroethane but a more stable *cis*-form in tetrachloroethane, we may argue in the following manner. Roughly, the dipole effects in dichloro- and tetrachloroethane are of the same magnitude and are sufficiently great to overcome the opposing interaction arising in the C−C bond and stabilize the *trans*-form of dichloroethane, whereas, when two more chlorine atoms are introduced into the molecule, the bond sections are distorted sufficiently, so that when overlapping is considered, the restriction in the bond is much greater than the dipole effect and the C_{2v} form is stabilized for tetrachloroethane.

The dipole interaction in dichloroethylene, CHCl=CHCl, is also comparable in magnitude with that in dichloroethane. In dichloroethylene, however, the *cis*-(C_{2v}) form is the more stable isomer. This indicates that the "overlapping energy difference" is considerably greater for the double bond than for the single bond. In other words a C=C double bond section is distorted more by the bonds and atoms on the C atom than the C−C single bond section by the same bonds and atoms.

MAY, 1940 JOURNAL OF CHEMICAL PHYSICS VOLUME 8

The Variation of the Transference Numbers of Potassium Chloride in Aqueous Solution with Temperature

R. W. ALLGOOD, D. J. LE ROY AND A. R. GORDON
Chemistry Department, University of Toronto, Toronto, Canada

(Received February 8, 1940)

The transference numbers of potassium chloride in aqueous solution have been determined for concentrations from 0.01N to 0.10N at temperatures from 15°C to 45°C by the moving boundary method. Both cation and anion boundaries were used. The results obtained by the two methods are in satisfactory agreement, the sum ($t_+ + t_-$) for a solution being unity within a few units in the fourth decimal place; the data reported here are also in close agreement with those reported by Longsworth for 25°C. For the whole range of temperature, the Longsworth function $t_+{}^{0\prime}$ is linear in the concentration. It is found, however, that the cation transference number decreases with rising temperature, in contradiction to the Kohlrausch generalization which predicts that transference numbers less than one-half should increase with rising temperature.

ALTHOUGH in recent years considerable information as to transference numbers of electrolytes at 25°C has been accumulated, precise transference data for other temperatures are still practically nonexistent. In this paper, we report the results of transference measurements by the moving boundary method on solutions of potassium chloride at temperatures from 15°C to 45°C. One reason for selecting this electrolyte and this temperature range was that such data were necessary to interpret thermodynamically the results of electromotive force measurements, which are now in progress in this laboratory, on cells with transference.

For cation boundaries, the autogenic cell, which had been previously used in the work on the acetates,[1] was employed; this cell is referred to in the tables as II. For anion boundaries, with

[1] D. J. Le Roy and A. R. Gordon, J. Chem. Phys. **6**, 398 (1938); **7**, 314 (1939).

potassium iodate as indicator solution, the simple sheared boundary cell (cell III) shown in Fig. 1 was used. With the large hollow stopcock S-turned 90° counterclockwise from the position indicated in the figure, potassium chloride and potassium iodate solutions are forced into the cell by air pressure through D and C; the cadmium anode and the silver-silver chloride cathode (each mounted in a ground glass joint) are placed in B and A; a clockwise rotation of S through 90° then forms the junction at the bottom of the graduated tube T. In spite of this rather crude method of forming the junction, the resulting boundary is extremely sharp and with no hint of haziness. As in the case of cell II, the tube T (internal diameter 2.5 mm) was calibrated by the method of MacInnes, Cowperthwaite and Huang.[2] As a rule the cadmium anode formed the closed side of the cell, although in some of the measurements at 25° (referred to in Table I as IIIa) the cathode side was closed. The circuit, the semi-constant current device, and the method of carrying out the current time readings were the same as those previously described.[1] The cells were mounted in a glass sided oil bath whose temperature was regulated to 0.01°C; temperatures were read on laboratory standard thermometers which had been calibrated against a platinum resistance thermometer with National Bureau of Standards certificate.

The potassium chloride and potassium iodate were British Drug Houses Analar, twice recrystallized; potassium chloride solutions were made up gravimetrically from conductivity water and the salt, which had been rapidly fused in platinum in an atmosphere of carefully purified dried nitrogen. All weights were reduced to vacuum, and in computing the volume concentrations density data from *International Critical Tables*[3] were employed. The indicator solutions were also made up gravimetrically from conductivity water and potassium iodate which had been previously dried in a desiccator over sulphuric acid. Carbon dioxide was removed from the solutions by bubbling carefully purified water-saturated air through them at 200 mm pressure[4] before they were forced into the cells. In each case a sample of the conductivity water used in making up the solution was treated similarly, and its conductance was then determined in order to compute the solvent correction.

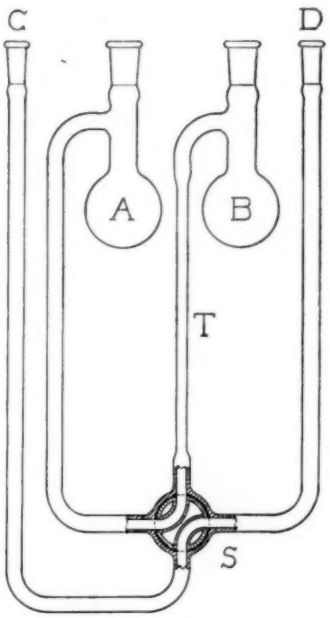

FIG. 1.

Table I summarizes the results. The first column gives the cell, the second the concentration C of the potassium chloride solution expressed in moles per liter, and the third the mean value for each run of $(t_+)_{obs}$ or of $(t_-)_{obs}$, the uncorrected transference numbers of the cation (II) or of the anion (III), respectively; these were computed by the relation $(t_+)_{obs} = VC/1000f$ where f is the number of faradays required to move the boundary through V cc; as a rule individual values of VC/f for a run showed a mean absolute deviation from the mean of a part in 3000 or less. The fourth and fifth columns of Table I give the solvent and volume corrections;[5] the latter is given by $-C\Delta V/1000$ where

[2] MacInnes, Cowperthwaite and Huang, J. Am. Chem. Soc. **49**, 1710 (1927).

[3] Int. Crit. Tab., Vol. 3, p. 87.

[4] By saturating the solutions at less than atmospheric pressure any chance of air bubbles forming in the cells during electrolysis was removed.

[5] For a discussion of these corrections see D. J. MacInnes and L. G. Longsworth, Chem. Rev. **11**, 171 (1932); L. G. Longsworth, J. Am. Chem. Soc. **57**, 1185 (1935).

Cell II

$$\Delta V = \tfrac{1}{2}\bar{V}_{CdCl_2} - t_+ \cdot \bar{V}_{KCl} - \tfrac{1}{2}V_{Cd}$$

Cell III

$$\Delta V = t_+ \cdot \bar{V}_{KCl} + \tfrac{1}{2}V_{Cd} - \tfrac{1}{2}\bar{V}_{CdCl_2}$$

Cell IIIa

$$\Delta V = V_{Ag} - V_{AgCl} + \bar{V}_{KCl} - (t_-)_{KIO_3} \cdot \bar{V}_{KIO_3}.$$

Here V_{Cd}, V_{Ag} and V_{AgCl} are the molal volumes of cadmium, silver and silver chloride, and $\bar{V}_{KCl}$, $\bar{V}_{CdCl_2}$ and $\bar{V}_{KIO_3}$ are the partial molal volumes of the three salts in solution. The sixth column of Table I gives the corrected value of t_+ or t_-, while the last column gives the mean value of t_+ for the solution.

There are two obvious checks on the accuracy of the data. First, the transference number from successive runs on the same solution must be independent of current density; in the measurements reported here this condition was always fulfilled, an increase of 100 percent in current density causing a random change in transference number no greater than the apparent error of an individual experiment. Second, when as in the majority of our measurements, both t_+ and t_- have been determined for the same solution, the sum of the two should be unity; a glance at the sixth column of Table I will show that this condition is fulfilled within a few units in the fourth decimal place.

It will be noticed in Table I that no results for anion boundaries at 45° are recorded in the table. The reason for this is that we have found that the Kohlrausch criterion for a stable boundary

$$(t_\pm/C)_{KCl} = (t_\pm/C)_{Indicator}$$

must be satisfied within ever narrower limits as the temperature rises. In the autogenic cell, this condition is obtained automatically, but in the sheared cell, the initial concentration of the

TABLE I.

Cell	C	$(t_\pm)_{obs}$	Sol. Corr.	Vol. Corr.	$t_\pm$	t_+
			15° *Centigrade*			
III	0.009935	0.5070	0.0005	−0.0001	0.5074	0.4926
III	.009941	.5068	.0005	−0.0001	.5072	.4928
II	.014207	.4919	.0004	+0.0001	.4924	.4926
III	.014207	.5069	.0004	−0.0001	.5072	
II	.015007	.4917	.0003	+0.0001	.4921	
III	.015007	.5072	.0003	−0.0001	.5074	.4924
III	.015007	.5072	.0003	−0.0001	.5074	
II	.020044	.4918	.0002	+0.0002	.4922	.4924
III	.020044	.5074	.0002	−0.0002	.5074	
II	.030303	.4918	.0001	+0.0002	.4921	.4921
III	.030303	.5080	.0001	−0.0002	.5079	
II	.060085	.4916	.0001	+0.0005	.4922	.4921
III	.060085	.5085	.0001	−0.0005	.5081	
II	.10024	.4915	.0000	+0.0008	.4923	.4922
III	.10024	.5088	.0000	−0.0008	.5080	
			25° *Centigrade*			
IIIa	.009926	.5091	.0005	0.0000	.5096	.4904
II	.014183	.4891	.0004	+0.0001	.4896	.4898
IIIa	.014183	.5096	.0004	0.0000	.5100	
II	.020004	.4894	.0002	+0.0002	.4898	.4899
III	.020004	.5100	.0002	−0.0002	.5100	
II	.030242	.4897	.0001	+0.0002	.4900	.4901
IIIa	.030242	.5096	.0001	0.0000	.5097	
IIIa	.072707	.5098	.0000	0.0000	.5098	.4902
III	.072707	.5104	.0000	−0.0005	.5099	
II	.094494	.4893	.0000	+0.0007	.4900	.4900
IIIa	.094494	.5100	.0000	0.0000	.5100	
II	.098572	.4894	.0000	+0.0007	.4901	
II	.098572	.4890	.0000	+0.0007	.4897	.4900
II	.098572	.4891	.0000	+0.0007	.4898	
IIIa	.098572	.5097	.0000	0.0000	.5097	
			35° *Centigrade*			
II	.009960	.4885	.0002	+0.0001	.4888	.4889
III	.009960	.5109	.0002	−0.0001	.5110	
II	.020068	.4883	.0002	+0.0001	.4886	.4886
III	.020068	.5113	.0002	−0.0001	.5114	
II	.029806	.4880	.0002	+0.0002	.4884	.4884
II	.030148	.4879	.0002	+0.0002	.4883	.4883
II	.030770	.4883	.0002	+0.0002	.4887	
II	.030770	.4882	.0002	+0.0002	.4886	.4886
III	.030770	.5114	.0002	−0.0002	.5114	
II	.060672	.4882	.0001	+0.0004	.4887	
II	.060672	.4880	.0001	+0.0004	.4885	.4884
III	.060672	.5121	.0001	−0.0004	.5118	
III	.060672	.5121	.0001	−0.0004	.5118	
III	.099542	.5116	.0001	−0.0007	.5110	.4890
III	.099542	.5115	.0001	−0.0007	.5109	
II	.100390	.4879	.0000	+0.0007	.4886	.4888
II	.100390	.4884	.0000	+0.0007	.4891	
			45° *Centigrade*			
II	.009923	.4865	.0002	+0.0001	.4868	.4868
II	.009923	.4864	.0002	+0.0001	.4867	
II	.019989	.4864	.0002	+0.0001	.4867	.4867
II	.019989	.4863	.0002	+0.0001	.4866	
II	.019994	.4865	.0003	+0.0001	.4869	.4869
II	.029424	.4864	.0002	+0.0002	.4868	.4868
II	.029424	.4864	.0002	+0.0002	.4868	
II	.060434	.4861	.0001	+0.0004	.4866	.4868
II	.060434	.4864	.0001	+0.0004	.4869	
II	.098929	.4869	.0001	+0.0006	.4876	.4876
II	.099083	.4864	.0000	+0.0006	.4870	.4871
II	.099083	.4866	.0000	+0.0006	.4872	

indicator solution can be varied at will. MacInnes and Longsworth[5] have stated (and our results confirm them) that at 25°C, a variation of 40 percent in the ratio C_{KCl}/C_{KIO_3} does not appreciably affect the measured transference number of the chloride ion; at 45°, the position is quite different. Fig. 2 shows the results of a series of measurements on a 0.04780N KCl solution at this temperature; the ordinates are the corrected values of t_- and the abscissas the concentration of the potassium iodate indicator solution. The horizontal line in the figure gives the value of t_- for this solution obtained from measurements on t_+ in cell II. A calculation of t_- for potassium iodate from rough conductance measurements on potassium chloride and potassium iodate solutions at 45° by means of the independent ionic mobility rule predicts 0.0328 normal as the correct indicator concentration for this strength of potassium chloride. The figure shows that a variation of as little as one percent from this concentration will cause an appreciable error in the measured transport number. We believe this is the explanation for the results of Samis[6] who found t_+ for 0.1N KCl at 40° to be 0.490, especially as he used falling boundaries, which are more sensitive to indicator concentration than are rising boundaries. At 35°C, indicator concentration is not so critical, and for a given potassium chloride solution there is an appreciable range in which t_- is not affected by potassium iodate concentration. It should be noted in passing that the curve of Fig. 2 is of radically different shape from the widely quoted curve of MacInnes and Longsworth[5] which gives the effect of indicator concentration on measured transference number for LiCl/KCl cation boundaries.

For many 1–1 electrolytes at 25°C, it has been found that the Longsworth function $t_+^{o\prime}$ is linear in C, i.e.,

$$t_+^{o\prime}=(t_+\cdot\Lambda'+\sigma\sqrt{C})/(\Lambda'+2\sigma\sqrt{C})$$
$$=t_+^{o}+AC. \quad (1)$$

Here t_+^{o} is the transference number at infinite dilution, A is a disposable constant, $\Lambda'=\Lambda_0-(\vartheta\Lambda_0+2\sigma)\sqrt{C}$, Λ_0 is the equivalent conductance at infinite dilution, and ϑ and σ have their theoretical values *viz.* $8.147\times10^5/(DT)^{\frac{3}{2}}$ and $40.93/(DT)^{\frac{1}{2}}\eta$ where D and η are the dielectric constant and viscosity of the solvent. The values of ϑ and σ (employing Wyman's dielectric constant data[7] and the viscosities as recorded in *International Critical Tables*[8]) are given in Table II. Except at 18° and 25° there are no precise values of Λ_0; however, a Shedlovsky extrapolation of the data in *International Critical Tables*[9] yields moderately accurate values for 0°, 50° and 100° and from the resulting plot of log Λ_0 *vs.* $1/T$, the values given in Table II were obtained; these are accurate enough for the present purpose.

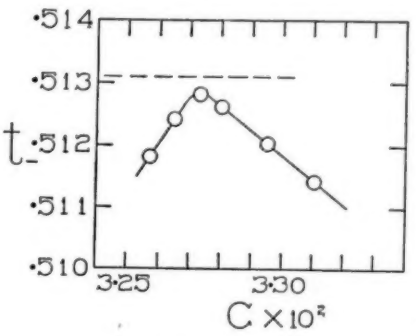

FIG. 2.

Figure 3 shows the resulting plots of $t_+^{o\prime}$ for the four temperatures, that for 25° also including the results of Longsworth.[10] It is evident from the figure that there is very satisfactory agreement between our results and his, and also that $t_+^{o\prime}$ is (within the limit of error of the measurements) linear in C for the whole range of temperature. The values of t_+^{o} and A corresponding to the plots of Fig. 3 are also recorded in Table II. Table III gives values of t_+ for a few round values of the concentration, computed from Table II by means of Eq. (1).

The most surprising result of the research, however, is that t_+ for potassium chloride *decreases* with rising temperature. Kohlrausch made the generalization many years ago that the faster the ion, the smaller the temperature coefficient of its mobility, a result similar to the Oholm rule for the temperature coefficient of the diffusion constant; hence all transference numbers should approach 0.5 with rising temper-

[6] C. S. Samis, Trans. Faraday Soc. **33**, 469 (1937).

[7] J. Wyman, Phys. Rev. **35**, 623 (1930).
[8] Int. Crit. Tab. Vol. 5, p. 10.
[9] Int. Crit. Tab. Vol. 6, p. 234.
[10] L. G. Longsworth, J. Am. Chem. Soc. **54**, 2741 (1932)

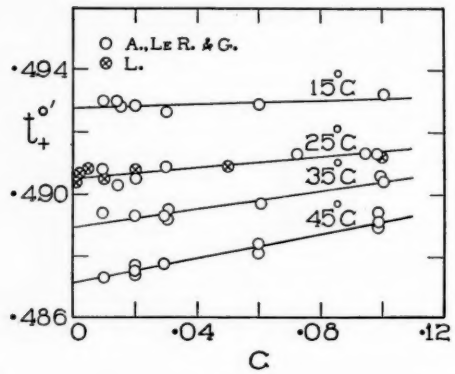

FIG. 3.

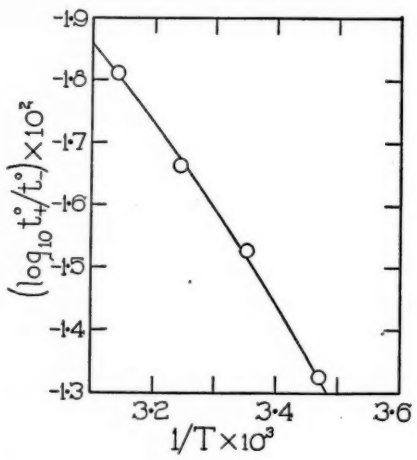

FIG. 4.

ature. Recently, Taylor,[11] discussing the Eyring theory of the transport process in solution,[12] has pointed out that the Kohlrausch rule is consistent with Eyring's argument; fast and presumably small ions will require smaller holes and consequently smaller activation energies of transport than will large slow ions. A little consideration shows, however, that this rule can only be a rough first approximation; due to the hydration of the cation, the mechanism of transport may well be different for cation and anion, and this difference may become prominent when, as in the case of potassium chloride, cation and anion have approximately the same mobility. It is possible, of course, on this basis to invent several moderately plausible explanations for our results—explanations, however, which possess the rather dubious advantage that there does not seem at the moment to be any way of proving or disproving them experimentally. For example: the mechanism of cation transfer might be a more or less continuous exchange of solvent molecules in the sheath surrounding the ion, while anion transfer might correspond to a jump from one "cage" of solvent molecules to another.[13]

TABLE II.

	15°	25°	35°	45°
Λ_0	121.0	149.9	180.5	213.4
ϑ	0.2233	0.2273	0.2318	0.2370
σ	23.23	29.89	37.35	45.42
t_+°	0.4928	0.4905	0.4889	0.4872
A	0.002_9	0.008_7	0.014_9	0.019_5

TABLE III. *t_+ for KCl solutions as a function of temperature and concentration.*

C	15°	25°	35°	45°
0.005	0.4926	0.4903	0.4887	0.4869
.01	.4925	.4902	.4886	.4868
.02	.4924	.4901	.4885	.4868
.05	.4923	.4900	.4885	.4869
.10	.4921	.4900	.4888	.4873

On the Eyring-Taylor theory, the tangent to a plot of log (t_+°/t_-°) against $1/T$ should yield the difference in the activational energies of transport of potassium and chloride ions at infinite dilution; Fig. 4 shows such a plot. The corresponding mean differences in the activation energy for the temperature ranges 15–25°, 25–35° and 35–45° are −150, −130 and −120 cal., respectively.

[11] H. S. Taylor, J. Chem. Phys. **6**, 331 (1938).
[12] H. Eyring, J. Chem. Phys. **4**, 283 (1936).
[13] M. J. Polissar, J. Chem. Phys. **6**, 833 (1938).

The Variation of the Differential Diffusion Constant of Sulphuric Acid with Temperature

E. A. HOLLINGSHEAD AND A. R. GORDON
Chemistry Department, University of Toronto, Toronto, Canada

(Received February 8, 1940)

The differential diffusion constant of sulphuric acid has been determined for concentrations from 0.025 mole per liter to 1 mole per liter at temperatures from 10°C to 35°C. Over the whole range of temperature, the variation of the diffusion constant with concentration is similar to that previously found at 25°. The mean activation energies of transport for the temperature intervals 10–15°, 15–25° and 25–35° are 4.9, 4.5 and 3.8 kcal, respectively.

AN earlier communication[1] from this laboratory reported values of the temperature coefficient of the differential diffusion constant for hydrochloric acid in aqueous solution; in this paper, we report similar data for sulphuric. The results are of interest since, in distinction from hydrochloric acid (a typical strong electrolyte) sulphuric acid is weak as far as its second ionization is concerned.

The apparatus, the method of analysis by interferometer, and the general experimental technique were similar to those previously used; as in the earlier work, the diffusion cells were recalibrated after every three or four runs with acid by means of 0.1 N KCl at 25°C, the value of $\bar{k}$ for the calibration[1,2] being as before 1.842×10^{-5} cm/sec.

Table I summarizes the results; the second and third columns give the initial concentrations of the inner and outer solutions in moles per liter; the fourth column gives the square root of the mean concentration of the experiment (the concentration for which the differential diffusion constant k is equal to the effective diffusion constant $\bar{k}$ computed by Eq. (2) of reference 2). The last column gives the mean value of k, obtained from four measurements each with a different cell; these individual values showed a mean absolute deviation from the mean of considerably less than one percent.

TABLE I.

°C	C_0'	C_0''	$((C_0'+C_0'')/2)^{\frac{1}{2}}$	$10^5\cdot k$
10	0.0536	0	0.164	1.270
10	.1027	0.0494	.276	1.210
10	.2006	0.0992	.387	1.210
10	.3964	0.3030	.591	1.220
10	.8050	0.6872	.864	1.300
15	.0505	0	.159	1.475
15	.1005	0	.224	1.445
15	.2014	0.1012	.389	1.385
15	.3998	0.2947	.589	1.395
15	.3991	0.2988	.591	1.400
15	.6152	0.5023	.748	1.430
15	.7912	0.6925	.861	1.465
35	.0504	0	.159	2.330
35	.0953	0	.218	2.290
35	.2030	0.1008	.390	2.265
35	.3998	0.3002	.592	2.280
35	.8103	0.6906	.866	2.430

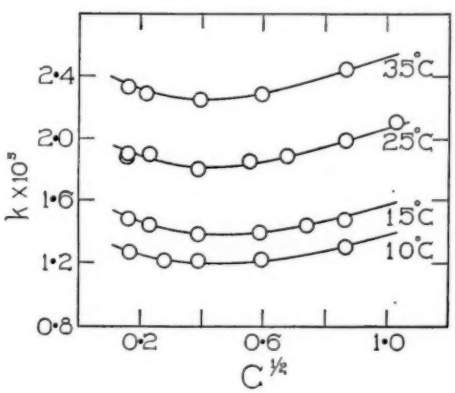

FIG. 1.

A calculation of the type described in reference 2 hardly seems justified in view of the uncertainties inherent in determining the thermodynamic factor[3] for an electrolyte such as sulphuric acid; a glance at Fig. 1, however, which also contains the data[2] previously reported for 25°C, shows that the curves of k *vs.* $\sqrt{C}$ are all of the same general shape. Table II gives values

[1] W. A. James and A. R. Gordon, J. Chem. Phys. **7**, 963 (1939).
[2] W. A. James, E. A. Hollingshead and A. R. Gordon, J. Chem. Phys. **7**, 89 (1939).
[3] A. R. Gordon, J. Chem. Phys. **5**, 522 (1937).

of the diffusion constant at round values of $\sqrt{C}$, corresponding to the continuous curves of Fig. 1.

A calculation of the mean activation energy of diffusion for 0.05 molal acid for the temperature intervals 10–15°, 15–25° and 25–35° gives 4.9, 4.5 and 3.8 kcal., respectively; these are to be compared with those for dilute hydrochloric acid[1] over the same temperature intervals, *viz.*, 4.4, 4.0 and 3.8 kcal. One difference between the two acids is that while for hydrochloric the activation energy is independent of concentration only up to 0.2 *N*, for sulphuric it is independent of concentration within the limit of error of the measurements for the whole range of concentration studied. If the behavior of hydrochloric acid is typical of strong electrolytes at moderate concentrations, this suggests that with sulphuric there must be some counterbalancing effect possibly due to the decreased ionization in the stronger solutions.

TABLE II.

$C^{\frac{1}{2}}$	10°	$\frac{10^5 \cdot k}{15°}$	25°	35°
0.15	1.28	1.49	1.94	2.35
.20	1.25	1.45_5	1.88	2.31
.30	1.21	1.40_5	1.83_5	2.26
.40	1.19_5	1.38_5	1.81	2.25
.60	1.21_5	1.41	1.86	2.29
.80	1.27	1.47	1.94	2.39
1.00	1.36_5	1.57	2.05	

MAY, 1940 JOURNAL OF CHEMICAL PHYSICS VOLUME 8

Dielectric Polarization in Solution

I. The Failure of the Clausius-Mosotti Equation

W. H. RODEBUSH AND C. R. EDDY
The Noyes Chemical Laboratory, University of Illinois, Urbana, Illinois

(Received February 24, 1940)

It has been assumed by recent writers, including Onsager, that the Debye-Clausius-Mosotti procedure would give satisfactory results for the polarization of a nonassociated polar solute in dilute solution in a nonpolar solvent. A consideration of the existing data for solutions of this type shows that this classic procedure must lead to erroneous and very misleading conclusions in regard to the polarization of the solute. The Onsager equation on the other hand gives excellent agreement with the experimental data and it is possible to calculate the moment in the vapor state by it, from the data in dilute solutions with results rather more satisfactory than those obtained by Böttcher from the dielectric constant of the pure liquid. For certain cases when the Clausius-Mosotti equation appears to hold, the agreement is believed to be fortuitous.

THE dielectric constant is the most significant property of solutions in which association takes place through hydrogen bonding. Infra-red studies[1] show the presence of hydrogen bonding but it appears that the most exact information as to the degree of polymerization and its variation with concentrations are to be obtained from measurement of the dielectric polarization. In the course of an investigation in which a great number of exact data have been obtained on the alcohols in solution in nonpolar solvents it has become evident that the interpretation of these data by the methods of Debye and his followers is difficult and probably misleading. The calculations of the polarization of the alcohols by the method which has been generally used leads to results which are bewildering particularly in very dilute solution where, if anywhere, the method should involve the least error. It has of course been recognized that the assumption of a constant polarization for the solvent is not sound but this defect alone could hardly account for the fantastic results obtained in very dilute solutions. It has also been generally recognized that the Clausius-Mosotti equation leads to the prediction of an

[1] See, for example, infra-red absorption studies by A. M. Buswell, W. H. Rodebush, *et al.*, in this journal and the *Journal of the American Chemical Society.*

infinite dielectric constant for all polar liquids. Thus the difference between ethyl alcohol and ethyl chloride would appear to be one of degree only. One would be led to assume that the association of ethyl alcohol actually reduced the dielectric constant while in the case of ethyl bromide some sort of dipole association was even more effective. This conclusion is of course contradicted by all the measurements of the colligative properties of these substances as well as the infra-red studies referred to above.

A number of writers have recently discussed the question from a theoretical point of view. Fuoss[2] has discussed solutions of molecules of large dipole moments (10–20 Debye units) in nonpolar solvents where dipole interaction may be expected to be considerable. Wyman[3] has made an empirical generalization for dipolar ions of large moment in polar solvents. Onsager[4] has considered the general case and Kirkwood[5] has extended the considerations of Onsager to a liquid such as water where association occurs. In this series of papers we wish to consider the behavior of molecules of small moment (1–3) Debye units in nonpolar solvents. To begin with we may note that this type of solution bears a close analogy to the cases studied by Wyman in that the polarity of the solute is relatively great as compared to that of the solvent. We shall make an empirical generalization similar to Wyman. But the justification for this generalization is to be found in the work of Onsager.

This we believe to be true in spite of the fact that Onsager states in his paper that the Clausius-Mosotti equation should be a satisfactory approximation in dilute solution and nonpolar solvents.

It must of course be recognized that the Clausius-Mosotti formula or its alternative forms the Lorentz-Lorenz expression holds for nonpolar liquids ($\epsilon = n^2$). The application of the Clausius-Mosotti formula to polar gases is of course no evidence for its general validity since here the internal polarization is negligible and the formula reduces to a form which is adequate by the simple laws of electrostatics. The difficulties with the Clausius-Mosotti equation become obvious as soon as we attempt to apply it to polar molecules.

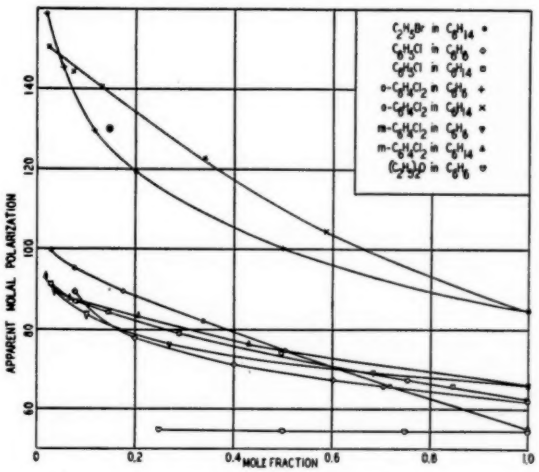

FIG. 1. Apparent molal polarization of polar solutes in nonpolar solvents as calculated by the Debye-Clausius-Mosotti theory. (See reference 6.)

In Fig. 1 are represented the polarizations of a number of halogen derivatives as calculated by the classical Debye-Clausius-Mosotti (hereinafter referred to as D-C-M) theory for which chemical evidence points to the lack of any sort of association and it should have been obvious from the beginning that the lack of any constancy in the polarization of these molecules even in the most dilute solutions indicates an internal inconsistency in the theory.[6]

It may of course be argued that the extrapolation of the polarization to infinite dilution leads to values of the moment which are often in agreement with the moment as obtained from measurements upon the vapor. To this it may be replied that this agreement is often obtained by the use of considerable corrections for a hypothetical atom polarization and that if the considerations of Onsager are correct no such agreement is to be expected. Finally, Böttcher[7] has shown that the value of the moment in the vapor state can often be calculated by the Onsager

[2] R. M. Fuoss, J. Am. Chem. Soc. **56**, 1027 (1934).
[3] J. Wyman, Jr., J. Am. Chem. Soc. **58**, 1482 (1936).
[4] L. Onsager, J. Am. Chem. Soc. **58**, 1486 (1936).
[5] I. G. Kirkwood, J. Chem. Phys. **7**, 911 (1939).

[6] All of the data for Figs. 1 and 2 are taken from the following articles: J. W. Williams and I. J. Krchma, J. Am. Chem. Soc. **49**, 1679 (1927); J. W. Williams and E. F. Ogg, J. Am. Chem. Soc. **50**, 98 (1928); C. P. Smyth, S. O. Morgan, and J. C. Boyce, J. Am. Chem. Soc. **50**, 1542 (1928); C. P. Smyth and S. O. Morgan, J. Am. Chem. Soc. **50**, 1554 (1928); H. Müller, Physik. Zeits. **34**, 689 (1933).
[7] C. J. F. Böttcher, Physica **6**, 59 (1939).

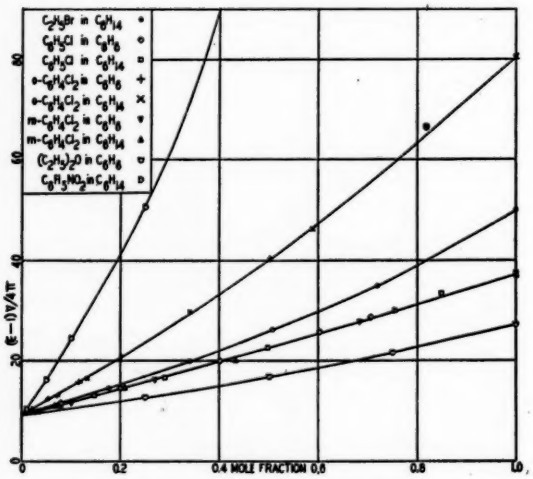

FIG. 2. Total polarization $\frac{\epsilon-1}{4\pi}\left(\frac{N_1M_1+N_2M_2}{d}\right)$ for polar solutes in nonpolar solvents.

equation from the dielectric constant of the pure liquid and in this paper we shall show that even better agreement can be obtained by the application of the Onsager equation to dilute solutions.

It would seem that the most serious defect of the D-C-M theory is the assumption that the permanent moment is a constant of the molecule regardless of its environment. Some years ago one of the authors[8] pointed out that a transformation toward the ionic type of binding must inevitably take place when a polar molecule goes into solution with a resultant enhancement of the dipole moment. Experimental work by Fairbrother[9] and Müller[10] tended to confirm this conclusion but in the absence of a satisfactory theory their results could only be taken as qualitative evidence. It remained for Onsager to show how the reaction field induced by the dipole in its environment produces this augmentation of the dipole moment. A further consequence of the reaction field is that the orienting effect of the "cavity" field calculated by the Clausius-Mosotti procedure practically disappears. As already stated Onsager believed this consideration not to be of great importance in dilute solutions of nonpolar solvents but a consideration of the polarization curves in Fig. 1 leads to the contrary conclusion.

[8] W. H. Rodebush, Trans. Faraday Soc. **30**, 778 (1934).
[9] F. Fairbrother, Trans. Faraday Soc. **30**, 863 (1934).
[10] H. Müller, Physik. Zeits. **34**, 689 (1933).

The Onsager equation for a solution of a polar molecule in a nonpolar solvent may be cast in the form

$$\frac{(\epsilon-1)V}{4\pi}=\frac{3\epsilon N_1V_1}{4\pi}\left(\frac{n_1^2-1}{2\epsilon+n_1^2}\right)+\frac{3\epsilon N_2V_2}{4\pi}\left(\frac{n_2^2-1}{2\epsilon+n_2^2}\right)+\frac{N_2N_0\mu\mu^*}{3kT}. \quad (1)$$

Where the subscripts (1) and (2) refer to nonpolar solvent and polar solute, respectively, n_1, n_2 are the refractive indices. N_1, N_2 are the mole fractions, V_1, V_2 the molal volumes, ϵ the dielectric constant and V, the volume of one mole of solution. N_0 is Avogadro's number. In this equation the molecules are assumed to be spheres and at the same time to fill the space without voids. Onsager of course recognizes the arbitrariness of this assumption. A further difficulty arises that the equation is not explicit in ϵ since μ and μ^* involve ϵ in a complicated way the exact relation for spherical molecules being

$$\mu\mu^*=\frac{\epsilon(n_2^2+2)^2(2\epsilon+1)}{3(2\epsilon+n_2^2)^2}\mu_0^2, \quad (2)$$

where μ_0 is the permanent moment of the molecule in the vapor state. Nevertheless for practical purposes Eq. (1) above is a useful form since in dilute solution the expression

$$\frac{\epsilon-1}{4\pi}V$$

becomes within the limits of experimental error a linear function of composition (mole fraction). Since

$$(\epsilon-1)/4\pi$$

represents the polarization at unit field for a gas we choose to call

$$\frac{\epsilon-1}{4\pi}V$$

the molal polarizability as distinguished from the D-C-M definition of polarization. In Fig. 2 are plotted values of

$$\frac{\epsilon-1}{4\pi}V$$

for a number of substances. If one differentiates Eq. (1) with respect to N_2 a very complicated expression must result since μ and μ^* are functions of N_2. For small values of N_2 however a number of terms may be neglected and since

$\epsilon=n_1^2$, we obtain

$$\frac{\partial[(\epsilon-1/4\pi)V]}{\partial N_2}=\frac{3\epsilon V_2}{4\pi}\frac{n_2^2-1}{2\epsilon+n_2^2}-\frac{V_1(n_1^2-1)}{4\pi}\left(1-\frac{1}{3\epsilon}\left(\frac{\partial\epsilon}{\partial N_2}\right)\right)+\frac{N_0\mu\mu^*}{3kT}. \quad (3)$$

This derivative with respect to N_2 we have chosen to call the partial molal polarization $\bar{P}_2$. Inspection of Fig. 2 shows that since Eq. (1) is linear over a considerable range of composition in dilute solution it is possible to determine the limiting value of the slope for $N_2=0$ with a considerable degree of precision. We believe this to be the most accurate method of calculating moments in solution and by use of the relation (2) above it is possible to make a comparison with the moment of the molecule in the vapor state.

In Table I values of the dipole moment calculated by various methods are compared with the values observed for the vapor where these are available. In the first column the values are calculated by the D-C-M equation from data on dilute solutions, while in the second column the values are calculated from the slopes by the Onsager equation as outlined above from the same data. The values in the third column were calculated by Böttcher from the dielectric constant of the pure liquid using the Onsager equation.

One notes on an inspection of Table I that the values obtained from the data on the dilute solutions by the two methods of calculation do not differ markedly, in most cases. The comparison with the data on the vapor is not as satisfactory as one might wish because of the lack of data and lack of agreement between different investigations where the data is available. For some substances when the two methods do not agree the Onsager equation gives better agreement with the vapor. This is not true however for the last three molecules listed. Here both methods of calculation yield values of μ much higher than those obtained in the vapor but the D-C-M method seems a little better. This is perhaps not surprising in view of the fact that the Debye polarization is constant for the whole range of composition for diethyl ether and for a limited range for the hydrogen halides. The case of diethyl ether is certainly interesting because it is the one case that has come to our attention where the Debye polarization is independent of composition and it might therefore be assumed to be a case where the Clausius-Mosotti theory really gives the correct picture.

We believe this conclusion to be erroneous, however. In the first place the moment as calculated by the Debye method does not agree with the value obtained from the vapor and for these last three substances in the table the value is now too large instead of too small as is usually the case. This agrees with the Onsager hypothesis of an increased moment due to the reaction field in solution and once this is admitted it follows that the Clausius-Mosotti theory cannot be correct. Furthermore one notes from Fig. 1 that the normal course of the polarization as calculated by the D-C-M method is a marked decrease with increasing concentration even in the most dilute solutions. The fact that diethyl ether or hydrogen chloride do not show this decrease must mean that the effective moment of the molecule increases even more rapidly with increasing dielectric constant in solution than is the case with the substances for which curves are shown in Fig. 1. Therefore these substances which appear to follow the D-C-M theory must differ in their actual behavior even more than ordinary from that constancy of moment postulated by the D-C-M theory. This existence of the variable moment renders the D-C-M method of calculation meaningless.

The Clausius-Mosotti theory evidently contains two fundamental errors. The first is the assumption of an unvarying permanent moment for the molecule in solution. The second is the

TABLE I. *Values of* μ_0.

	D-C-M Method	Onsager equation		Measured in vapor state
		Dilute Solution	Pure Liquid	
Nitrobenzene	3.90	3.88	4.20	4.20
Ethyl bromide	1.86	2.03	1.90	2.00
Chlorobenzene	1.55	1.63	1.52	1.70
o-dichlorobenzene	2.25	2.33	2.24	—
m-dichlorobenzene	1.48	1.55	1.42	—
Diethyl ether	1.25	1.35	1.47	1.14
Hydrogen chloride	1.28	1.36	—	1.03
Hydrogen bromide	1.01	1.02	—	0.78

inclusion of the reaction field in the total orienting field acting on the molecule. These two effects cause deviations in opposite directions. Ordinarily the second effect predominates so that the D-C-M polarization decreases with increasing concentration but in the case of diethyl ether when there is reason to believe the augmentation of the moment is greater than that predicted by the Onsager equation the two effects neutralize each other so that the polarizations calculated by the D-C-M method appears independent of concentrations.

It does not follow of course the relation of Onsager, Eq. (2), is correct for all molecules since as he himself has pointed out the model from which it is calculated may have little resemblance to real molecules. One can scarcely hope to obtain any single relation of the type of (2) above which will fit all types of molecules. One sees that in general that the curves for

$$\frac{\epsilon-1}{4\pi}V$$

as plotted (Fig. 2) are concave upward which indicates that the increase in effective moment with increasing dielectric constant is greater than Eq. (2) would indicate, the effect of course being most pronounced for molecules of larger moment. It should be noted that diethyl ether which is the outstanding case where the D-C-M polarization is linear does not as might have been anticipated show any greater deviation from the linearity predicted by the Onsager equation than does ethyl bromide.

From the foregoing it might be concluded that since neither theory can be relied upon to give the exact value of the moment in the vapor state in every case and since both theories often lead to the same value for this moment, then one theory is as good as the other. Onsager of course, showed that in the limiting case of infinite dilution the equations of the two theories can be cast in the same mathematical form provided that the refractive indices of solute and solvent are the same. That this identical form may be obtained in some cases does not mean, however, that either form of equation is equally good for extrapolation to infinite dilution. The calculation of the apparent molal polarization by the D-C-M method involves the exaggeration of experimental errors and unpredictable variations in case complicating effects such as association are present. An apparent molal quantity is not suitable for extrapolation to infinite dilution since it involves small differences between observed quantities and as we have seen only the extrapolated value at infinite dilution can have any significance. The one exception to this statement is the case where the apparent molal polarization is constant or even a linear function of concentration, but a glance at Fig. 1 shows that this is seldom the case. An alternative method is of course to determine the limiting value of the slopes of the total polarization as calculated by the D-C-M method but this is of course not feasible since the total polarization is not linear. The extrapolation by the D-C-M method involves the judgment of the calculator and one must feel that these judgments have been affected in some cases by a knowledge of the μ_0 values for the vapor so that the figures in Table I cannot be regarded as purely objective and unique values.

Müller[11] has avoided this obvious difficulty in extrapolation by assuming as we have done, the linearity of the dielectric constant as a function of concentration. It appears to us that he should extend his measurements over a wider range of concentrations than he has reported in order to make a satisfactory extrapolation. When this is done we predict with Onsager that his μ-values will in general not be in agreement with those found for the vapor. On the other hand we have seen that the quantity

$$\frac{\epsilon-1}{4\pi}V$$

is linear within the experimental error over a considerable range of concentration so that the slope, which may be considered a partial molal polarization, can be obtained with accuracy. This partial molal polarization becomes a significant quantity by Onsager's theory. Furthermore, our calculations together with those of Böttcher show that the theory of Onsager has a real validity over the whole range of concentration. In a succeeding paper we shall attempt to interpret the behavior of alcohols and other associated molecules by this theory.

[11] H. Müller, Physik. Zeits. **35**, 346 (1934).

LETTERS TO THE EDITOR

This section will accept reports of new work, provided these are terse and contain few figures, and especially few halftone cuts. The Editorial Board will not hold itself responsible for opinions expressed by the correspondents. Contributions to this section should not exceed 600 words in length and must reach the office of the Managing Editor not later than the 15th of the month preceding that of the issue in which the letter is to appear. No proof will be sent to the authors. The usual publication charge ($3.00 per page) will not be made and no reprints will be furnished free.

Some Heat Capacity Data for Isopropyl Alcohol Vapor

Some heat capacity data for isopropyl alcohol vapor have long been needed in connection with various thermodynamic studies involving this compound. Accordingly, using a "constant flow" method, we have now made experimental determinations of its molal heat capacity (C_p) at a constant pressure of 1 atmosphere at three temperatures. Briefly, our method involved the passing of preheated isopropyl alcohol vapor at a uniform rate through a copper calorimeter to which a measured amount of energy was supplied electrically. The temperature rise of the vapor, determined accurately by thermocouples and a White potentiometer, was about 3°. By passing the vapor at different rates, a suitable correction could readily be made for radiation and conduction losses at each temperature; and thus the experimental C_p values given in Column 2 of Table I were derived. They are probably accurate to within 1.5 percent.

TABLE I. *Heat capacity values for isopropyl alcohol vapor.*

	C_p FOR 1 ATMOS. (IN CAL./DEG. PER MOLE)		
TEMP. °K	EXPERIMENTAL	BY EQ. (1)	BY EQ. (2)
427.9	28.4	28.3	26.9
457.7	30.5	30.6	28.5
480.3	32.4	32.3	29.6

These three heat capacity results fit the linear equation

$$C_p = -4.54 + 0.0767T \qquad (1)$$

with an average deviation of only 0.3 percent. The values thereby calculated are given in the third column of the table. In Fig. 1 this equation is represented by the solid line and our experimental results by the large dots.

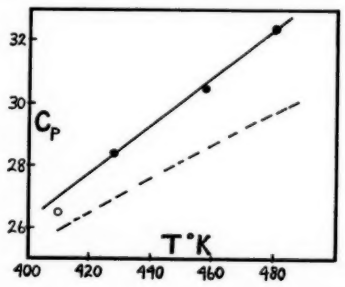

FIG. 1. The molal C_p values for isopropyl alcohol vapor plotted against the absolute temperature. The dots represent experimental values in the present study and the circle the value obtained by Bennewitz and Rossner.

After the start of our investigation Bennewitz and Rossner[1] published a single experimental value, $C_p = 26.5$ cal. per mole, for the heat capacity of isopropyl alcohol vapor at 410°K. This is represented by the circle in the figure; it lies 1.5 percent below our empirical line. For estimating heat capacity values for the vapors of various organic compounds these authors also developed a semi-theoretical method, which has been subsequently modified for practical purposes by Fugassi and Rudy.[2] Using the power series constants suggested by these latter investigators, we have also derived the equation

$$C_p = -1.91 + 12.4(10^6)T^{-3} + 0.0798T - 0.000030T^2 \qquad (2)$$

which is represented by the broken line in the figure. Through its use we have obtained the calculated values in the fourth column of the table. These are 5.3, 6.6 and 8.6 percent, respectively, below our experimental data.

GEORGE S. PARKS
C. HOWARD SHOMATE*

Department of Chemistry,
Stanford University,
Stanford University, California,
April 4, 1940.

[1] Bennewitz and Rossner, Zeits. f. physik. Chemie **39B**, 126 (1938).
[2] Fugassi and Rudy, Ind. Eng. Chem. **30**, 1029 (1938).
* Holder of the Standard Oil Company Fellowship at Stanford University for 1938–1939.

A Note on Electronic Absorption Spectra in Solution

It has been proposed to explain the various effects of solvents on absorption spectra, in particular those of diatomic molecules, by the addition of a potential barrier, $W''(r)$, to the $U(r)$ curves of the ground and excited electronic levels.[1] That part of the function, which is determined by the cage of solvent molecules about the absorbing molecule, can be evaluated by considering the work necessary to increase the internal surface area of the solvent cage in order that the molecule may be accommodated when the nuclear separation is increased during a vibration. By assuming that the solvent cage has spherical symmetry and that this is unaltered by small increases in r, one obtains an approximation to $W''(r)$ by evaluating the work done against the surface tension, γ, as a function of r. It must, however, be realized that this method is valid for the evaluation of $W''(r)$ only when the assumption of spherical symmetry is a good one, i.e., when r is close to r''_e. The eigenfunctions of those vibrational levels which are re-

sponsible for the bulk of the absorption are appreciable only over values of r close to r''_e, where the above method may be applied.

For nonassociated solvents—

$$W'(r) = 4\pi\gamma(r^2 - r''_e{}^2),$$

$W''(r)$ being zero when $r = r''_e$.

$W''(r)$ has been calculated for the solvent $CHCL_3$ over the region where the eigenfunctions $R''_0(r)$ and $R''_1(r)$ for the $^1\Sigma^+_g$ state of Br_2 are appreciable. Addition of this to the potential function for gaseous Br_2 molecules, $U''_g(r)$, gives a $U''_s(r)$ curve for the dissolved molecules which approaches that of the harmonic oscillator to within 0.002A at $v''=0$ and to within 0.009A at $v''=1$. The use of the Hermitic in preference to the anharmonic eigenfunctions in calculating the $\epsilon - \nu$ curve for Br_2 dissolved in $CHCl_3$ by Bayliss and Rees[1] is therefore justified on the basis of this evaluation of $W''(r)$.

In the hydroxylic solvents, where, as has been pointed out,[1] the quasi-crystalline nature of the solvent implies a semirigid cage of radius, h, work must be done to increase the internal surface area of this cage to accomodate the molecule of radius r''_e. In this case, $W''(r)$ will be zero at $r = h$ and is expressed therefore as—

$$W''(r) = 4\pi\gamma(r^2 - h^2),$$

$W''(r''_e)$ being $4\pi\gamma(r''_e{}^2 - h^2)$.

As the component A[2] of the visible absorption continuum of Br_2 involves the transitions $^3\pi_{0^+u} \leftarrow {}^1\Sigma^+_g$ and $^1\pi_u \leftarrow {}^1\Sigma^+_g$,[3] the displacement of the vibrational eigenfunctions of Br_2 on solution in water renders calculation of the whole absorption curve impossible with the present data. The position of the absorption maximum can, however, be determined without the introduction of any further assumptions. From the data of Bernal and Fowler,[4] h can be shown to have the value 1.7A for water. $W''(r)$ has been calculated for water and added to the $U''_g(r)$ curve for Br_2. The resultant $U''_s(r)$ curve has its minimum at 2.255A and is 990 cm^{-1} higher than the minimum of $U''_g(r)$. From the $U'_s(r)[= U'_g(r) + W''(r)]$ curve for the A component of the visible absorption, the value of ν_{max} for Br_2 in water has been shown to be 25,500 cm^{-1}, the calculated shift in ν_{max} on solution of Br_2 in water being 1400 cm^{-1}. The observed shift is 1750 cm^{-1}.[5,6]

The $U'(r)$ curves for I_2 are not known with any accuracy in the region of the continuous levels, but, by making $U'(r)$ correct at r''_e and giving it the same slope as the Morse curve for the component with $\nu_{max} = 19{,}700$ cm^{-1}, the shift of the absorption maximum is calculated to be 1300 cm^{-1} for I_2 in water, whereas the observed shift is 1800 cm^{-1}.[7,8]

A. L. G. REES*

Department of Physical and Inorganic Chemistry,
Imperial College,
London, S.W. 7.
March 19, 1940.

[1] Bayliss and Rees, J. Chem. Phys. **8**, 377 (1940).
[2] Acton, Aickin and Bayliss, J. Chem. Phys. **4**, 474 (1936).
[3] Bayliss and Rees, J. Chem. Phys. **7**, 854 (1939).
[4] Bernal and Fowler, J. Chem. Phys. **1**, 515 (1933).
[5] Child and Walker, Trans. Faraday Soc. **34**, 1506 (1938).
[6] Aickin, Bayliss and Rees, Proc. Roy. Soc. **A169**, 234 (1938).
[7] Getman, J. Am. Chem. Soc. **50**, 2883 (1928).
[8] Groh, Zeits. f. anorg. Chemie **162**, 287 (1927).
* Beit Research Fellow.

The Hindered Rotation in $CH_2D \cdot CH_2Br$

As in the case of tetrachloroethane[1] we would predict that $CH_2D \cdot CH_2Br$ is an equilibrium mixture of two rotational isomers, a *cis*-form in which the D atom is opposed to the Br atom, and two spectroscopically identical *trans*-forms, in which the D atom is opposed to either of the two H atoms of the $-CH_2Br$ group. Since the curve of potential energy as a function of the internal rotational angle has *three identical equally spaced minima and maxima*, the statistical weight of this *trans*-isomer is exactly 2. As a result, the intensity ratio of the Raman lines from the two isomers is

$$\frac{I_{trans}}{I_{cis}} = \frac{(\text{number of } trans)}{(\text{number of } cis)} \cdot A = 2A \approx 2,$$

where A is the ratio of the intensity contributed by a single *trans*-molecule vibrating in a particular mode, to the intensity contributed by a single *cis*-molecule vibrating in a corresponding mode: This factor has a value not very different from 1.[1]

Furthermore, from analogy with other *cis*- and *trans*-isomers, and as a result of calculations based on a simple potential function for these isomers, it can be shown that a symmetrical vibration in a *cis*-form has a *lower* frequency than the corresponding vibration in the *trans*-form. Accordingly, we would predict that the Raman spectrum of $CH_2D \cdot CH_2Br$ consists of a number of double lines, in which the intensity of the line with higher frequency (in any doublet arising from symmetrical modes) would be about twice that of the line with lower frequency.

The best measure of the splitting of a doublet is obtained for the C-Br stretching vibration, the frequency of which is the most sensitive to the configuration of the molecule. We have obtained the Raman spectra of $CH_3 \cdot CH_2Br$ and $CH_2D \cdot CH_2Br$. The intensities of the lines (in the C-Br stretching region) were obtained from microphotometer tracings.

The $CH_3 \cdot CH_2Br$ gave one line at 561.0 cm^{-1} corresponding to the C-Br stretching vibration, whereas $CH_2D \cdot CH_2Br$ gave two lines at 557.5 and 536.5 cm^{-1} with the intensity ratio $I_{557}/I_{536} = 1.6$.

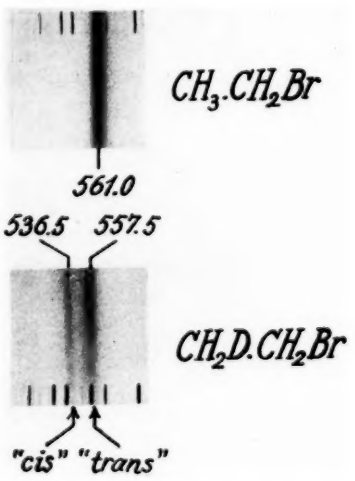

FIG. 1.

This is in agreement with the predictions based on the theory of hindered rotation.[2]

In Fig. 1, prints of the Raman spectra of $CH_3 \cdot CH_2Br$ and $CH_2D \cdot CH_2Br$ are given, showing the two lines corresponding to the *cis*- and *trans*-forms in the deuterium compound.

As can be seen (Fig. 1) there are broad faint components on the low frequency side of each line in the $CH_2D \cdot CH_2Br$ spectrum. The ethylbromide-d_1 was prepared by addition of DBr to C_2H_4. Since exchange reactions could take place during the preparation, it is likely that the sample of $CH_2D \cdot CH_2Br$ used for the Raman spectrum was contaminated with a small quantity of di-deuterium ethylbromides. Since there are 6 isomers of this compound, with C-Br frequencies not very different, it is understandable that the effect is observed as bands.

The good agreement between experiment and theory in this case adds yet another argument in favor of the D_{3h} configuration for ethane.[2]

A. Langseth
H. J. Bernstein*
B. Bak

Universitetets kemiske Laboratorium,
Copenhagen, Denmark,
March 1, 1940.

[1] A. Langseth and H. J. Bernstein, this issue, p. 410.
[2] A. Langseth, H. J. Bernstein and B. Bak, this issue, p. 415.
* 1851 Exhibition Research Scholar.

Simple Method for Calculating Moments of Inertia

In a recent article,[1] Dr. Bryce Crawford showed how the generalized moments of inertia can be calculated for a molecule containing internal torsional motions. His usage of the momental dyad is also advantageous for molecules which are rigid ($N=0$). This special case provides a simple means for calculating the principle moments of inertia for complicated molecules for which the directions of the principle axes are not apparent. Thus, from his Eq. (15), the products of the three principle moments of inertia, I_1, I_2 and I_3, is equal to the determinant of the momental dyad:

$$I_1 I_2 I_3 = \begin{vmatrix} A & -D & -E \\ -D & B & -F \\ -E & -F & C \end{vmatrix}.$$

Where $M = \sum_i m_i$,

$$A = \sum_i m_i(y_i^2+z_i^2) - \frac{1}{M}(\sum_i m_i y_i)^2 - \frac{1}{M}(\sum_i m_i z_i)^2,$$

$$B = \sum_i m_i(x_i^2+z_i^2) - \frac{1}{M}(\sum_i m_i x_i)^2 - \frac{1}{M}(\sum_i m_i z_i)^2,$$

$$C = \sum_i m_i(x_i^2+y_i^2) - \frac{1}{M}(\sum_i m_i x_i)^2 - \frac{1}{M}(\sum_i m_i y_i)^2,$$

$$D = \sum_i m_i x_i y_i - \frac{1}{M}(\sum_i m_i x_i)(\sum_i m_i y_i),$$

$$E = \sum_i m_i x_i z_i - \frac{1}{M}(\sum_i m_i x_i)(\sum_i m_i z_i),$$

$$F = \sum_i m_i y_i z_i - \frac{1}{M}(\sum_i m_i y_i)(\sum_i m_i z_i).$$

Here m_i is the mass and x_i, y_i and z_i are the Cartesian coordinates of the ith atom. The reference frame may have its origin at any place within the molecule and the directions of the axes are arbitrary. In the calculation of rotational partition functions, only this product of the three moments of inertia is required.

Also it is easy to show that the three principle moments of inertia may be obtained separately as the roots, I, of the secular equation:

$$\begin{vmatrix} A-I & -D & -E \\ -D & B-I & -F \\ -E & -F & C-I \end{vmatrix} = 0.$$

These equations should greatly facilitate the calculation of moments of inertia for all those molecules which do not contain a plane of symmetry.

Joseph O. Hirschfelder

Department of Chemistry,
University of Wisconsin,
Madison, Wisconsin,
March 18, 1940.

[1] Bryce L. Crawford, Jr., J. Chem. Phys. **8**, 273 (1940).

The Directional Oxidation of a Single Crystal of Copper by Heating in Air at Reduced Pressure

When a single crystal of copper is treated with an etching liquid, the reactivity of the crystal has been shown to vary with the crystal plane along which the surface is prepared.[1] Experiments are herein reported which show that the reactivity also varies with the crystal plane when the crystal is reacting with oxygen gas. This variation in reactivity should be of importance in a study of the mechanism of gaseous reactions on the surfaces of solids.

A single crystal of copper in the form of a sphere, $\frac{5}{8}$ in. in diameter, was prepared and surfaced by the method[2] previously described. The crystal was then heated for four hours in air at a pressure of 0.3 mm of mercury and at a temperature of approximately 1000°C. The crystal was allowed to cool to room temperature in air at this same pressure. The very striking oxidation pattern shown in Fig. 1 was obtained. The dark square in the center is

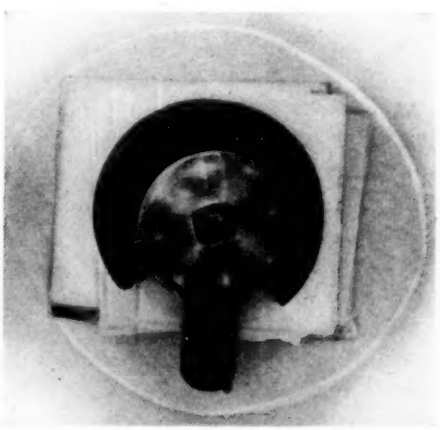

Fig. 1. Oxidation pattern of a single crystal of copper heated in air at reduced pressure.

located at the (100) pole position and the four light spots opposite the four sides of the square and near the outside edge of the sphere are located at the (110) pole positions. The colors in the pattern, when the crystal was illuminated by diffuse white light (by placing a tube of white paper above the sphere), varied from bright red in the squares at the (100) pole positions to a silvery metallic luster in the small apparently unoxidized areas at the (111) pole positions. At least eight areas having visibly different degrees of oxidation could be recognized. The lighter irregular spot within the darker square area at (100) pole position is due to a reflection from the source of illumination during photography and should be disregarded. When the surface was examined under a microscope with a magnification of 600, fine circular striations could be seen over areas, 3 to 5 mm in diameter, with the centers of the circles located at the (110) and (111) pole positions. From the reflections seen with the unaided eye using a beam of light normal to the surface, the (110) and (111) planes, respectively, appeared to be developed over these two areas. When the crystal was heated in hydrogen at atmospheric pressure and a temperature of 340°C, the bright oxide colors disappeared but a gray foggy pattern could still be identified. At a temperature of 580°C the pattern had disappeared and the surface had largely recovered its highly polished appearance. The circular striations as seen under the microscope had become very faint.

A second crystal was heated for three hours in air at a pressure of 0.3 mm of mercury and at a temperature of about 580°C. It was then allowed to cool to room temperature at this same pressure of air. A more irregular tarnish had appeared over surface but a definite pattern, quite different from the first, could be identified. Several types of deep striations or ridges could be seen on the surface with the aid of a microscope, the most striking of which were bounded by the sides of an equilateral triangle and located at the (111) pole positions. When the crystal was heated in hydrogen at 580°C the oxide colors disappeared but the surface retained a gray fogginess. When examined under a microscope most of the striations could still be seen but had decreased in prominence. A third crystal was heated in air at a temperature of about 580°C and a pressure of about 4 mm and a somewhat different oxidation-pattern was produced.

From these experiments the following conclusions had been drawn: (1) The reactivity of a single crystal of copper with oxygen gas varies with the crystal plane along which the surface is prepared. (2) The oxidation-pattern depends on both the pressure of the gas and the temperature. (3) Since no appreciable striations or patterns were produced on heating a highly polished crystal at 560°C in either a high vacuum or an atmosphere of hydrogen, the oxygen gas in reacting must cause the atoms in the surface to rearrange and to develop preferred crystal planes at a temperature considerably below the melting point of the copper. (4) On reducing the oxidized surface with hydrogen the striations and ridges in the surface were greatly reduced in prominence. If the oxidation is slight (yet sufficient to photograph), the surface practically recovers its original appearance of a high polish.

A detailed description of the experiments will be presented later.

ALLAN T. GWATHMEY
ARTHUR F. BENTON

School of Chemistry,
University of Virginia,
Charlottesville, Virginia,
April 6, 1940.

[1] G. Tammann and F. Sartorius, Zeits. f. anorg. allgem. Chemie 175, 97 (1928); K. W. Hausser and P. Scholz, Wiss. Veröffent. Siemens-Konzern 5, 144 (1927); A. T. Gwathmey and A. F. Benton, Trans. Electrochem. Soc., in press.
[2] A. T. Gwathmey and A. F. Benton, see reference 1.